

Dissertation zur Erlangung des Doktorgrades  
der Fakultät für Chemie und Pharmazie  
der Ludwig-Maximilians-Universität München

**Molecular analyses of  
resistance and sensitivity mechanisms  
to anti-EGFR directed tumor therapy**

**Denis Joachim Irmer**

aus

**Recklinghausen**

2008

## **Erklärung**

Diese Dissertation wurde im Sinne von § 13 Abs. 3 bzw. 4 der Promotionsordnung vom 29. Januar 1998 von Herrn PD Dr. Jens Oliver Funk betreut und von Herrn Prof. Dr. Christoph W. Turck vor der Ludwig-Maximilians-Universität München vertreten.

## **Ehrenwörtliche Versicherung**

Diese Dissertation wurde selbständig, ohne unerlaubte Hilfe erarbeitet.

München, den 01.03.2008

.....  
Denis Joachim Irmer

Dissertation eingereicht am:	07.12.2007
1. Gutachter:	Herrn PD Dr. Jens Oliver Funk
2. Gutachter:	Herr Prof. Dr. Christoph W. Turck
Mündliche Prüfung am:	25.02.2008

*Science is when fiction is confused with reality.*

# Contents

## Contents

## Abbreviations

<b>1. Introduction .....</b>	<b>1</b>
<b>1.1 Receptor tyrosine kinases (RTKs) .....</b>	<b>2</b>
1.1.1 ErbB family of RTKs .....	3
1.1.2 Modes of EGFR activation.....	4
1.1.3 EGFR-mediated signal transduction.....	5
1.1.4 Physiological importance and functions of EGFR.....	7
<b>1.2 Role for EGFR in cancer.....</b>	<b>7</b>
1.2.1 Cancer physiology .....	7
1.2.2 Modes of EGFR-mediated cell transformation.....	9
1.2.3 EGFR kinase domain mutations .....	10
1.2.4 The role of Epithelial-mesenchymal transition (EMT) for metastasis and EGFR .....	12
<b>1.3 EGFR-targeting cancer therapy.....</b>	<b>14</b>
1.3.1 Tyrosine kinase inhibitors .....	15
1.3.2 EGFR-targeting monoclonal antibodies .....	16
1.3.3 Mechanisms of cellular and clinical resistance and sensitivity to EGFR-directed cancer therapy .....	18
1.3.3.1 Biomarkers for resistance to EGFR-directed cancer therapy .....	18
1.3.3.2 Biomarkers for sensitivity to EGFR-directed cancer therapy.....	19
1.3.3.3 Cellular resistance models .....	21
<b>1.4 Aim of this study.....</b>	<b>22</b>
<b>2. Material and methods .....</b>	<b>23</b>
<b>2.1 Materials .....</b>	<b>23</b>
2.1.1 Laboratory instruments .....	23
2.1.2 Software .....	24
2.1.3 Laboratory chemicals .....	24



2.1.4 Consumables.....	26
2.1.5 Enzymes.....	26
2.1.6 Antibodies.....	27
2.1.7 “Kits” .....	28
2.1.8 Vectors and oligonucleotides.....	28
2.1.8.1 Oligonucleotides.....	28
2.1.8.2 Starting vectors .....	29
2.1.8.3 Vectors constructed in this work.....	29
2.1.9 DNA- and protein size standards.....	30
2.1.10 Media and buffers.....	31
2.1.11 Cell culture media and supplements .....	34
2.1.12 Growth factors and cancer therapeutics.....	34
2.1.13 Bacterial strains.....	35
2.1.14 Mammalian cell lines .....	35

## **2.2 Methods..... 36**

<b>2.2.1 Methods in molecular biology.....</b>	<b>36</b>
2.2.1.1 Introduction of plasmid DNA into bacteria .....	36
2.2.1.2 Plasmid preparation from bacteria.....	37
2.2.1.3 Agarose gel electrophoresis .....	37
2.2.1.4 Elution of plasmid DNA from agarose gels .....	37
2.2.1.5 Nucleic acid quantification and determination of purification quality.....	37
2.2.1.6 Polymerase chain reaction (PCR) .....	38
2.2.1.7 Automated fluorescence DNA sequencing .....	39
2.2.1.8 Enzymatic manipulation of DNA .....	40
2.2.1.8.1 Restriction digestion of plasmid DNA.....	40
2.2.1.8.2 Dephosphorylation of vector DNA at 5’ strand ends .....	40
2.2.1.8.3 Preparation of DNA for ligation .....	41
2.2.1.8.4 Ligation of manipulated DNA with T4 Ligase .....	41
2.2.1.8.5 Site-directed mutagenesis of vector constructs .....	42
2.2.1.9 RNA expression analyses .....	43
2.2.1.9.1 Isolation of total RNA from mammalian cells .....	43
2.2.1.9.2 Reverse transcription of mRNA for cDNA synthesis .....	43

2.2.1.9.3 Quantitative real-time PCR analyses with Taqman <sup>®</sup> Low Density Arrays (LDA).....	44
2.2.1.9.4 Quantification of the genome-wide mRNA expression with Affymetrix whole genome DNA chip arrays .....	46
2.2.1.9.5 Statistical methods for evaluation and interpretation of the whole genome expression analyses .....	46
<b>2.2.2 Methods in mammalian cell culture and pharmacology.....</b>	<b>46</b>
2.2.2.1 General cell culture conditions and techniques .....	46
2.2.2.2 Calculation of cell numbers .....	47
2.2.2.3 Freezing and thawing of cell lines .....	47
2.2.2.4 Light microscopy .....	47
2.2.2.5 Generation of stably transfected NIH3T3 cell lines .....	47
2.2.2.6 Generation of long-term gefitinib or cetuximab-treated human cancer cell lines.....	48
2.2.2.7 Monolayer growth inhibition assays with Wst-1 reagent.....	49
2.2.2.8 Colony formation assay in a soft-agar matrix .....	50
2.2.2.9 Short-term treatment of cell lines with EGF and cancer therapeutics for protein lysate preparation.....	51
2.2.2.10 Detection of EGFR surface expression via fluorescence assisted cell sorting (FACS) .....	51
2.2.2.11 Internalization of radioactively labeled <sup>125</sup> I-cetuximab in A431 cell lines.....	52
2.2.2.12 In vivo pharmacology with murine tumor xenografts upon treatment with cancer therapeutics.....	52
<b>2.2.3 Methods in protein analyses and biochemistry.....</b>	<b>53</b>
2.2.3.1 Preparation of protein lysates.....	53
2.2.3.1.1 Protein extraction from cell lines .....	53
2.2.3.1.2 Protein extraction from murine xenograft tumors .....	53
2.2.3.2 Determination of protein concentrations.....	54
2.2.3.3 SDS-polyacrylamide-gelelectrophoresis (SDS-PAGE).....	54
2.2.3.4 Transfer of proteins on nitrocellulose membranes.....	54
2.2.3.5 Immunoblot detection of proteins .....	55

2.2.3.6 Examination of receptor tyrosine kinase (RTK) activation levels using immunoblot arrays .....	55
<b>3. Results .....</b>	<b>57</b>
<b>3.1 Impact of clinically relevant mutations in the EGFR kinase domain for EGFR-directed tumor therapy .....</b>	<b>57</b>
3.1.1 Studies on stably transfected NIH3T3 cells .....	57
3.1.1.1 Validation of the cellular model system .....	57
3.1.1.2 Examination of cellular signal transduction in NIH3T3 cells .....	58
3.1.1.3 Cellular transformation by EGFR mutants .....	60
3.1.1.4 Growth inhibition of NIH3T3 cells under drug treatment in a 3D soft-agar matrix .....	61
3.1.2 Examination of NSCLC cell lines endogenously expressing EGFR....	62
3.1.2.1 ErbB receptor and ligand expression levels in NSCLC cell lines...	62
3.1.2.2 Growth inhibition of NSCLC cells under drug treatment .....	65
3.1.2.3 Examination of cellular signal transduction in NSCLC cells.....	68
3.1.2.4 Tumor regression of NSCLC cells under drug treatment in murine xenografts .....	71
3.1.2.5 Identification of response predicting marker genes through gene expression profiling in drug-sensitive and resistant NSCLC cell lines.....	74
<b>3.2 Establishment and characterization of cancer cell lines treated long term with EGFR-directed cancer drugs .....</b>	<b>78</b>
3.2.1 Identification and selection of cancer cell lines with primary drug resistance and sensitivity .....	78
3.2.2 Examination of sensitivity and cross-sensitivity of long-term-treated A431 cells.....	80
3.2.3 Morphological changes in cell lines with primary drug sensitivity.....	85
3.2.4 Characterization of biological and biochemical changes in long-term treated A431 cells .....	89
3.2.4.1 Examination of EGFR levels and dynamics in A431 cells .....	89
3.2.4.2 Analyses of molecular markers for epithelial-mesenchymal transition (EMT) in A431 cells.....	92

3.2.4.3 Identification of scavenger pathways compensating for EGFR blockade in A431 cells .....	94
3.2.5 Examination of differential gene expression in cancer cell lines upon long-term treatment with EGFR-specific cancer drugs.....	99
<b>4. Discussion .....</b>	<b>105</b>
4.1 Response to gefitinib is neither exclusively nor strictly determined by presence of EGFR kinase mutations.....	105
4.2 Cellular sensitivity to cetuximab is determined by factors other than EGFR kinase domain mutations .....	106
4.3 Basal expression profiling of NSCLC cells identifies candidate genes putatively predicting response to EGFR-targeting therapy .....	108
4.4 Long-term exposure of A431 to gefitinib, but not to cetuximab, causes gain of resistance to EGFR-directed drugs .....	109
4.5 Cetuximab and gefitinib long-term treated A431 cells show moderately altered expression patterns and different dynamics of EGFR.....	110
4.6 Cetuximab and to a minor extent gefitinib, block epithelial- mesenchymal transition (EMT) in long-term cultured A431 cells .....	111
4.7 Activation of HGFR may compensate for cetuximab-mediated blockage of EGFR.....	112
4.8 Cells lines with primary resistance or sensitivity to EGFR-targeting drugs show differential basal expression patterns after long-term exposure to cancer therapeutics .....	113
4.9 Perspectives .....	114
<b>5. Summary/Zusammenfassung .....</b>	<b>116</b>
<b>6. References.....</b>	<b>118</b>
<b>Acknowledgements .....</b>	<b>144</b>
<b>Curriculum Vitae.....</b>	<b>146</b>

## Abbreviations

2D	Two-dimensional
3D	Three-dimensional
A	Ampere
Ab	Antibody
ADAM	A disintegrin and metalloprotease domain
ADCC	Antibody-dependent cellular cytotoxicity
Amp	Ampicilline resistance
AREG	Amphiregulin
ATP	Adenosintriphosphate
Axl	AXL receptor tyrosine kinase
BAD	BCL-2 antagonist of cell death
BAX	BCL-2-associated X protein
BCA	Bicinchoninic acid
BCR-ABL	Breaking cluster region - Abelson murine leukemia
bp	Base pairs
BSA	Bovine serum albumin
BTC	Betacellulin
°C	Degree Celsius
C3	Complement factor 3
CCL5	Chemokine ligand 5
CDC	Complement-dependent cytotoxicity
CDH1	E-Cadherin
cDNA	Complementary DNA
c-Fos	Cellular homologue of v-fos (FBJ murine osteosarcoma viral oncogene)
c-Jun	Cellular homologue of v-jun (avian sarcoma virus 17 oncogene)
cm <sup>2</sup>	Square centimetres
CML	Chronic myeloid leukemia
CR	Cysteine-rich

## Abbreviations

---

CRC	Colorectal cancer
CXCL6	Chemokine ligand 6
DMEM	Dulbecco's modified eagle medium
DMSO	Dimethylsulfoxide
DNA	Desoxyribonucleic acid
dNTP	Desoxy-nucleosidtriphosphat
dsDNA	Double-stranded DNA
DTT	Dithiothreitol
EC <sub>50</sub>	Effective concentration 50%
ECL	Enhanced chemiluminescence
EDTA	Ethylene-diamine-N,N,N',N',tetraacetic acid
e.g.	Exempli gratia
EGF	Epidermal growth factor
EGFR	Epidermal growth factor receptor
EGTA	Ethylene glycol-bis(2-aminoethyl)-N,N,N',N'-tetraacetic acid
EMT	Epithelial-mesenchymal transition
EPGN	Epigen
EphA	Ephrin type-A receptor
ErbB	V-erb-a erythroblastic leukemia viral oncogene homolog
EREG	Epiregulin
ERK	Extracellular signal-regulated kinase
Fab	Antigen binding fragment
FACS	Fluorescence assisted cell sorting
FAM	5'Carboxy-fluorescein
FCS	Fetal calf serum
FDA	Food and drug administration
FGF	Fibroblast growth factor
FGFR	Fibroblast growth factor receptor
FITC	Fluorescein-iso-thio-cyanat
g	Gramm
GPCR	G protein-coupled receptor
Grb2	Growth factor receptor binding protein 2

## Abbreviations

---

h	Hour(s)
H <sub>2</sub> O	Water
HB-EGF	Heparin-binding EGF-like growth factor
HER	Human EGFR-related
HGF	Hepatocyte growth factor
HGFR	Hepatocyte growth factor receptor
HRP	Horse radish peroxidase
HSPG	Heparane sulfate proteoglycans
Ig	Immunoglobulin
IGF1	Insulin-like growth factor 1
IGF1R	Insulin-like growth factor 1 receptor
IHC	Immunohistochemistry
IL1	Interleukine 1
i.p.	Intra peritoneal
IP3	Inositol-1,4,5-trisphosphate
JAK-2	Janus kinase 2
JNK	c-Jun N-terminal kinase
k	Kilo
kb	Kilobase
kDa	Kilodalton
KRAS	v-Ki-ras2 Kirsten rat sarcoma viral oncogene homolog
l	Liter
LB	Lysogeny broth
LDA	Low density array
LREA	Amino acid motive (Lysin-Arginine-Glutamic Acid-Arginine)
LPA	Lysophosphatidic acid
μ	Micro
m	Milli
M	Molar
MAP	Mitogen-activated protein
MAPK	MAP kinase (Erk1/2)
MEK	MAPK/ERK Kinase

## Abbreviations

---

MET	Mesenchymal-epithelial transition
MgCl <sub>2</sub>	Potassium chloride
Mig6	Mitogen-inducible gene 6
MiliQ water	MiliQ filtered deionized water
min	Minute(s)
MMP	Matrix metalloprotease
mRNA	Messenger ribonucleic acid
n	Nano
NaCl	Sodium chloride
NFkB	Nuclear factor k in B-cells
nm	Nanometer
NP-40	Nonidet P40
NRG	Neuregulin
NSCLC	Non-small cell lung cancer
OD	Optical density
PBS	Phosphate-buffered saline
PCR	Polymerase chain reaction
PDGF	Platelet-derived growth factor
PDGFR	Platelet-derived growth factor receptor
PE	Phycoerythrin
PI	Propidium iodide
PI3K	Phosphatidylinositol 3-kinase
PI3P	Phosphatidylinositol trisphosphate
PMA	Phorbol 12-myristate 13-acetate
PTEN	Phosphatase and tensin homolog
PTP	Protein tyrosine phosphatase
Raf	Homologue of v-raf (murine sarcoma viral oncogene)
Ras	Homologue of v-ras (rat sarcoma viral oncogene)
RNA	Ribonucleic acid
rpm	Rotations per minute
RPMI	Roswell Park Memorial Institute
RT	Room temperature



## Abbreviations

---

RTK	Receptor tyrosine kinase
SCCHN	Squamous cell carcinoma of the head and neck
SDC2	Syndecan 2
SDS	Natriumdodecylsulfate
SDS-PAGE	SDS polyacrylamide gel electrophoresis
Sec	Second(s)
Ser	Serine
Src	Homologue of v-src (sarcoma viral oncogene)
STAT	Signal transducer and activator of transcription
TACSTD	Tumor-associated calcium signal transducer
TAE	Tris-acetate-EDTA
TAMRA	1-(4,4'-Dimethoxytrityloxy)-3-[O-(N-carboxy-(tetramethyl-rhodamine)- 3-aminopropyl)]-propyl-2-O-succinoyl-l-aa
TBST	Tris-buffered saline supplemented with Tween-20
Thr	Threonine
TGF $\alpha$	Transforming growth factor alpha
TNF $\alpha$	Tumor necrosis factor alpha
TKI	Tyrosine kinase inhibitor
Tris	Tris(hydroxymethyl)aminomethan
TSPAN	Tetraspanin
Tween 20	Polyoxyethylen(20)-sorbitan-monolaureate
Tyr	Tyrosine
U	Unit for enzymatic activity
UV	Ultraviolet
V	Volume
VEGF	Vascular endothelial growth factor
VEGFR	Vascular endothelial growth factor receptor
WHO	World health organization
Wt	Wild-type
Y	Tyrosine

## 1. Introduction

According to the World Health Organization (WHO), an estimated 11 million people are diagnosed with cancer worldwide and over 7 million die from cancer every year; however, the number of unreported cases is expected to be far higher. In Germany over 400,000 people died from cancer in 2002, which means that - at current rates - every fourth living German citizen will die from cancer. Carcinoma of the breast (for women), prostate (for men), colorectal tract and lung are responsible for the majority of cancer cases and deaths. Obviously cancerogenesis is a process that develops differently in different organs, where often numerous subclasses of tumors can be distinguished from histology. Furthermore, carcinomas typically pass through specific hallmarks during development, where finally all events leading to tumor formation are due to a complex interplay of molecular factors dependent on the individual situation in the single patient.

In addition to classical tumor therapies, which include surgical removal of tumors, radiation and chemotherapy a spectrum of innovative strategies are being developed specifically targeting cellular molecules, which are either unique for or overrepresented in cancer tissue. A number of these oncogenes, which dominantly drive tumor development by deregulating proliferation or differentiation of normal tissue, have so far been identified and various inhibitors against these entities are in development or already in clinical use (often in combination with conventional forms of therapy). Yet, the complexity of processes in tumorigenesis, as well as the heterogeneity of patient cohorts leads to often only moderate efficacy of these regimens, combined with high costs for individuals and for society as a whole. It is therefore of immanent importance to better understand the molecular mechanisms underlying cancerogenesis, to identify criteria by which tumor response towards a specific regimen can be robustly predicted and to classify patients prior to therapy according to individual suitability of treatment. It is a tempting, yet still inconceivable, conception that in the future there could be standard screening systems available, which are applied upon tumor diagnosis and which allow identification of the optimal individualized medication for every patient in need.

## 1.1 Receptor tyrosine kinases (RTKs)

Cells communicate through various ways either directly via cell-cell contacts or indirectly via secretion and specific binding of messenger proteins, which allows a concerted and controlled action within tissues, organs and the organism. Reversible phosphorylation and dephosphorylation of proteins, which are part or endpoints of signal transduction pathways, has been identified to be a central mechanism of intracellular signal processing (Cohen, 2002). This is substantiated by the fact that over 500 genes coding for kinases and 130 genes coding for phosphatases have been identified by the Human Genome Project (Shawver et al., 2002). Kinases specifically catalyze phosphorylation of serine/threonine or tyrosine residues on target proteins and may occur in the cytoplasm or bound to membranes (Cohen, 2002). Due to their high regulatory potential and their eminent role as driving forces for tumorigenesis, kinases are adequate target structures for specific anti-cancer therapy concepts.

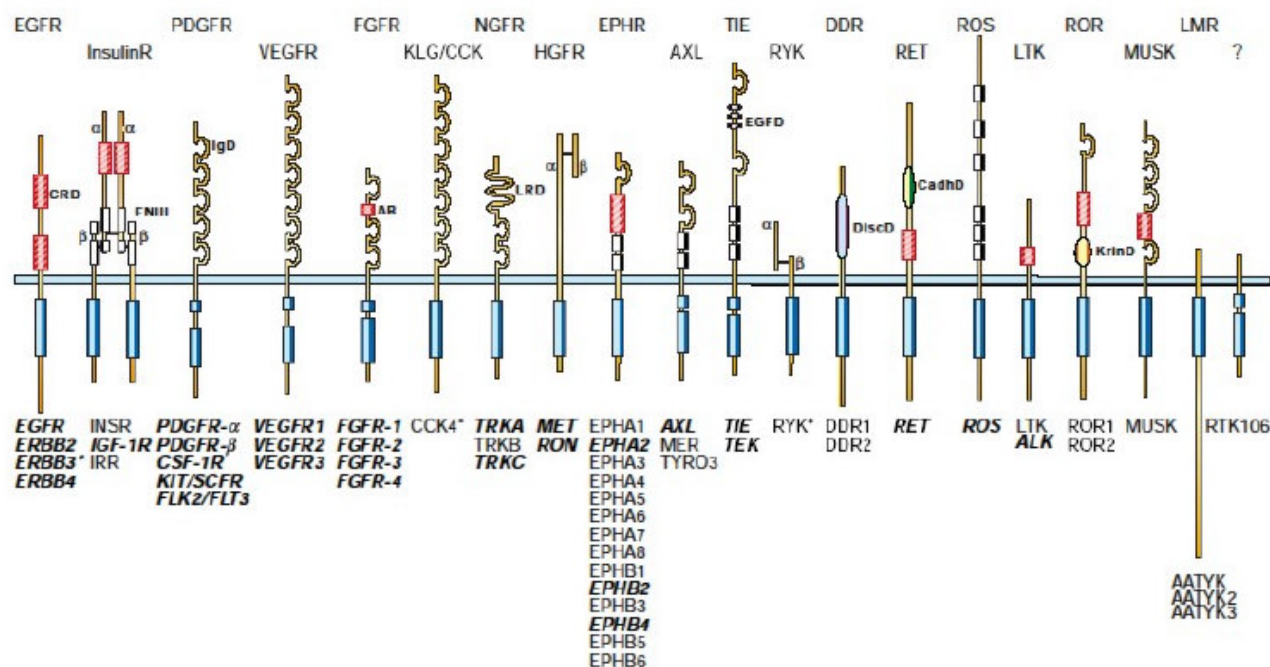


**Figure1 Subfamilies of receptor tyrosine kinases.** Abbreviation in the figure: AB: acidic box; CadhD: cadherin-like domain; CRD: cysteine-rich domain; DiscD: discoidin-like domain; EGFD: epidermal growth factor-like domain; FNIII: fibronectin type III-like domain; IgD: immunoglobulin-like domain; KrinD: kringle-like domain; LRD: leucine-rich domain (from Blume-Jensen and Hunter, 2001).

Receptor tyrosine kinases (RTK) are transmembrane proteins with an intrinsic tyrosine kinase activity. They contain a highly glycosylated extracellular domain, which is engaged in protein-protein interactions, such as ligand binding or complex formation with other receptors and is therefore highly variable between different RTKs. The cytoplasmic domain of RTKs is highly conserved and is composed of the catalytic center, as well as of regulatory regions controlling the (auto-) phosphorylation of the receptor. A transmembrane domain connects the extracellular and intracellular domains. Beyond their common features, the known 58 RTKs are characterized by a wide structural and modular diversity (Blume-Jensen and Hunter, 2001) (figure 1).

All RTKs, with the exception of the insulin receptor (Van-Obberghen et al., 1994), are present as monomers in the membrane and dimerize upon ligand binding, which is paralleled by receptor activation. In the case of the fibroblast growth factor (FGF), binding to the receptor (FGFR) is dependent on stabilization with heparane sulfate proteoglycans (HSPGs), which are localized in the extracellular matrix and on cellular surfaces (Spivak-Kroizman et al., 1994). The signaling capacity of activated RTK receptors can be blocked by antagonistic ligands, by the action of protein tyrosine phosphatases (PTPs) or by receptor degradation (Schlessinger, 2000). Activated RTKs are further subject to internalization and vesicular trafficking, which has been shown to significantly influence the receptor capacity for downstream signaling (Wiley, 2003; Mukherjee et al., 2006).

### 1.1.1 ErbB family of RTKs

The ErbB family encompasses four members, all of which are transmembrane receptor tyrosine kinases (RTKs), including EGFR (epidermal growth factor receptor), ErbB2/Neu/Her2, ErbB3/Her3 and ErbB4/Her4. All four receptors contain two cysteine-rich regions in their extracellular domain. Activation of ErbB family is controlled by the expression and secretion of natural ligand proteins. Ligand binding induces activation of the intrinsic kinase, which catalyzes trans-phosphorylation of the receptor dimers at specific tyrosine residues within their intracellular domain. Phosphorylation of tyrosine residues serves to recruit specific adaptors and other signaling proteins leading to the activation and modulation of intracellular signaling pathways (Pawson et al., 2001). ErbB2 forms dimers with all other ErbB family members, yet cannot bind any known natural ligands by itself (Graus-Porta et al.,

1997), while ErbB3 has a non-functional kinase domain and can only signal in heterodimeric complexes (Guy et al., 1994). Interestingly, it has been observed that ErbB2 containing heterodimers are preferentially formed and that ErbB2 has a high intrinsic kinase activity, readily trans-phosphorylating tyrosine residues of the dimerization partner receptor (Graus-Porta et al., 1997).

### 1.1.2 Modes of EGFR activation

The EGFR gene is located on chromosome 7 and encodes a mature 170kDa protein that encompasses 1186 amino acids. The EGFR ectodomain consists of 621 amino acids and is subdivided into four structural domains (I-IV), where ligand binding domains I and III are leucine-rich repeats (L1 and L2) and domains II and IV are cysteine-rich (CR1 and CR2). Binding of ligands to EGFR forms a complex with 2:2 stoichiometry, where the two receptors are directly bound to each other by interaction between their domains II, while the ligands are on opposite sites from the dimer interface (Ogiso et al., 2002; Garrett et al., 2002) (see figure 2).

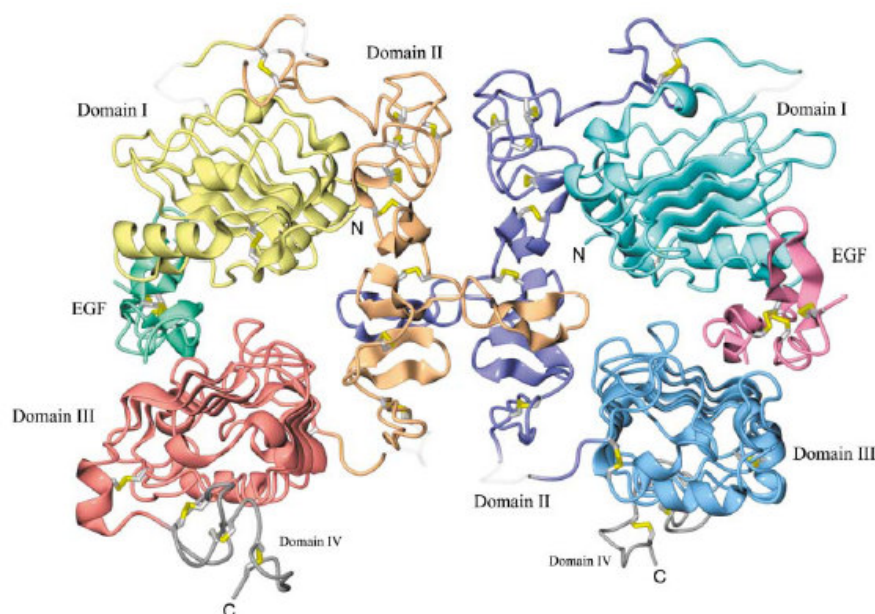


**Figure 2 Crystal structure of the interaction between EGFR and EGF in a 2:2 stoichiometry.** Ribbon diagram with the approximate two-fold axis oriented vertically. The EGF on the left side of the 2:2 EGF•EGFR complex is pale green. Domains I (yellow), II (orange), III (red), and IV (grey) in the left receptor of the dimer are as well highlighted in color. Most of domain IV is disordered (from Ogiso et al., 2002).

Recently, it has been shown that inactive EGF receptor dimers may occur, which are intrinsically auto-inhibited. It has been postulated that allosteric binding of EGF induces sterical changes leading to formation of an asymmetric dimer, which releases the receptors from inhibition and allows receptor activation (Zhang et al., 2006).

Ligand-mediated activation of EGFR can be accomplished by eight ligands, namely amphiregulin (AREG), betacellulin (BTC), epidermal growth factor (EGF), epiregulin (EREG), heparine-binding epidermal growth factor (HB-EGF), transforming growth factor  $\alpha$  (TGF $\alpha$ ) (Riese and Stern, 1998), epigen (EPGN) (Strachan et al., 2001) and cripto (Salomon et al., 1999). All these ligands have an EGF-like domain that consists of 30 to 50 amino acids and forms three disulphide bonded intramolecular loops. Many ErbB ligands are part of a transmembrane precursor and need to be proteolytically processed before getting freed from the membrane. Cleavage of ligand precursors is catalysed by metalloproteases, whose activity is again controlled by G-protein coupled receptors, allowing substantial cross-talk in between these receptor classes (Prenzel et al., 1999; Fischer et al., 2003). There is also evidence that already the membrane tethered precursors of e.g. TGF $\alpha$  may bind to EGFR on adjacent cells and trigger events of signal transduction (Wong et al., 1999). In addition, intracellular kinases, such as Janus kinase 2 (JAK-2) (Yamauchi et al., 1997) or Src (v-src sarcoma viral oncogene homolog) can also directly phosphorylate tyrosine residues on EGFR. In essence, the interplay of ErbB receptors, ligands and other proteins causes a highly complex signaling output, which is sensitively concerted by the expression levels and activity of the involved proteins and which allows a fine regulation of intracellular signal responses and feedback mechanisms. Another mode of EGFR activation includes mutations that may cause a ligand- independent constitutive activation of the receptor. Such genetic alterations are frequent in EGFR driven cancerogenesis and thus are discussed in sections 1.2.2 and 1.2.3.

### 1.1.3 EGFR-mediated signal transduction

The intracellular domain of the EGF receptor contains a serine (Ser-1142), a threonine (Thr-654) and seven tyrosine residues (Tyr-845, 992, 1045, 1068, 1086, 1148, 1173) that can be phosphorylated upon appropriate inputs. Which tyrosine residues of EGFR are phosphorylated and thus, which signaling pathways are

switched on is determined by the composition of the ErbB receptor dimer and the specific ligand involved (Olayioye et al., 1998). Important vertical intracellular signal transduction pathways, which can be activated by EGFR include the phosphatidylinositol-3 kinase (PI3K)/Akt, as well as the Ras/Raf/MEK/MAPK and the JAK/STAT signaling cascades (Schlessinger, 2000; Yarden, 2001). Furthermore, a broad range of different adapter proteins may specifically bind to designate residues upon receptor phosphorylation and trigger horizontal signal transmission (figure 3).

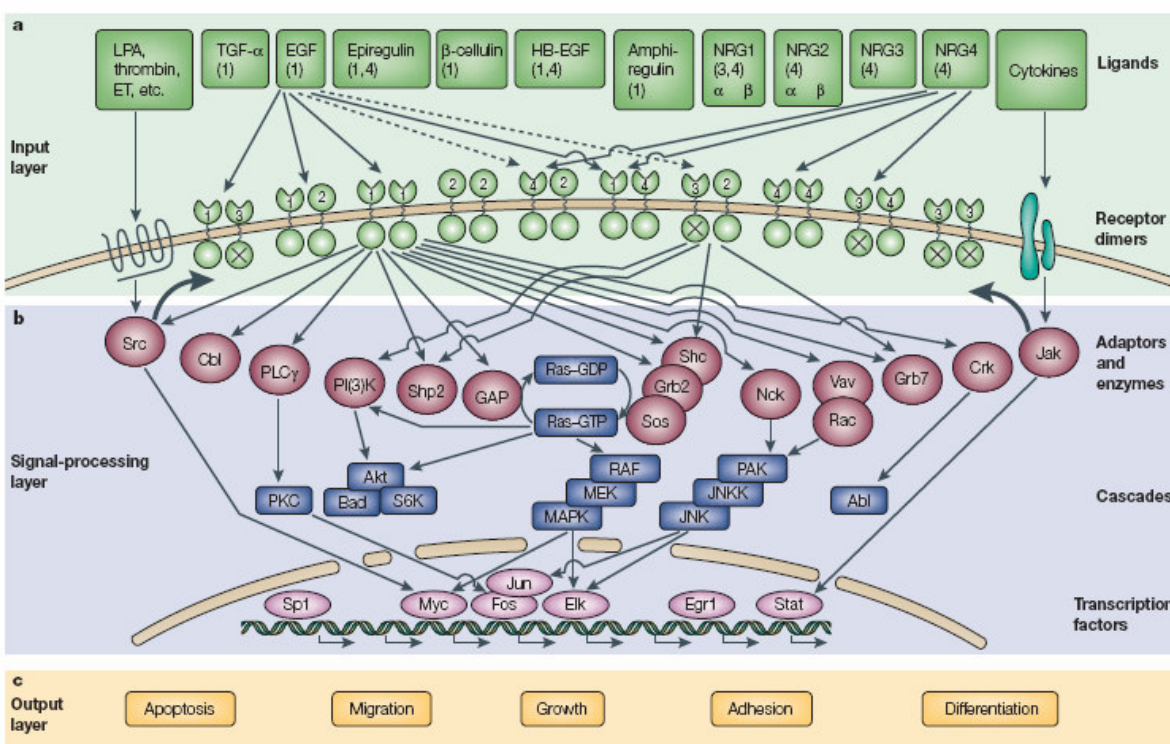


**Figure 3 Details from the ErbB receptor signaling network.** The input signal may vary with regard to the formed receptor pair and the bound ligands (green; receptor specificity for each ligand is indicated in brackets behind ligand name; ErbB receptor designation is indicated by number). For sake of simplicity only binding and signal of EGF at EGFR homodimers and NRG4 at ErbB2/ErbB3 heterodimers are displayed. Signal transmission is ensured by adaptor proteins (violet), which specifically bind to activated receptor dimers. Transactivation of ErbB receptors (thick arrows) is exemplarily portrayed for Lysophosphatidic acid (LPA) activated GPCR via Src kinase (left) and Jak-mediated transactivation of ErbB receptors through activated cytokine receptors (right). Activation and attenuation of transcription factors (pink) is the endpoint of each signaling cascade (blue), which allows fine control of an particular output (yellow) (from Yarden, 2001).

Due to its many different modes and its wide-reaching levels of signal transduction, EGFR may control a multitude of cellular actions. This includes e.g. protection against programmed cell death (apoptosis): activation of the PI3K/Akt cascade causes phosphorylation of Akt, which inhibits activity of the pro-apoptotic protein Bad



(BCL-2 antagonist of cell death) (Datta et al., 1997) and may activate the anti-apoptotic transcription factor NF $\kappa$ B (nuclear factor  $\kappa$  in B-cells) (Madrid et al, 2000). Other outcomes are e.g. controlled by the Ras/Raf/Mek/MAPK cascade: EGFR-mediated activation of Ras causes translocation of phosphorylated MAPK into the nucleus, which supports activation of specific transcription factors, such as c-Jun and c-Fos. This cascade is highly conserved and triggers various effects, including control of proliferation, differentiation, angiogenesis and migration (Hunter, 1998; Yoon et al., 2006).

#### **1.1.4 Physiological importance and functions of EGFR**

Expression of ErbB receptor and EGF orthologs has also been found in *Caenorhabditis elegans* and *Drosophila melanogaster*, where they play roles in cellular differentiation processes and embryogenesis (Moghal et al., 2003; Shilo et al., 2003). EGFR knockout mice have been found to die during embryogenesis or early post birth. These mice have defects in epidermal cells of the skin, lung, gastrointestinal tract, eyes and teeth and display severely impaired gut development (Miettinen et al., 1995; Sibilio et al., 1995; Threadgill et al., 1995). Knockouts in EGFR ligands showed some functional redundancy, while combined loss of TGF $\alpha$ , EGF and AREG causes defects of the lung, skin, eyes and mammary glands as well as accelerated hair and weight loss (Luetteke et al. 1999). The essential role of EGFR for renewal and homeostasis of the skin has been shown in mice with tissue-specific expression of a dominant negative EGF receptor (Murillas et al., 1995), but no further conditional tissue-specific knockouts have been reported so far. Yet, the fact that expression of EGFR can be found in most mature organs underlines its importance for the adult organism and suggests that more details of its functions will be deciphered in the future.

### **1.2 Role for EGFR in cancer**

#### **1.2.1 Cancer physiology**

Cancer is a genetic disease, caused by loss (tumor suppressor genes), amplification or mutation (oncogenes) of certain genes or major chromosomal changes. The majority of cancers are somatic, which means that they are occurring in the affected tissue during tumorigenesis. Yet, many tumors also have a heritable dimension



caused by germline transmission of predisposing genetic alterations that contribute to the development of cancer. Cancerogenesis is a process, which can be subdivided into several intermediate stages. Over the full course of cancer development, which starts with somatic cells and ends up with a severely malignant successor cells, several hallmarks are passed through (see figure 4; Hanahan and Weinberg, 2000).

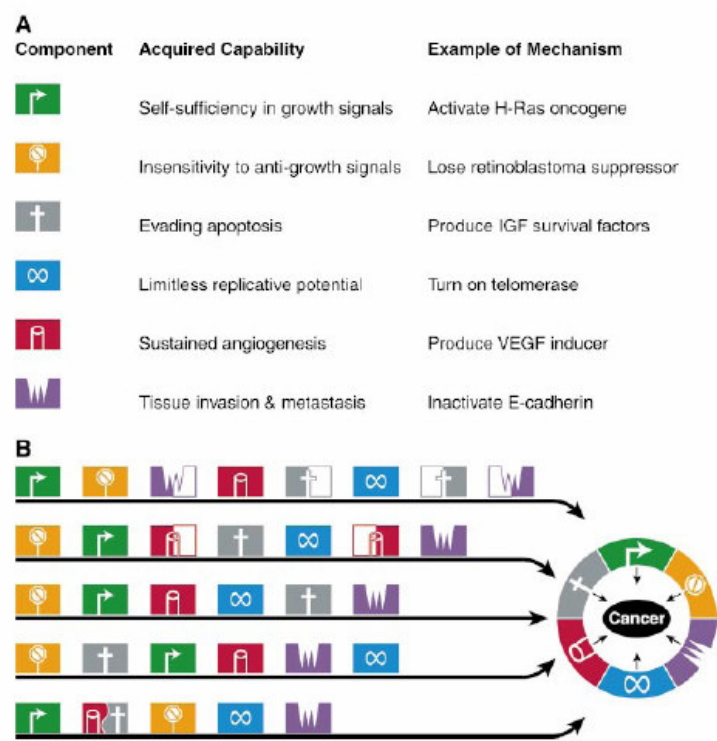


**Figure 4 Expected parallelism of oncogenic events leading to a malign cancer phenotype.** The cancerogenesis model developed by Hanahan and Weinberg postulates that cancers need to acquire six capabilities for reaching full malignancy (A). The order by which these hallmarks are passed through, however, may be variable and is thought to be dependent on cancer types and subtypes (B) (from Hanahan and Weinberg, 2000).

At a early stage somatic cells gain self-sufficiency on the generation of growth signals. Other early steps include insensitivity to growth inhibitory signals, gain of the capacity to evade apoptosis and the acquisition of unlimited replicative potential. Local outgrowth of tumors causes high cellular densities leading to stress and high demand of nutrients and oxygen for the fast-growing cells. Further genetic alterations may thus confer the cancer cells with the potential to promote angiogenesis. Finally malign tumors may start to leave the tumor tissue through the vascular system and

metastasize into other organs of the body. The order by which the cells acquire these capabilities, however, is thought to vary from tumor to tumor.

### 1.2.2 Modes of EGFR-mediated cell transformation

In many tumors natural ligands of EGFR, such as EGF or TGF $\alpha$ , are produced and secreted either by tumor cells themselves or by the stromal tissue. Overexpression of EGFR together with autocrine ligand secretion and concomitant receptor activation provides multiple advantages to tumors by promoting cell proliferation, survival, angiogenesis, invasion and metastasis (Salomon et al., 1995; Huang and Harari, 1999; Normanno et al., 2005). EGFR is frequently expressed in carcinomas of the head and neck (80-100%) (Salomon et al., 1995; Grandis et al., 1996), Non-small cell lung cancer (40-80%) (Rusch et al., 1997; Fontanini et al., 1998), glioblastomas (40-60%) (Ekstrand et al., 1991; Rieske et al., 1998), as well as in pancreatic carcinomas (30-50%) (Uegaki et al., 1997) and ovarian cancer (35-70%) (Bartlett et al., 1996; Fischer-Colbrie et al., 1997). Several studies correlate EGFR expression with reduced survival of patients (Veale et al., 1993; Resnick et al., 2004), the same correlation has also been observed for tumor expression of TGF $\alpha$  and EGF (Hirai et al., 1998; Tateishi et al., 1990).

Another mechanism of EGFR-mediated cancerogenesis is transactivation of the receptor through non-classical mechanisms. This includes transactivation of EGF receptor by GPCRs through metalloprotease-mediated EGF-like ligand shedding (Fischer et al., 2003). Furthermore, cross-talk between other RTKs, integrins, cytokine-receptors, ion-channels and EGFR have been described (Prenzel et al., 2000; Gschwind et al., 2001).

Deregulated EGFR-mediated signaling may also be triggered through mutations of ErbB genes. The most common mutation is a deletion of EGFR, encompassing residues 6-273, called EGFRvIII (de2-7 EGFR). Even though EGFRvIII is unable to bind EGF-like ligands, it is constitutively phosphorylated and elicits downstream signaling pathways qualitatively and quantitatively slightly different from ligand-activated wild-type EGFR (Pedersen et al., 2001). In xenograft models EGFRvIII can confer enhanced tumorigenicity (Damstrup et al., 2002; Feldkamp et al., 1999) and clinically this mutation has been detected for example in NSCLC (5-39%) and glioma (57-86%) biopsies (Moscatello et al., 1995; Frederick et al., 2000; Okamoto et al., 2003; Ji et al., 2006). Recently, EGFR ectodomain mutations have found to occur

frequently in glioblastoma patients (13,6%), however their clinical impact has not yet been studied (Lee et al., 2006b). In contrast, activating EGFR kinase domain mutations that were found in NSCLC patients have been subject of enormous research activities.

### **1.2.3 EGFR kinase domain mutations**

In May 2004 two groups independently reported on EGFR kinase domain mutations found in NSCLC patients with clinical response to the EGFR-targeting cancer drug gefitinib (Lynch et al., 2004a; Paez et al., 2004). Gefitinib is a tyrosine kinase inhibitor (TKI), which is in clinical use for lung cancer and that is discussed in detail in section 1.3.1. More than 15 mutations at different sites in or close to the EGFR kinase domain have been described so far, small deletions in exon 19 encompassing the LREA motive (~48% of mutations), point mutations, such as L858R (~38%), in-frame deletion/insertions in exon 20 (~6%) being the most abundant ones (Janne et al., 2005; Pao and Miller, 2005) (figure 5).

The first two mutations are also referred to as classical EGFR kinase domain mutations, to underline that they confer sensitivity for gefitinib to NSCLC patients and cell lines. Up to now, EGFR kinase domain mutations have only been sporadically described in other tumors, such as colorectal (<0.3%) and head and neck cancer (0-7%) (Barber et al., 2004; Lee et al., 2005; Sihto et al., 2005).

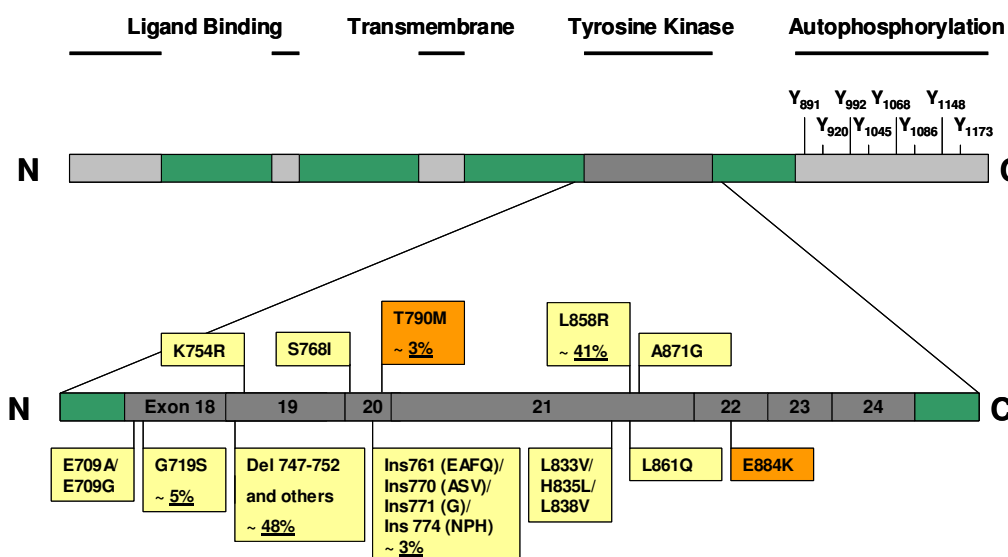


**Figure 5 EGFR kinase domain mutations found in NSCLC patients with relevance for clinical response to gefitinib therapy.** Structural organization of EGFR and localization of clinically relevant mutations in the kinase domain of NSCLC patients. Mutations are highlighted in yellow boxes and their proportional frequencies are indicated for the most abundant clinical mutations. Mutations that may confer resistance to EGFR-directed TKIs are highlighted in orange boxes (from Irmer et al., 2007a).

The initial observation that EGFR mutations on their own do not affect binding affinities of gefitinib (Fabian et al., 2005) triggered a variety of non-clinical analyses using different in vitro and animal models with the aim to better understand the molecular and cellular mechanisms of the EGFR mutations in tumor homeostasis. Clinical investigations showed that EGFR mutations appear to be more frequent in females, never-smokers and in patients with adenocarcinomas. Furthermore, Asians show a much higher prevalence for EGFR mutations (20–40%) than Caucasians (<10%) (Pao and Miller, 2005; Calvo and Baselga, 2006). Many retrospective studies have been performed on NSCLC patients, all correlating expression of mutated receptor with sensitivity to gefitinib (Irmer et al., 2007a). Furthermore, encouraging data on gefitinib monotherapy as first-line regimen in chemo-naïve NSCLC patients have been reported: pre-selection of patients based on EGFR mutations increased gefitinib or erlotinib response rates from 22.7–30 to 75–90% (Asahina et al., 2006; Giaccone et al., 2006; Niho et al., 2006). In contrast, a secondary mutation (T790M, discussed in section 1.3.3.1) may occur in NSCLC patients who carry classical kinase mutations, which reverts hypersensitivity and causes resistance to EGFR-targeting TKIs (Pao et al., 2005a). Additionally, it was proposed that occurrence of

the EGFR mutation E884K dominantly renders tumors resistant to erlotinib, another TKI, but not to gefitinib in NSCLC patients (Choong et al., 2006).

Laboratory studies with cells expressing transfected or endogenous EGFR revealed that mutated receptors are constitutively activated. This is often reflected by a high basal activation of signaling components downstream from EGFR, including phosphorylation of Akt and STAT3/5. Compared with this, phosphorylation of MAPK seems to be exclusively affected in stably transfected cells or in those expressing endogenous receptors. Activation of mutated EGFR or downstream signaling can be very effectively inhibited by gefitinib treatment in most in vitro models (Sordella et al., 2004; Amann et al., 2005; Greulich et al., 2005).

Only very limited data are available for the impact of these mutations on NSCLC therapy with EGFR-targeting monoclonal antibodies, such as cetuximab, which are also in clinical use as cancer therapeutics (see section 1.3.1 for detailed information). However, initial examinations indicate that clinical response to cetuximab in NSCLC does not seem to correlate with the presence of EGFR mutations (Lynch et al., 2004b; Mukohara et al., 2005, Tsuchihashi et al., 2005). This impression is supported by studies with cell lines and examinations on murine xenograft models (Amann et al., 2005; Perez-Torres et al., 2006).

#### **1.2.4 The role of Epithelial-mesenchymal transition (EMT) for metastasis and EGFR**

The conversion of epithelial cells to mesenchymal cells is a critical event in embryogenesis and organ development that was first observed in 1908 (Lillie, 1908). Epithelial cells are normally part of a thin epithelium, where cell-cell junctions and adhesions closely interconnect them, which confers mechanical rigidity and a polarized structural organization to tissues. In contrast, mesenchymal cells have a non-uniform morphology with elongated shapes, do not build tight cell-cell contacts, lack polarity and display an increased migratory capacity (Shook and Keller, 2003). The process that transduces a cell with epithelial morphology to a state with mesenchymal morphology has been designated EMT (epithelial-mesenchymal transition) and was shown to be regulated by a complex interplay of various factors (Thiery, 2002). EMT is a fundamental event of epithelial remodeling during development in many metazoan organisms (Gilbert, 1997) and is essential e.g. for gastrulation during embryogenesis in vertebrates (Shook and Keller, 2003).

Furthermore, EMT is a crucial prerequisite for the mobilization of cancer cells, leading to invasive growth, triggering cellular intravasation into the endothelium and finally metastazation over the body (Thompson et al., 2005). EMT is reversible and can be reversed by a process called mesenchymal-epithelial transition (MET).

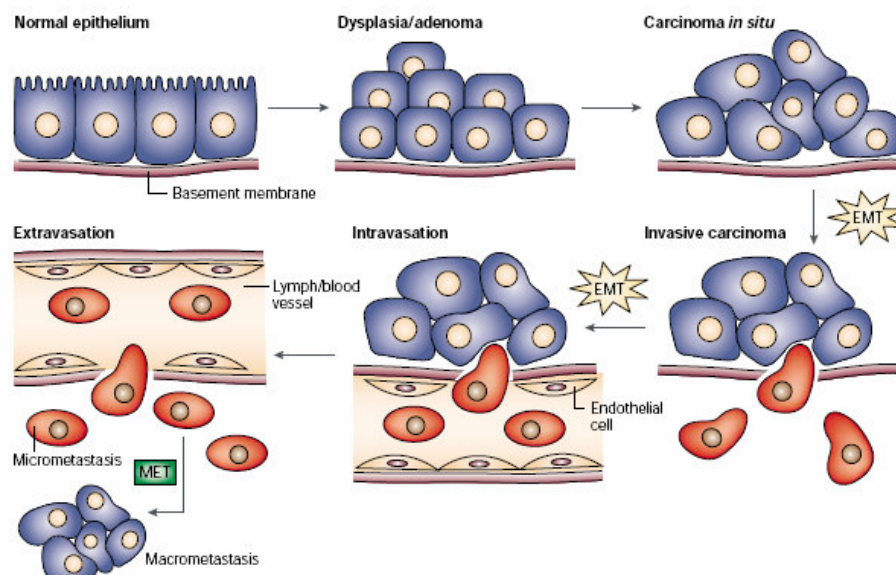


**Figure 6 Modes and sites of EMT and MET in the emergence and propagation of carcinoma.** Regular cells from polarized epithelium may proliferate upon transformation and give rise to adenoma. Further genetic alterations or the presence of paracrine ligands elicit further outgrowth into carcinoma in situ. EMT then leads to disintegration of the basal layer that permits passage of cancer cells into the endothelium, where they are shuttled to other sites. Micrometastases may form after extravasation in distant tissues, where finally macrometastases can arise after a mesenchymal-epithelial transition (MET) of cells (from Thiery, 2002).

Proteins indicating the progress of EMT have been identified to serve as markers permitting categorization of clinical samples and cancer cell lines. The phenotypic markers of EMT are: elongated morphology, as well as an increased scattering, migration and invasion of originally epithelial cells. The most important molecular hallmarks are loss of E-Cadherin expression, increase of vimentin and N-Cadherin expression and nuclear localization of  $\beta$ -Catenin (Lee et al. 2006a). However, typically not all of these features are strictly observed when studying EMT in cell cultures. E-Cadherin is the key component of intercellular junction complexes, where it forms tight connections in between cells through their endodomains, while their intracellular domains bind to the actin microfilaments (Gumbiner, 2005). Cell-cell contacts formed by N-Cadherin, however, are much weaker (Lee et al., 2006a).

The action of RTKs has been found to play a central role in triggering EMT. Hepatocyte growth factor receptor (HGFR), together with its natural ligand hepatocyte growth factor/scatter factor (HGF/SF), was the first RTK proven to mediate EMT (Sonnenberg et al., 1993). EGF-mediated activation of EGFR has also been shown to induce EMT in epithelial breast cancer cells (Lee et al., 2006a). The postulated mode of EGFR-mediated EMT induction includes interaction of activated EGFR with the transcription factor STAT3 (signal transducer and activator of transcription 3) and subsequent shuttling into the nucleus (Lo et al., 2005). It has been reported earlier that EGFR may induce EMT through a STAT3-dependent mechanism, which causes a Liv1-mediated activation of the transcription factor Snail (Yamashita et al., 2004). Snail is a zinc finger transcription factor, which centrally controls the transcription of genes involved in EMT, including repression of E-Cadherin (Cano et al., 2000; Batle et al., 2000). Interestingly, recent reports point towards a role of EMT for determining response of cancer cell lines to treatment with EGFR-targeting TKIs. According to these examinations, cells that have undergone EMT are resistant to this regimen (Yauch et al., 2005; Thomson et al., 2005).

### ***1.3 EGFR-targeting cancer therapy***

Since cancer treatment via EGFR inhibition was suggested for the first time in the 1980's (Sato et al., 1983), a variety of EGFR-directed therapeutics have been developed and some of them already came into clinical use. These drugs belong to two major classes: monoclonal antibodies and tyrosine kinase inhibitors (TKIs). Currently, there are five EGFR-directed drugs, which are approved for cancer treatment: two TKIs and three antibodies. Clinically approved EGFR inhibitors usually show favourable tolerability with manageable adverse events and preclinical as well as clinical studies have shown beneficial anti-tumor effects in combination with radiation or chemotherapy. Moreover, innovative combination therapies targeting other oncogenic factors, such as mTOR (mammalian target of rapamycin) or VEGFR (vascular endothelial growth factor receptor) are currently in the focus of refined EGFR-directed therapy concepts (Adjei et al., 2006). A variety of other EGFR-directed drugs are currently in clinical phase II and III. These include reversible bi-specific EGFR/ErbB2 and EGFR/VEGFR inhibitors, as well as irreversible bi-specific EGFR/ErbB2 TKIs and additional EGFR-directed monoclonal

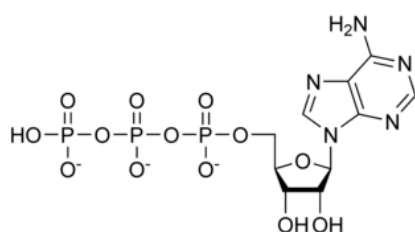
antibodies (Heymach et al., 2006). Common effects of EGFR inhibition include inhibition of cell proliferation, induction of apoptosis, delay in cell cycle progression, anti-angiogenic effects, inhibition of invasion and metastasis and sensitizing of tumors to chemotherapy or radiation (Normanno et al., 2003).

### 1.3.1 Tyrosine kinase inhibitors

TKIs are designed to fit into specific binding pockets of their target structures usually located close to the kinase domain, comprising amino acids of the ATP binding pocket of EGFR (Noble et al. 2004). Binding of the TKI to EGFR blocks its capacity for autophosphorylation and thereby inhibits activation. Due to their small size and formulation, TKIs can infiltrate tumors and enter into cells quite efficiently, where they display a direct and rapid onset of action.

Two EGFR-directed TKIs, gefitinib (ZD1839/Iressa from Astra Zeneca) and erlotinib (CP-358,774/Tarceva/OSI-774 from OSI Pharmaceuticals/Genentech/ Roche) have already been approved for clinical use in NSCLC after failure of standard treatment. Both are reversible, pharmacologically similar drugs (de Bono and Rowinsky, 2002; Laskin and Sandler, 2004).

**Adenosinetriphosphate**



**Gefitinib**

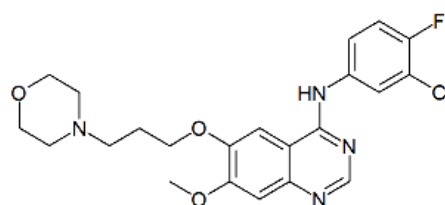


**Figure 8 Chemical structures of adenosinetriphosphate (ATP) and gefitinib.** Gefitinib (N-(3-chloro-4-fluorophenyl)-7-methoxy-6-(3-morpholin-4-ylpropoxy)quinazolin-4-amine) is a low molecular weight quinazolin derivate that functions as an ATP competitive inhibitor of the EGFR kinase.

Phase II studies further revealed single-agent activity of gefitinib in squamous cell carcinoma of head and neck (Cohen et al., 2003; Caponigro et al., 2004) and promising activity of gefitinib in colorectal cancer in combination with standard radio- or chemotherapy (Williams et al., 2004; Douglass et al., 2003). On the other hand,



phase II trials with gefitinib in breast cancer have been overall unsatisfactory (Baselga et al., 2004).

Even though gefitinib is quite specific for EGFR, dose-limiting side effects and occasionally severe complications (e.g. intestinal lung disease) are observed in the clinic (Dancey and Sausville, 2003; Cohen et al., 2004). Affinity chromatography with a gefitinib derivative and subsequent analyses of bound proteins by 2D gel electrophoresis revealed a number of cellular targets for this drug, in addition to EGFR ( $IC_{50} < 0,014 \mu M$ ). In vitro kinase assays determined low  $IC_{50}$  values of gefitinib e.g. for EphB4, BRK and Lyn ( $IC_{50} < 1 \mu M$ ), as well as medium activity of gefitinib against HGFR ( $IC_{50} = 3,2 \mu M$ ) (Brehmer et al., 2005). Together with the notion that gefitinib concentrations in breast tumors can be as high as 5 to  $25 \mu M$  (Baselga et al., 2002; Albanell et al., 2002; Ranson et al., 2002), this allows the conclusion that the observed side effects are not exclusively due to inhibition of EGFR. On the other hand, this facet could also yield chances for therapy since the effects against other tyrosine kinases might extend therapeutic utility of the drug.

### 1.3.2 EGFR-targeting monoclonal antibodies

In comparison to TKIs, monoclonal antibodies may elicit different modes of action, which include competition for ligand binding and induction of receptor internalization (Ono et al., 2006). Another important aspect of antibodies is their interaction with the host immune system that may for instance lead to complement-dependent (CDC) and antibody-dependent cellular cytotoxicity (ADCC) (Mellstedt, 2003). Further advantages of monoclonal antibodies over TKIs are their prolonged half-life (associated with decreased drug administrations) and low toxicities.

Three EGFR-directed antibodies are in clinical use: Cetuximab (C225/Erbitux from ImClone Systems/Bristol-Myers Squibb/Merck KGaA) is a 152kDa human-mouse chimeric anti-EGFR monoclonal antibody containing the human IgG1 constant region that is approved for the treatment of advanced colon rectal cancer (CRC) and squamous cell carcinoma of the head and neck (SCCHN) (Janmaat and Giaccone, 2003; Harding and Burtneess, 2005). Nimotuzumab (TheraCim/hR-3 from YM BioSciences/Oncoscience) is a humanized monoclonal antibody that was originally developed by a Cuban research institute and is clinically used in certain Asian and South American countries (Allan, 2005). Lastly, panitumumab (ABX-EGF/Vectibix from Abgenix/Amgen), a fully human anti-EGFR antibody generated using the

XenoMouse technology was approved by the FDA for the treatment of chemotherapy-resistant CRC (Davis et al., 1999).

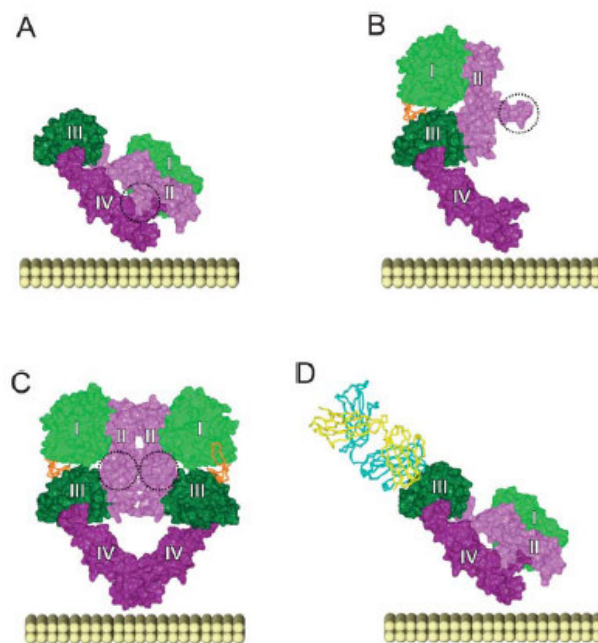


**Figure 9 Schematic illustration of EGFR in the EGF or cetuximab bound state.** Figure A shows the ectodomain of EGFR (domain I is colored in light green, domain II in light purple, domain III in dark green and domain IV in dark purple) in the autoinhibited (tethered) state (A). Figure B shows structure of the 1:1 EGF:EGFR ectodomain (dimerization-competent state; EGF is colored in orange) (B), while figure C displays the structure of the 2:2 EGF:EGFR ectodomain (dimerized, activated state) (C). Figure D shows the ectodomain of EGFR in the cetuximab bound state, where domain III of EGFR is tethered to the antibody causing receptor arrest in the autoinhibited state (the cetuximab Fab Cα light chain is colored in yellow and the Cα heavy chain is colored in cyan) (D) (from Hubbard, 2005).

Co-crystallization of the EGFR ectodomain with the antigen binding fragment (Fab) of cetuximab revealed that the antibody binds exclusively to domain III of the receptor. This epitope overlaps with the binding site of EGF, however, binding studies show that affinity of cetuximab to EGFR is 50 fold higher than the receptor's affinity to EGF. Through its mode of receptor binding, the antibody sterically inhibits juxtaposition of domains I and III and could thereby prevent a putative spontaneous (ligand independent) formation of the dimerization competent receptor conformation (Li et al., 2005b).

### **1.3.3 Mechanisms of cellular and clinical resistance and sensitivity to EGFR-directed cancer therapy**

Clinical resistance against monoclonal antibodies and TKIs is common and may either be intrinsic (primary resistance) or can be acquired during drug treatment (secondary resistance). An impressive examination of TKI resistance has been published for the Bcr-Abl (Breaking Cluster Region - Abelson Murine Leukemia) kinase in chronic myeloid leukemia (CML) where mutations conferring resistance to the Bcr-Abl-targeting TKI imatinib can arise during treatment, but may also be detected at low frequency in patients that had not received the drug before (Roche-Lestienne et al., 2002).

#### **1.3.3.1 Biomarkers for resistance to EGFR-directed cancer therapy**

Biomarkers are products of organisms that are indicative for the biological response of the organisms to drug exposure or other environmental conditions. Extensive efforts are made to identify tumor biomarkers that allow prognosis of response of cancer patients to EGFR-targeting drugs. Recently, a mechanism that may at least account for some cases of resistance to gefitinib was revealed in NSCLC patients. Clinical and laboratory examinations showed that an EGFR-T790M mutation, which confers resistance to gefitinib treatment, may occur additionally to EGFR kinase domain mutations L858R and deletion mutations of the LREA motive within the kinase domain of EGFR (Gow et al., 2005; Kobayashi et al., 2005, Pao et al., 2005a). The presence of this particular resistance conferring mutation in NSCLC patients appears to be independent from TKI treatment, but subpopulations of tumor cells expressing this EGFR variant might be enriched during the TKI regimen (Toyooka et al., 2005, Inukai et al., 2006). Yet, cetuximab treatment of mouse xenografts carrying subcutaneously transplanted cells that endogenously express EGFR-L858R-T790M causes marked tumor regression, while gefitinib treatment had only marginal effects (Perez-Torres et al., 2006). In contrast, cell lines expressing the EGFRvIII mutation are rather growth resistant against treatment with gefitinib (Learn et al., 2004) and cetuximab (Li et al. 2007).

Another, principal cause for resistance to EGFR-directed therapy - concerning TKIs and therapeutic antibodies - is aberrant activation or overexpression of other RTKs. Since cancerogenesis generally involves genetic alteration of various factors, it is unlikely that inhibition of a single oncogene like EGFR will lead to a complete stasis

or death of tumor cells. Constitutive activation or amplification of e.g. insulin-like growth factor-1 receptor (IGF1R) (Laban et al., 2003), HGFR (Ma et al. 2003; Christensen, et al. 2005) or FGFR family members (Adhane et al., 1991) is common in various cancers and might compensate for blockage of EGFR. Exemplarily, it was observed that a breast cancer cell line with sensitivity to the ErbB2-targeting antibody herceptin was rendered resistant to this drug by transfection with IGF1R (Lu et al., 2001). Furthermore, the ligands FGF and IGF1 were found to block the inhibitory effects of cetuximab on cellular survival and activation of downstream signaling in colon cancer and glioblastoma cell lines (Liu et al., 2001; Chakravarti et al., 2002).

Since EGFR-directed drugs act at an early point of the signal transduction cascade, they cannot affect tumorigenic alterations in downstream signaling pathways. Inhibition of EGFR-mediated signaling through PI3K/Akt and Ras/Raf/MEK/MAPK pathways is thought to be crucial for sensitivity to EGFR-targeting tumor drugs. Tumorigenic activation of the Ras/Raf/MAPK pathway may be responsible for causing resistance to EGFR-directed therapy. Gain-of-function mutations of KRAS are described in various cancers, including NSCLC and may confer resistance to EGFR-targeting TKIs (Pao et al., 2005b). By the same token, persistent activation of PI3K/Akt signaling paralleled by cellular resistance to gefitinib can be caused by loss of the phosphatase PTEN (phosphatase and tensin homolog), a negative regulator of PI3K (She et al., 2003; Bianco et al., 2003). Amplification of PI3K or Akt expression (Robertson, 2005), as well as growth advantage conferring genetic alterations in the PI3KCA gene (Samuels et al., 2004) might also cause a clinically relevant activation of the pathway.

### **1.3.3.2 Biomarkers for sensitivity to EGFR-directed cancer therapy**

Facing the multitude of putative and known mechanisms leading to resistance against EGFR-directed tumor therapy, the question if there are any factors, which alone allow a robust prediction of response to this regimen is at hand. Such biomarkers for sensitivity can either be dominant over certain resistance causing alterations discussed above, or they can be subordinate to them, gaining relevance in absence of resistance conferring factors. This scenario makes it practically very difficult to decipher the relative value of putative biomarkers for sensitivity. As discussed in section 1.2.3, EGFR kinase domain mutations appear to be a rare

exception in biomarker research, for they represent one of the few quite dominant sensitivity markers known.

EGFR gene amplification has been positively correlated with tumor response to TKI regimen (Takano et al., 2005; Cappuzzo et al., 2005). However it is not clear whether this translates to increased EGFR protein levels detectable by immunohistochemistry (IHC) (Hirsch et al., 2006). A similar picture arises for cetuximab, where EGFR expression assessed by IHC did not correlate with response to the antibody in colorectal cancer (Saltz et al., 2004; Cunningham et al., 2004); however amplification of gene copy number as assessed by FISH (fluorescence in-situ hybridization) did (Moroni et al., 2005).

Conflicting results exist also for the relevance of high levels of phosphorylated Akt or STAT3/5 for predicting gefitinib sensitivity in patients. Most probably this depends on the simultaneous activation of EGFR in the same tissue, indicating dependence of these downstream signaling components on a paralleled EGFR phosphorylation (Cappuzzo et al., 2004; Haura et al., 2005). High expression of ErbB2, ErbB3 or ErbB ligands was also postulated to be predictive for gefitinib response. However forced expression of e.g. ErbB3 in gefitinib-resistant cells did not render them sensitive, indicating that this candidate is only of subordinate value for response prediction (Amann et al., 2005; Engelman et al., 2005).

Whole genome expression profiling analyses was used to compare candidate gene expression in gefitinib sensitive and resistant cell lines. Detection of differential expression patterns within sensitive or resistant groups may thus reveal biomarkers for response prognosis. Microarray profiling of a panel of NSCLC cells independently identified increased ErbB3, E-cadherin and tumor-associated calcium signal transducer 2 (TACSTD2) levels as potential indicators for cellular response to gefitinib (Coldren et al., 2006). Another expression analyses with tumor samples from gefitinib-treated NSCLC patients identified amphiregulin (AREG) as a potential biomarker expressed high in non-responders to this TKI (Kakiuchi et al., 2004). Another study from Yauch and colleagues also found E-Cadherin expression as a marker for sensitivity for erlotinib (Yauch et al., 2005). A proteomics study on two colorectal cancer cell lines with variable responses towards cetuximab has been published where different patterns of proteins primarily associated with metabolic functions have been identified (Skvortsov et al., 2004).

### 1.3.3.3 Cellular resistance models

Systematic laboratory studies to approach the problem of relapse of cancer patients that first responded efficiently to EGFR inhibitor therapy are rare. To address this problem, *in vitro* experiments have been conducted with primary sensitive cancer cell lines, which were made resistant against a specific drug by long-term exposure and dose escalation. Various cellular alterations that might be responsible for resistance of these cells towards the therapeutic have been identified by comparisons with untreated cells of the same origin and similar passage number.

The first such approach was performed with erlotinib, applying the human squamous cancer cell lines HN5 and A431, which are sensitive to EGFR-targeting drugs. Erlotinib-resistant cells expressed significantly lower levels of EGFR than medium-treated control cells. Furthermore, total levels and activation of Akt was increased and mRNA expression analyses revealed up-regulation of FGFR, PDGFR (platelet-derived growth factor receptor) and fibronectin levels (Perez-Soler et al., 2003)

Equivalent approaches with gefitinib were undertaken with different NSCLC cell lines that carry EGFR kinase domain mutations that sensitize cells to gefitinib or erlotinib treatment. The changes observed in resistant cells include: increased ligand-induced internalization of EGFR, down regulation of EGFR expression, loss of the EGFR kinase domain mutation, gain of the resistance conferring EGFR-T790M mutation, decreased EGFR-dependent Akt/NF $\kappa$ B signaling, loss of PTEN, as well as increased activation of Akt and increased sensitivity towards TNF $\alpha$  induced apoptosis (Kwak et al., 2005; Ando et al., 2005; Kokubo et al., 2005; Engelman et al., 2006).

Two studies focusing on a long-term exposure of cells to EGFR-targeting therapeutic antibodies have been published so far. In one study, two pancreatic carcinoma cells with either primary sensitivity or resistance to cetuximab were exposed to the drug for 6 weeks under cell culture conditions. A relative decrease of EGFR surface levels as well as an up-regulation of the pro-apoptotic protein BAX (BCL2-associated X protein) (as compared to untreated control) was seen for the sensitive but not for the resistant cell lines. Interestingly transactivation of EGFR through FGF in the presence of cetuximab was observed for the primary resistant, but not for the sensitive cell lines (Huang et al., 2003). The latter finding could be indicative for a compensatory activation of FGFR upon EGFR blockage in pancreas carcinoma as possible mode of resistance to cetuximab (Liu et al., 2001).

In another study, cetuximab-resistant A431 cells from relapsed xenograft tumors were isolated after 280 days of treatment with the antibody. Interestingly, total EGFR expression was unaltered and long-term-treated cells retained normal in vitro sensitivity to cetuximab as compared to the parental cell line. Yet, cells isolated from the relapsed xenograft showed increased in vivo resistance to cetuximab and expressed increased levels of VEGF (vascular endothelial growth factor), paralleled with higher levels of angiogenesis in vivo (Viloria-Petit et al., 2001).

#### **1.4 Aim of this study**

The aim of this study was to investigate the action of EGFR-targeting compounds, exemplified by the TKI gefitinib and the monoclonal antibody cetuximab in cellular model systems. The ultimate goal of the work was to identify possible modes of sensitivity and resistance of model cell lines to these two classes of EGFR-specific cancer drugs.

One approach utilized stably transfected cells or NSCLC cell lines endogenously expressing EGFR kinase domain mutations. The first model aimed to study the impact of EGFR mutations have on gefitinib or cetuximab therapy in a cellular system with a consistent genetic background. Furthermore, a panel of NSCLC cell lines was characterized in order to study the relevance of factors suggested to be involved in determining sensitivity or resistance to EGFR-targeting compounds. In addition, expression profiling of NSCLC cells was performed to identify novel candidate genes predictive for cellular response to gefitinib or cetuximab.

In another approach, a panel of cancer cell lines was long-term exposed to gefitinib or cetuximab in order to monitor cellular alterations and to identify cellular factors that confer resistance to cancer cells upon treatment with these therapeutics. Two primary sensitive and two cell lines with primary resistance to EGFR-targeting therapeutics included in this examination were characterized in terms of sensitivity to cetuximab and gefitinib. Furthermore, a primary sensitive cell line was examined in detail in regard to the biological and molecular alterations conferred by long-term treatments. Finally, a candidate based expression analyses was carried out to identify genes that are differentially expressed in primary sensitive and resistant cell lines after long-term cultivation.

## 2. Material and Methods

### 2.1 *Material*

#### 2.1.1 Laboratory instruments

Agarose gel chambers (Mini-/ Wide Mini- SUB Cell - GT)	BioRad
Bacteria shaking incubator	New Brunswick
Bioanalyzer (3100)	Applied Biosystems
Blotting chamber	BioRad
Cell counting chamber (Neubauer chamber)	Zeiss
Cell culture incubator	Heraeus
Centrifuges, table (5417R)	Eppendorf
Centrifuge, cell culture (Omnifuge 2.0 RS)	Haereus
Centrifuge, laboratory (RC5C)	Sorvall
DNA Sequencer (3100 Genetic Analyser)	Applied Biosystems
Electronic Pipet (Accujet)	Brand
Heating thermostat	Haereus
Immunoblot documentation system (Versa Doc™)	BioRad
Laboratory shaker (ST5)	Hecht-Assistent
Light microscope (Axiovert 25, AxioStar Plus)	Zeiss
Magnet stirrer (MR3001K)	Heidolph
Microwave	Neff
Multipette	Eppendorf
Nanodrop	Peqlab
PCR apparatus (Gene Amp PCR System 9700)	Applied Biosystems
pH-meter (pH211)	Hanna
Pipettes (Reference)	Eppendorf
Plate reader spectroscope (Mithras LB940)	Berthold
Power supply, agarose gels (EPS601)	Amersham Pharmacia
Power supply, SDS-PAGE (Power Pac 200)	BioRad
Precellys apparatus	Peqlab
Precision balances	Mettler
	Satorius
Real-time PCR system (ABI Prism 7900 HT)	Perkin Elmer



Sonification ultrasound-homogenizator (HD2070)	Bandelin
SDS-PAGE chambers (Criterion)	BioRad
UV documentation system	Syngene
Vortex apparatus (VFC)	Janke & Kunkel
Water treatment apparatus (Mili Q UF plus)	Milipore

### 2.1.2 Software

Agarose gel documentation (GeneSnap™)	Syngene
Cell Quest™, FACSComp™	Becton Dickinson
Design of oligonucleotides (PrimerSelect™)	DNASTAR
DNA/protein sequence analyses (EditSeq™, MegAlign™, SeqMan™II)	DNASTAR
Immunoblot documentation (Quantity One®)	BioRad
Pharmacology data processing (GraphPad Prism®)	Graph Pad
Plate reader spectrometer software (MicroWin 2000™)	Berthold
SDS 2.1 real time data analyses software	Applied Biosystems
Text processing, data processing and graphic software	Microsoft Office

### 2.1.3 Laboratory chemicals

Acetic acid	Merck
Agar-agar	Merck
Agarose	Invitrogen
Ampicilin	Applichem
Aprotonin	Sigma-Aldrich
Bovine serum albumin (BSA), fraction V	Applichem
Bromphenol blue	Merck
Calcium chloride	Merck
Di-sodium hydrogen phosphate	Merck
DMSO	Applichem
dNTP mix (10mM ea. dNTP)	New England Biolabs
Ethanol	Merck
Ethidium bromide	Sigma-Aldrich
Glycin	Merck
Isopropanol	Merck

---

Kanamycin	Applichem
Lipofectamine <sup>TM</sup> 2000 reagent	Invitrogen
Loading dye solution for nucleotides (6x)	Fermentas
LumiLight Western blotting substrate	Roche
Magnesiumchloride-hexahydrate	Merck
Methanol	Merck
Mercaptoethanol	Merck
Nonidet P40	Roche
Nuclease-free water	Promega
Peptone (from Casein pancreatic digestion)	Merck
Phosphatase inhibitor cocktail set II	Calbiochem
Ponceau S	Merck
Protease inhibitor cocktail set III	Calbiochem
Potassiumchlorid-dihydrate	Merck
Propidium Iodide	Molecular Probes
S.O.C.S. medium	Invitrogen
Sodium acide	Merck
Sodium acetate	Merck
Sodium chloride	Merck
Sodium dihydrogenphosphate	Merck
Sodium dodecylsulfate (SDS)	Sigma-Aldrich
Starting Block <sup>TM</sup> (PBS) buffer	Pierce
TAE buffer (50x)	Invitrogen
Tris	Merck
Triton X-100	Merck
Tween-20	Merck
XT MOPS running buffer (20x)	BioRad
XT reducing agent (20x)	BioRad
XT sample buffer (4x)	BioRad
Yeast extract	Applichem
Zeocin	Invitrogen

### 2.1.4 Consumables

7900 HT Micro Fluidic Card (Real Time PCR; LDA)	Applied Biosystems
Acrodiscs® PF syringe filter (Supor membrane)	Pall
Blotting fiber pads	BioRad
Blotting sandwiches (nitrocellulose membrane)	BioRad
Cell culture dishes, plates & flasks (Nuncleon™ Surface)	NUNC
FACS tubes	Becton Dickinson
Laboratory tubes (15ml/ 50ml)	Becton Dickinson
Multipette CombiTips	Eppendorf
PCR tubes, MicroAmp® tubes (Real Time PCR; LDA)	Applied Biosystems
PCR tubes, standard	Biozyme
Petridishes for microbiology	Greiner
Pipett tips	Eppendorf
Plastic pipettes	Costar
Precellys ceramic bead columns (1,4mm beads)	PeqLab
Reaction tubes (1,5ml/ 2ml)	Eppendorf
RNAeasy solution	Invitrogen
RNAse-free pipett tips (Safeseal Premium)	Biozyme
Sterile filtration units (SFCA)	Nalgene
Steriflip® sterile filtration units (ExpressPlus membrane)	Milipore
Syringes for sterile filtration	Terumo

### 2.1.5 Enzymes

Anarctic phosphatase (5U/μl)	New England Biolabs
DNA-polymerase I (Klenow) (5U/μl)	New England Biolabs
Pwo polymerase (1U/μl)	PeqLab
Restriction enzymes (listed in section 2.2.1.7.1)	New England Biolabs
T4-DNA-ligase (400U/μl)	New England Biolabs

### 2.1.6 Antibodies

#### Primary Antibodies

Antigen	Dilution	Source	Catalog number	Supplier
Cofilin	1:500 in TBST/BSA	rabbit	#3312	Cell Signaling
E-Cadherin (clone 67A4)	1:200 in TBST/Skim Milk	rabbit	#SC-21791	Santa Cruz
EGFR (clone 1005)	1:250 in TBST/Starting Block	rabbit	#SC-03	Santa Cruz
EGFR, PE-labeled	10mg/ml	rat	#MCA 1784-PE	Serotec
ErbB2 (clone 44E7)	1:500 in TBST/Starting Block	mouse	#2248	Cell Signaling
ErbB3 (clone 66219)	1:500 in TBST/BSA	mouse	#Mab-348	R&D Systems
ErbB4	1:200 in TBST/BSA	rabbit	#SC-283	Santa Cruz
HGFR	1:500 in TBST/BSA	rabbit	#SC-161	Santa Cruz
N-Cadherin (clone 13A9)	1:750 in TBST/Skim Milk	mouse	#05-915	Upstate
Phospho-Akt (Ser473)	1:750 in TBST/Starting Block	rabbit	#9271	Cell Signaling
Phospho-EGFR (Tyr1068)	1:1000 in TBST/BSA	rabbit	#2234	Upstate
Phospho-MAPK (Ser217/Ser221)	1:1000 in TBST/BSA	rabbit	#9122	Cell Signaling
Phospho-HGFR (Tyr1234/Tyr1235)	1:150 in TBST/BSA	rabbit	#3126	Cell Signaling
Vimentin (clone LN6)	1:200 in TBST/Starting Block	mouse	#IF01	Calbiochem

#### Secondary Antibodies

Mouse-IgG	1:2000	horse	#7076	Cell Signaling
Rabbit-IgG	1:2000	goat	#7074	Cell Signaling
Mouse-IgG - FITC	10µg/ml	goat	#349031	Becton- Dickinson

### 2.1.7 “Kits”

BigDye® Terminator v3.1 cycle sequencing kit	Applied Biosystems
First strand cDNA synthesis kit for RT-PCR	Roche
HiSpeed plasmid Maxi kit	Quiagen
Jetquick gel extraction spin kit	Genomed
One cycle target labeling assay	Affymetrix
Plasmid mini purification kit	Quiagen
Proteome Profiler™ array (Human phospho-RTK array kit)	R&D Systems
Quik Change® II XL site-directed mutagenesis kit	Stratagene
RNeasy® Mini kit	Quiagen
Sigma Spin™ Post reaction clean up columns	Sigma
Spectral calibration reagent kit	Applied Biosystems
TaqMan® Universal PCR master mix	Applied Biosystems

### 2.1.8 Vectors and oligonucleotides

#### 2.1.8.1 Oligonucleotides

All oligonucleotides were purchased from Operon Biotechnologies.

##### 1) Oligonucleotides for site-specific mutagenesis:

###### **EGFR\_T790M\_fdw**

GTG CAA CTC ATC ATG CAG CTC ATG CCC

###### **EGFR\_T790M\_rev**

GGG CAT GAG CTG CAT GAT GAG TTG CAC

##### 2) Oligonucleotides for EGFR sequencing:

###### **cEGFRS4**

CAA CAT GTC GAT GGA CTT CCA

###### **cEGFRS5**

GCA AAG TGT GTA ACG GAA TAG G

###### **cEGFRS6**

GTG AAA ACA GCT GCA AGG CC

###### **cEGFRS7**

GCC TAA GAT CCC GTC CAT CG

**cEGFRS8**

AAT CCT CGA TGA AGC CTA CG

**cEGFRS9**

AGA GTG ATG TCT GGA GCT ACG GGG TGA C

**cEGFRS10**

CCA GCG CTA CCT TGT CAT TC

**cEGFRAS2**

GGC AGT TCT CCT CTC CTG C

**cEGFRAS3**

CTG TGG ATC CAG AGG AGG AGT AT

**cEGFRAS5**

AGA GTT CTC CAC AAA CTC CC

**cEGFRAS6**

TTC GCA TGA AGA GGC CGA TCC

**cEGFRAS7**

CCA GTT GAG CAG GTA CTG GGA

**cEGFRAS8**

GGG TTC AGA GGC TGA TTG TGA T

**2.1.8.2 Starting vectors**

<b>Vector name/designation</b>	<b>cloned by person/ sold by company</b>
EGFR-pcDNA3.1/v5-His	Pia Stroh, Merck KGaA
EGFR-del747-753-pcDNA3.1/v5-His	Yvonne Wilhelm, Merck KGaA
EGFR-L858R-pcDNA3.1/v5-His	Yvonne Wilhelm, Merck KGaA
pEF5/FRT/v5-D-TOPO® (Cat.# K6035-01)	Invitrogen
pcDNA3.1/v5-His® TOPO® (Cat.# K4800-01)	Invitrogen

**2.1.8.3 Vectors constructed in this work****EGFR- pEF5/FRT/v5**

EGFR was cut out via KpnI/PmeI restriction site from EGFR-pcDNA3.1/v5-His and was cloned via KpnI/EcoRV restriction sites into to the pEF5/FRT/v5 vector plasmid.

**EGFR-L858R - pEF5/FRT/v5**

EGFR-L858R was cut out via KpnI/PmeI restriction site from EGFR-pcDNA3.1/v5-His and was cloned via KpnI/EcoRV restriction sites into to the pEF5/FRT/v5 vector plasmid.

**EGFR-del747-753 - pEF5/FRT/v5**

EGFR- del747-753 was cut out via KpnI/PmeI restriction site from EGFR-pcDNA3.1/v5-His and was cloned via KpnI/EcoRV restriction sites into to the pEF5/FRT/v5 vector plasmid.

**EGFR-del747-753/T790M - pEF5/FRT/v5**

Amino acid exchange mutation T790M was introduced into EGFR-del747-753 - pEF5/FRT/v5 plasmid by the Quick Change<sup>®</sup> II XL site directed mutagenesis kit under use of oligonucleotide primers EGFR\_T790M\_fdw and EGFR\_T790M\_rev.

**EGFR-L858R/T790M - pEF5/FRT/v5**

Amino acid exchange mutation T790M was introduced into EGFR-L858R - pEF5/FRT/v5 plasmid by the Quick Change<sup>®</sup> II XL site-directed mutagenesis kit under use of oligonucleotide primers EGFR\_T790M\_fdw and EGFR\_T790M\_rev.

All constructs were validated via DNA sequencing (sequencing primers are noted in section 2.1.8.1).

**2.1.9 DNA- and protein size standards**

1kb Plus DNA ladder	Invitrogen
MagicMark <sup>®</sup> XP Western standard	Invitrogen
SeeBlue <sup>®</sup> Plus2 prestained protein standard	Invitrogen

### 2.1.10 Media and buffers

**Acid stripping solution**

NaCl	0,5M
Acetic acid	0,2M

Filled up with sterile MiliQ water and adjusted pH 2,8

**Basal agar, soft-agar assay**

Agar-agar	1,0% (w/v)
-----------	------------

Filled up with sterile water, autoclaved

**Blocking buffer, immunoblot**

Bovine serum albumine (BSA)	5% (w/v)
-----------------------------	----------

Filled up with TBST

**LB agar**

LB medium

Agar-agar	1,5% (w/v)
-----------	------------

Filled up with sterile water, autoclaved

**LB medium**

Peptone (trypsin digested)	1% (w/v)
Yeast extract	0,5% (w/v)
NaCl	0,5% (w/v)

Filled up with sterile water, autoclaved



**Lysis buffer, Laemmli**

Glycerol	192mM
SDS	0,1% (v/w)
Tris, pH 6,8	25mM
Bromphenol blue	0,005% (v/w)

Filled up with sterile MiliQ water

*Added freshly:*

XT reducing agent (20x)	5% (v/w)
Phosphate inhibitor mix (100x)	1% (v/w)
Protease inhibitor mix (100x)	1% (v/w)

**Lysis buffer, RIPA (4x)**

NaCl	600 mM
Tris, pH 7,4	200 mM
Nonidet P-40	4% (w/v)
SDS	2% (w/v)
EGTA	4mM

Filled up with sterile MiliQ water

*Diluted with water and added freshly:*

XT reducing agent (20x)	5% (v/w)
Phosphate inhibitor mix (100x)	1% (v/w)
Protease inhibitor mix (100x)	1% (v/w)

**MEM medium (2x), soft-agar assays**

Fetal calf serum (FCS)	20% (v/v)
L-glutamine (200mM)	2% (v/v)
Sodium pyruvate (100mM)	2% (v/v)
Sodium bicarbonate (7,5%)	6% (v/v)

Filled up with sterile MiliQ water

**Ponceau staining solution**

Ponceau S	0,25% (w/v)
Acetic acid	10% (v/v)
Filled up with MiliQ water	

**TBST**

TBS (20x)	5% (v/v)
Tween-20 (20%)	0,25% (v/v)
Filled up with MiliQ water	

**Top agar, soft-agar assay**

Agar-agar	0,8% (w/v)
Filled up with sterile water, autoclaved, stored at 4 °C	

**Transfer buffer, Electroblothing**

Tris, pH 8,3	12mM
Glycine	96mM
Methanol	20% (v/v)
Filled up with MiliQ water, adjusted to pH 8,0	

**Tris-buffered saline (TBS), 20x**

Tris, pH 7,4	500mM
NaCl	3M
Filled up with MiliQ water and adjusted to pH 7,4	

**Wash buffer, FACS**

BSA	1% (w/v)
Sodium azid	0,03% (w/v)
Filled up with TBST	

**Wash buffer, immunoblot**

BSA 1% (w/v)

Filled up with TBST

**2.1.11 Cell culture media and supplements**

Mammalian cell lines were cultured in specific medium as designated in section 2.1.13. All cell cultivation media were purchased from GIBCO. Human cancer cell lines were treated long term with cetuximab or gefitinib in medium supplemented with FCS purchased from Pan Biotech and tested in cell culture before use.

Cell dissociation solution (1x)	Sigma
EDTA-Trypsine (2,5%)	Invitrogen
Hygromycin (50mg/ml)	Invitrogen
L-glutamine (200nM)	Invitrogen
MEM alpha powder	Invitrogen
Sodium pyruvate (200nM)	Invitrogen
Sodium bicarbonate (200nM)	Invitrogen

**2.1.12 Growth factors and cancer therapeutics**

Cetuximab (Erbitux)	Merck
Gefitinib (Iressa)	Astra Zeneca
Matuzumab (EMD72000), FITC labeled	Merck (labeled by Mr. Jürgen Schmidt, TA Oncology)
Paclitaxel	Sigma
EGF, human recombinant	Upstate
HGF	R&D Systems
<sup>125</sup> I-Cetuximab	Merck (labeled by Biotrend)
PMA (phorbol 12-myristate 13-acetate)	Calbiochem
TNF $\alpha$	R&D Systems

**2.1.13 Bacterial strains**

DH5 $\alpha$ , chemically competent (transformation)                      Invitrogen  
 XL Blue, chemically competent (site-directed mutagenesis)      Stratagene

**2.1.14 Mammalian cell lines**

<u>A431</u> (ATCC Cat.# CRL-1555)	
DMEM + 10% FCS	Humane epidermoid cancer cell line

<u>A549</u> (ATCC Cat. # CCL-185) <u>Calu-3</u> (ATCC Cat. # HTB-55) <u>Calu-6</u> (ATCC Cat. # HTB-56) <u>H1650</u> (ATCC Cat. # CRL-5853) <u>H1781</u> (ATCC Cat. #CRL-5894) <u>H1975</u> (ATCC Cat. #CRL-5908) <u>H292</u> (ATCC Cat. #CRL-1848) <u>H322</u> (Dr. Christa Burger, Merck) <u>H4006</u> (kind gift from Dr. Jon Kurie, MD Anderson Cancer Center, Houston, USA) <u>H460</u> (ATCC Cat. # HTB-177) <u>HCC2279</u> (kind gift from Dr. Jon Kurie, MD Anderson Cancer Center, Houston, USA) <u>HCC-827</u> (ATCC Cat. #CRL-2868)	
RPMI + 10% FCS + 2mM L-glutamine + 1mM sodium pyruvate	Human NSCLC cell lines

<u>Difi</u> (Dr. Christa Burger, Merck)	
DMEM/F12 (1:1) + 10% FCS	Human colorectal cancer cell line

<u>Hela</u> (Dr. Christa Burger, Merck)	
DMEM + 10% FCS	Human cervical cancer cell line

<u>MCF-7</u> (ATCC Cat.# HTB-22)	
DMEM + 10% FCS	Human breast cancer cell line

<u>MDA-MB-231</u> (ATCC Cat.# HTB-26)	Human breast cancer cell line
DMEM + 10% FCS	

<u>NIH3T3</u> (Cat.# F-2900, Invitrogen)	
DMEM + 10% FCS + 100µg/ml zeocin	Murine embryonic fibroblast cell line

<u>NIH3T3</u>	
stably transfected with EGFR variants (see section 2.2.2.5)	
DMEM + 10% FCS + 200µg/ml hygromycin	Murine embryonic fibroblast cell line

<u>SCOV-3</u> (Dr. Christa Burger, Merck)	
DMEM + 10% FCS	Human ovarian cancer cell line

<u>SW707</u> (Dr. Christa Burger, Merck)	
DMEM + 10% FCS	Human colorectal cancer cell line

## 2.2 Methods

### 2.2.1 Methods in molecular biology

#### 2.2.1.1 Introduction of plasmid DNA into bacteria

Bacterial plasmid DNA was introduced into an *E. coli* strain via transformation of commercially available competent cells. Aliquots (50µl) of chemically competent *E.coli* DH5α (Invitrogen) were thawed on ice and then incubated with 10-50ng plasmid DNA. After 15 min incubation on ice, cells were subjected to a 1-minute heat shock at 42°C and directly chilled on ice for 5 min. A volume of 200µl SOCS medium was added to the 1,5ml tube, which was then incubated at 37°C for 40 min. When the plasmid DNA was for re-transformation, a volume of 50µl cell suspension was plated on LB-agar dishes containing the respective selection antibiotic (50µg/ml for ampicillin and kanamycin, 40µg/ml for zeocin). When plasmid DNA was from a ligation reaction, one volume of 50µl and one volume of 200µl were plated on the respective LB-agar dishes. Agar plates were incubated overnight at 37°C.

### 2.2.1.2 Plasmid preparation from bacteria

Overnight cultures of *E. coli* cells carrying the plasmid of choice were inoculated with one colony from an agar plate transferred in flasks containing LB-medium and a selective antibiotic. The cell suspension was centrifuged and the bacterial plasmid DNA was isolated from the pellet with a kit according to the recommendations in the manufacturers manual (HiSpeed Plasmid Maxi kit or Mini Preparation kit).

### 2.2.1.3 Agarose gel electrophoresis

Nucleic acids were fractionated by size through horizontal agarose gel electrophoresis. This method has been used to analyse and purify specific DNA molecules from total DNA and RNA in a complex mixture. Agarose gels (containing 0,7-1,5% agarose) were poured after mixing agarose with TAE buffer, heating in a microwave and addition of ethidium bromide (0,01%). After solidification of the gel, samples were mixed with 1/5-volume loading buffer (5x) and loaded into the respective wells. A current of 100 Volt was applied for 20-100 min. After completion of the run, DNA was visualized under UV light, photos were taken and documented with an integrated gel documentation system (Syngene). The size and mass of specific DNA molecules was estimated by the usage of size markers separated on gel in parallel to the loaded samples.

### 2.2.1.4 Elution of plasmid DNA from agarose gels

Specific DNA molecules were cut out from the agarose gel and subsequently purified from agarose by the help of a kit (Jetquick Gel Extraction Spin kit). Agarose slices were transferred to 1,5ml tubes and DNA was purified according to the manufacturers guidelines in the manual.

### 2.2.1.5 Nucleic acid quantification and determination of purification quality

The exact quantification and quality determination of isolated DNA and RNA was performed by UV/Vis spectroscopy with a Nano-Drop 1000 UV/Vis spectrometer (Nanodrop). This apparatus measures the absorption at 260nm (for the nucleic acid content) and 280nm (for the protein content) in the test solution. The ratio ( $r$ ) 260nm/280nm is therefore indicative of the purity of the sample, with  $1,8 < r < 2$  as the optimal range. The concentrations of nucleic acids can be determined according to

their  $OD_{260nm}$ , where an  $OD_{260nm}=1$  correlates to 50 $\mu$ g/ml double-strand DNA and 40 $\mu$ g/ml RNA, respectively. For RNA isolations, integrity of RNA molecules was tested determining the ratio of 28S and 18S RNA by the help of a kit (mRNA Pico Kit) and analyses via a spectrometer (Bioanalyzer 3100). Intact RNA has a 28S/18S RNA ratio of 2,0 and here ratios between 1,8 and 2,0 were considered as acceptable.

#### 2.2.1.6 Polymerase chain reaction (PCR)

PCR allows the rapid amplification of specific DNA fragments from complex mixtures of DNA molecules. The applications of the PCR are numerous, since it has been refined and can be used for various methods that base on the classical PCR technique. The methods used in this work that relate to the classical PCR reactions include the detection of DNA fragments in biological isolates, directed mutagenesis and quantitative real-time PCR.

The reaction mixture for DNA fragment detection is:

- 1 $\mu$ l template DNA (10-20ng)
- 5 $\mu$ l buffer (10x)
- 1 $\mu$ l dNTP mixture (10mM ea.)
- 0,5 $\mu$ l oligonucleotide I (100 $\mu$ M)
- 0,5 $\mu$ l oligonucleotide II (100 $\mu$ M)
- 1 $\mu$ l Pwo polymerase (1U/ $\mu$ l)

The employed PCR program was dependent on the length of the template fragment, on the used oligonucleotides and on the purpose of the PCR reaction. This is reflected by variable elongation times and variable annealing temperatures. The variable annealing temperatures for the oligonucleotides are indicted in the material section of this work. The variable elongation times are dependent on the length of the fragment to be amplified. An elongation time of 1 min per 1kb template was calculated for reactions with the proofreading Pwo DNA-polymerase. The terminating elongation step was run for the cycle elongation time multiplied by four. Steps 2) to 4) were repeated over 30 cycles.

The standard protocol used for the PCR reaction was:

- 1) 2 min at 95 °C (initial denaturation)
- 2) 45 sec at 95 °C (denaturation)
- 3) 30 sec at variable temperature [60 °C to 68 °C] (annealing)
- 4) Variable time [30 sec to 4 min] at 72 °C (elongation)
- 5) Variable time [2 to 16 min] at 72 °C (terminating elongation)

### 2.2.1.7 Automated fluorescence DNA sequencing

For the determination of the sequence of defined stretches of DNA molecules, an automated fluorescence DNA-sequencing reaction, which emerges from the Sanger DNA sequencing method, has been used (Sanger et al., 1977). A PCR reaction with the DNA template of interest and a single primer is performed with a high molar amount of desoxynucleotides and a low molar amount of fluorescence tagged dideoxynucleotides (using different dyes for each of the four nucleotides). The catalyzed integration of dideoxynucleotides into the amplified DNA molecules leads to termination of the amplification reaction, which causes the generation of a heterogeneous mixture of DNA molecules with different lengths. These are separated via a capillary electrophoresis and subsequently the fluorescence tags can be detected with a laser, which allows the identification of the DNA sequence over length of approximately 400 nucleotides.

The PCR reaction has been performed with the following reaction mixture:

- |      |  |
|------|--|
| 1µl  | DNA (c.a. 20ng)  |
| 1µl  | oligonucleotide primer (5pmol) (see section 2.1.8.1 for sequences) |
| 2µl  | reaction buffer (5x)   |
| 4µl  | Big Dye reaction mix (includes dNTPs, ddNTPs, Ampli-Taq FS)        |
| 12µl | nuclease-free water  |

The reaction was performed with the following PCR protocol (25 cycles):

- |                 |
|-----------------|
| 10 sec at 96 °C |
| 10 sec at 62 °C |
| 4 min at 60 °C  |



### 2.2.1.8 Enzymatic manipulation of DNA

#### 2.2.1.8.1 Restriction digestion of plasmid DNA

Enzymatic digestion of purified DNA molecules was performed with specific restriction enzymes under optimal temperature and buffer conditions, as indicated in the following table. All restriction enzymes and buffers were received from New England Biolabs.

Restriction enzyme	Reaction buffer	Temperature optimum
EcoRV	3	37 °C
KpnI	1	37 °C
PmeI	4	37 °C
KpnI/EcoRV	2	37 °C
KpnI/PmeI	2	37 °C

Different reaction conditions were used for analytic (reaction time: 2 h) or preparative digestions (reaction time: overnight).

Reaction mixture (total volume 20µl) for analytic digestions:

- 1µl DNA (50-200 ng)
- 2µl reaction buffer (10x)
- 0,5µl restriction enzyme I
- (0,5µl restriction enzyme II - optional)
- 16,5µl (16,0µl) nuclease-free water

Reaction mixture (total volume 50µl) for preparative digestions:

- 2µl DNA (1-2 µg)
- 5µl reaction buffer (10x)
- 1,5µl restriction enzyme I
- (1,5µl restriction enzyme II - optional)
- 41,5µl (40,0µl) nuclease-free water

#### 2.2.1.8.2 Dephosphorylation of vector DNA at 5' strand ends

Target vector DNA was enzymatically dephosphorylated at its 5' end to prevent self-ligation in the ligation reaction. Antarctic phosphatase catalyzes the hydrolysis of the

phosphate group at the 5' end of nucleic acid strands and at desoxynucleotides and thereby generates 5' OH ends at its substrates. The reaction was performed for 15 min at 37°C and the following reaction mixture has been used.

Reaction mixture for the 5' end dephosphorylation of vector DNA by Antarctic phosphatase

- 2µl Antarctic phosphatase buffer
- 1µl Antarctic phosphatase (5 units)
- 10µl DNA (<1µg)
- 7µl H<sub>2</sub>O

The reaction was stopped via heat inactivation (5 min at 65°C).

#### **2.2.1.8.3 Preparation of DNA for ligation**

Restriction digested and 5' end dephosphorylated DNA was purified by centrifugation in Sigma Spin™Post Reaction Clean Up Columns as recommended by the manufacturer.

#### **2.2.1.8.4 Ligation of manipulated DNA with T4 Ligase**

The enzyme T4 ligase catalyzes the formation of phosphodiester bonds between juxtaposed 3' OH and 5' phosphate DNA strand ends in an ATP dependent reaction. T4 ligase is capable to ligate double-stranded DNA with blunt or cohesive ends and therefore e.g. allows the integration of DNA inserts into DNA target vector plasmids. The reaction was performed at 16°C overnight and subsequently the whole ligation reaction mixture was subjected to bacterial transformation as described.

The reaction was set up in the following mixture (total volume 10µl) in PCR tubes:

- 1µl digested, dephosphorylated and purified vector DNA (5-10ng)
- 5µl digested and purified insert DNA (c.a. 25 ng)
- 1µl ligase buffer (10x)
- 1,5µl T4 ligase (400U/µl)
- 1,5µl nuclease-free water

To estimate the ligation efficacy, control ligations were performed with the reaction mixture without insert DNA (ratio of self-ligated vector) or with the reaction mixture without T4 Ligase (ratio of uncut vector/insert DNA) and also subjected to bacterial transformation. The calculation of the ratio of colonies on the agar plates from control reactions to colonies from bacteria with plasmids from the complete reaction mixture, allows estimating the ratio of colonies with correctly ligated vectors.

#### 2.2.1.8.5 Site-directed mutagenesis of vector constructs

For the introduction of site-specific nucleotide exchanges into DNA vector plasmids the Quik Change<sup>®</sup> II XL site-directed mutagenesis kit has been applied. Two complementary oligonucleotides containing the mutation of choice were used together with PfuTurbo proofreading DNA-polymerase to amplify the template vector plasmid, which produces plasmids with the mutation. Plasmids were incubated with DpnI enzyme, which specifically degrades methylated template DNA isolated from *E. coli* while DNA amplified with Pfu-polymerase in vitro remained intact and was transformed into XL1-Blue competent cells. All steps were performed as recommended by the manufacturer of the kit.

The sample mix for the PCR reaction was:

5µl reaction buffer (5x)  
1µl DNA template (10ng)  
1µl Primer 1 (125ng)  
1µl Primer 2 (125ng)  
2µl dNTP mix (10mM each)  
1,5µl PfuTurbo DNA polymerase (2,5U/µl)  
Filled up to 50µl with nuclease-free water.

The PCR program was run with the following parameters:

- 1) 30 sec at 95°C (initial denaturation)
- 2) 30 sec at 95°C (denaturation)
- 3) 1 min at 55°C (annealing)
- 4) 1 min/kb of plasmid length at 68°C (elongation)

For introduction of the T790M mutation into pEF5/FRT/V5-EGFR vector plasmids (see section 2.1.8.1), elongation time was 10 min per cycle and 16 cycles (of steps 2-4) were performed. All steps were carried out as recommended by the manufacturer of the kit.

### **2.2.1.9 RNA expression analyses**

Analyses of the mRNA expression in differentially treated cells has been used to display the biological differences caused by specified treatment condition within one or more cell lines.

#### **2.2.1.9.1 Isolation of total RNA from mammalian cells**

Total cellular RNA was isolated from human cancer cell lines with the help of a commercially available kit according to manufacturer's recommendations (Rneasy Mini Kit). The preparation process was conducted carefully with RNase-free pipette tips and reaction tubes. Working gloves were changed frequently and working surfaces were rinsed with RNase Away solution.

#### **2.2.1.9.2 Reverse transcription of mRNA for cDNA synthesis**

Isolated total RNA that was used for quantitative mRNA expression analyses via Taqman<sup>®</sup> Low Density Arrays (LDA; micro fluidic cards) was transcribed into complementary DNA (cDNA) with the First strand cDNA synthesis kit for RT-PCR. The initial template concentration of total RNA was 1µg per 20µl reaction mixture. The cDNA synthesis was performed by using a hexamerix ("random") primer mixture.

Synthesis of cDNA was carried out with the following reaction mixture:

2µl reaction buffer (10x)  
4µl MgCl<sub>2</sub> (25mM)  
2µl random hexameric primer mixture  
1µl RNase inhibitor (1000U/µl)  
0,8µl AMV reverse transcriptase (~ 500 U/µl)  
2µl total RNA (1µg)

Filled up to 20µl with nuclease-free water.

The following steps followed the manufacturer's guidelines. Samples were frozen at 80°C, if not used directly for cDNA analyses with Real-time PCR.

Reverse transcription and sample processing of the RNA which was analysed by Affymetrix Whole Genome DNA chips is described in section 2.2.1.7.6.4.

### **2.2.1.9.3 Quantitative real-time PCR analyses with Taqman® Low Density Arrays (LDA)**

Real-time PCR allows an online documentation of the quantitative increase of the amplification product during the running PCR. This allows determination of the relative starting amount of cDNA in the sample and thus enables comparisons of mRNA expression in between samples from different sources. In this work Taqman® Low-density arrays (LDAs; micro fluidic cards) were employed to compare the mRNA expression levels from long-term gefitinib or cetuximab treated A431 cell in comparison to medium-treated control cells.

Real-time PCR with LDAs allow parallel probing with 12 to 380 probes for different candidate genes on one single chip system. Fluorescence-tagged oligonucleotides with specificity for respective candidate genes are used as probes. They are covalently linked with a rhodamine-derivate (TAMRA) as a reporter dye at their 5' end and with a fluorescein-derivate (FAM) as a signal quencher at their 3' end. During the PCR reaction, probes are hybridizing with the cDNA templates. This triggers Ampli-Taq polymerase binding to the 5' end of the oligonucleotides and release of the TAMRA dye through the 5'-3' exonuclease activity of the polymerase. Free TAMRA dye produces fluorescence signals (emission at 530nm), whose intensity is correlated with the amount of amplification product, which were detected by an ABI Prism 7900 HT apparatus. A signal threshold (Ct) is defined for every probe, which is reached after variable cycle numbers by every sample under examination. A high Ct value therefore corresponds to a low amount of cDNA template in the respective sample. To determine efficiencies (Eff) of PCR reaction with the different probes, variable concentrations of reference cDNA were loaded i) on a LDA chip carrying probes for endogenous control genes ("housekeeper" genes; Eff<sub>control</sub>) and ii) on a LDA chip carrying probes for candidate genes (Eff<sub>candidate</sub>).

Concentrations of cDNA from different samples were determined via capillary electrophoresis and adjusted via dilution before starting PCR reactions.

The reaction mixture for Taqman-PCR was:

25µl H<sub>2</sub>O

25µl cDNA (200ng/µl)

50µl Universal Master Mix (Cat.# 4304437; Applied Biosystems)

Relative quantification of candidate gene mRNA was performed by normalization against a mean value calculated from a panel of household genes, whose expression has been shown to constant under treatment of cells with EGFR-directed cancer therapeutics (Radonić et al. 2004). Relative expression of candidate genes in drug treated (dt) in relation to untreated cells (ut) has been calculated by the following formula:

Relative Expression of candidate gene =

$$\text{Eff}_{\text{candidate}}^{(\text{Ctdt} - \text{Ctut})} \times \text{Eff}_{\text{control}}^{(\text{Ctdt} - \text{Ctut})}$$

Ct<sub>dt</sub> = Threshold cycle in drug treated cells

Ct<sub>ut</sub> = Threshold cycle in untreated control cells

Eff<sub>candidate</sub> = Efficacy of specific candidate gene

Eff<sub>control</sub> = Efficacy of control gene

A relative expression value >1 means that the corresponding candidate gene expressed higher in cells treated with the respective drug than in untreated control cells. All measurements with probes for candidate genes were performed as triplicates, measurements with probes for endogenous control genes as duplicates. The evaluation of data probed via Taqman<sup>®</sup> LDAs (micro fluidic cards) was kindly performed by Mr. Jens Baumgärtner in the laboratory of Mr. Tobias Haas, LSA, Merck KGaA.

#### **2.2.1.9.4 Quantification of the genome-wide mRNA expression with Affymetrix whole genome DNA chip arrays**

Transcription of cDNA, sample labeling, clean up and hybridization control was accomplished with the Affmetrics Gene Chip One Cycle Target Labeling and Control Reagents kit as described in the manufacturer's protocol and analysed on an Affymetrix Gene Chip Array Station. Whole genome expression analyses was kindly performed by Mrs. Melanie Kühnl in the laboratory of Dr. Detlef Güssow, TAR, Merck KGaA.

#### **2.2.1.9.5 Statistical methods for evaluation and interpretation of the whole genome expression analyses**

Preprocessing of the probe-level Affymetrix data was conducted using VSN (variance stabilization and calibration) (Huber et al., 2002), followed by computing probe set summaries with the median polish algorithm of RMA (Irizarry et al., 2003). In a global prefiltering step, only probe sets with a) intensity values above 100 in at least two cell lines, b) a standard deviation above 0,5 on the logarithmic scale (base 2), and c) matches to RefSeq transcripts of unique human genes, were chosen for the analyses. For the analyses of NSCLC cell lines, differentially expressed genes in the comparison of sensitive and resistant cell lines were identified using a moderated t-test. All microarray analyses were performed using Bioconductor software (Gentleman et al., 2004). Statistic data prefiltering and processing was kindly performed by Dr. Anja von Heydebreck, Bioinformatics, Merck.

### **2.2.2 Methods in mammalian cell culture and pharmacology**

#### **2.2.2.1 General cell culture conditions and techniques**

All adherent mammalian cells lines used for this work, were cultured in cell line specific full medium, as indicated in section 2.1.13. Incubation of cell lines was at 37°C and 5% CO<sub>2</sub>. For passaging, cells were washed once with D-PBS and detached from the plate by incubation with 1,5ml Trypsin/EDTA (2,5%) for 1-5 min at 37°C. Detached cells were resuspended in 20ml full medium, the suspension was centrifuged for 3 min at 1200rpm and 4°C and the cell pellet was again carefully resuspended in a defined volume of full medium. Depending on the specific

experimental purpose, the cell suspension was then transferred to variable formats of cell culture dishes.

#### **2.2.2.2 Calculation of cell numbers**

A small volume of a cell suspension (50-200µl) was mixed with an equivalent volume of trypane blue solution (0,4%) and transferred to a Neubauer counting chamber. Only unstained (viable) cells are counted under the microscope, since trypane blue can penetrate only dead cells. To calculate the number of viable cells per millilitre of the suspension, the number of cells counted in one big square (which is subdivided into 9 small squares) gets multiplied by factor  $1 \times 10^4$  (counting chamber dilution factor) and by factor 2 (dilution factor for trypane blue). Cell numbers of four big squares were determined and their mean value was used for calculation.

#### **2.2.2.3 Freezing and thawing of cell lines**

Cell lines were frozen in liquid nitrogen for long-term storage purposes. After trypsinizing, centrifugation and resuspension of cells in full medium, aliquots of the suspension (500µl) were transferred to cryo vials. An equivalent volume of freezing medium (full medium + 20% FCS + 20% DMSO) was added to the cryo vials, the cell suspension was carefully mixed and chilled stepwise (2 h at  $-20^{\circ}\text{C}$ , 2 days at  $-80^{\circ}$ ) and finally stored in liquid nitrogen.

#### **2.2.2.4 Light microscopy**

Phase contrast microscopy has been used for documentation of cellular morphology. Cells were seeded in variable densities on 6-well cell culture dishes and morphology was observed under a light microscope at 40x and 400x magnifications. Microscope was adjusted according to the guidelines of Köhler (Köhler, 1893) before use. Photos were taken and processed by an integrated photo documentation system.

#### **2.2.2.5 Generation of stably transfected NIH3T3 cell lines**

For the generation of murine NIH3T3 cells stably transfected with variants of EGFR, genetically manipulated NIH3T3 cells, which are part of the Flp-In™ transfection system, have been used (Cat.# R761-07, Invitrogen). These cells possess a genome wide unique Flp recombination target (FRT) site, which is located in the coding



sequence of a zeocin resistance gene. For generation of stably EGFR expressing Flp-In cell lines, NIH3T3 cells were co-transfected with the pEF5/FRT/v5 expression vector transferring resistance to hygromycin and coding for EGFR and the Flp recombinase expression plasmid pOG44. Flp recombinase catalyses site-specific DNA recombination and therefore allows integration of EGFR into the FRT locus. Upon integration of the plasmid, cells lose zeocin resistance, but gain resistance to hygromycin, allowing specific selection of stably transfected cells.

For transfection  $5 \times 10^5$  cells per well were seeded in a 6-well culture plate and allowed to attach on the surface overnight. Transfection of cells was performed with Lipofectamine™2000 reagent according to the manufacturer's recommendations. Transfected cells were incubated under standard cell culture conditions and medium was changed 6 h post transfection. After incubation for two days, selective medium containing hygromycin (200 µg/ml) was added to the cells. This step was repeated once each day for 4 days and plates were checked every day for viable cells. One well with untransfected cells was as well treated with selection medium. No viable cells could be observed after two days of selection with hygromycin in this control well. Surviving cells from the transfections were permanently propagated in selective medium, expanded, frozen and used for experiments. Since the integration locus of EGFR is constant in every case, subcloning of colonies was not necessary. Stable expression of EGFR in the respective cell lines has been validated via FACS analyses (see section 2.2.2.10).

#### **2.2.2.6 Generation of long-term gefitinib or cetuximab-treated human cancer cell lines**

Human cancer cell lines were treated for 8-15 months with gefitinib or cetuximab to examine the effects of long-term exposure to these drugs in vitro. Cells were thawed from low passage cryo stocks and cultured with their specific medium in 75T cell culture flasks. Treatment medium containing gefitinib or cetuximab was sterile filtrated and changed every 3-4 days. When necessary, cells were passaged and seeded in low density on fresh flasks with treatment medium. Biological activity of therapeutics after sterile filtration was shown once and activity after storage at 4 °C was shown periodically by monolayer growth assays with Difi cells, which are hypersensitive to gefitinib and cetuximab.

The starting concentrations of the therapeutics correspond to the EC<sub>50</sub> concentration of the therapeutic in the respective cell line and are indicated in the table below. Concentrations of gefitinib were stepwise escalated once the cells resumed growth under the current doses. To reduce the bias through off-target effects, maximum concentration for dosis escalation with gefitinib was 10µM.

With the exception of Difi cells, no EC<sub>50</sub> value could be determined for cetuximab in a monolayer growth-inhibition assay. Therefore A431, H460 and SW707 cells were treated with constant concentrations of cetuximab, while Difi cells were also doses escalated with cetuximab.

Cell line	Starting Concentration		Final Concentration	
	Gefitinib	Cetuximab	Gefitinib	Cetuximab
A431	0,5µM	33µg/ml (150nM)	10µM	33µg/ml (150nM)
Difi	0,05µM	0,22µg/ml (1nM)	1µM	5µg/ml (25nM)
H460	5µM	33µg/ml (150nM)	10µM	33µg/ml (150nM)
SW707	5µM	33µg/ml (150nM)	10µM	33µg/ml (150nM)

### 2.2.2.7 Monolayer growth inhibition assays with Wst-1 reagent

Monolayer growth assays were performed to study the growth inhibitory effect of gefitinib and cetuximab on human cancer cells. Cells were counted, centrifuged, resuspended in full medium, seeded in flat bottom 96-well plates (50µl per well) and allowed to attach to the plate. The number of cells seeded on per well varied by the cell line (1x10<sup>3</sup> cells per well for SW707 and H460, 3x10<sup>3</sup> cells per well for Calu3 and Difi and 2x10<sup>3</sup> cells per well for all other cell lines). After full attachment to plates, 50µl starvation medium (without serum) containing the therapeutics in variable concentrations was given to the wells. Cells were incubated under standard cell culture conditions for five days. For evaluation 10µl of Wst1 reagent were added to each well and incubated for 2 h. Wst1 is a tetrazolium salt, which is cleaved to produce formazan by viable cells. Finally, absorbance at 440 nm was determined via a spectrometer (Mithras plate reader). To determine the pharmacological background for each cell line, cells were treated with 100µM Paclitaxel, which effectively kills all cells in the respective well. EC<sub>50</sub> values were calculated by the Graph Pad Prism software, after subtraction of the pharmacological background, normalization to the mean value of medium-treated control cells, log-transformation

of the x-axis and sigmoidal dose-response (variable slope) regression. Quantification of every data point was carried out at least as triplicate.

#### **2.2.2.8 Colony formation assay in a soft-agar matrix**

Colony formation assays were performed to study the growth inhibitory effect of gefitinib and cetuximab on human cancer cells in an agar matrix format. In this assay cells cannot attach to a culture plate surface, but are exposed to contact-free growth conditions. This assay therefore requires special tumorigenic capabilities, other than those displayed under cellular adherence at culture plate surfaces.

For assay preparation, equal volumes of 2x MEM-full medium (warmed to room temperature) and basal agar (warmed to ~ 52°C) were mixed and 750µl of this mixture is transferred to each well on 24-well plates. These plates were either used directly for soft-agar assays or stored at 4°C. Cells were trypsinized, resuspended and counted, then centrifuged and resuspended in a defined volume of 2x MEM-full medium. The cell number per well was variable, depending on the cell line (a cell number of  $5 \times 10^3$  cells per well was used for the H460 cell line;  $1,5 \times 10^4$  cells per well for stably transfected NIH3T3 cells;  $5 \times 10^4$  cells per well for Calu3 and H1781 cell lines and  $3 \times 10^4$  cells per well for all other cell lines). Top agar solution (warmed to ~ 52°C) was carefully mixed with cell suspension and 750µl of this mixture is transferred on top of the solidified basal agar layer. Plates are incubated overnight under standard cell culture conditions.

Treatment solutions were prepared from serum-free medium supplemented with variable doses of EGF or therapeutics and added on top of the agar layers. Treatment solutions were 5x concentrated, sterile filtrated and added in a volume of 375µl per well (total volume of assay is 1875 µl). Plates were cultured under standard conditions for 6-10 days. For evaluation 200µl of Cell Titer Blue solution are added to the wells and incubated for 2-8 h. Cell titer blue solution contains resazurin, which is processed by respiratory chain components of viable cells to produce the fluorescent product resorufin. The fluorescence signal was quantified with a plate reader (excitation: 540nm, emission: 600nm). The  $EC_{50}$  values were determined as described for the monolayer growth assays. Quantification for every data point was carried out at least as triplicate.

### **2.2.2.9 Short-term treatment of cell lines with EGF and cancer therapeutics for protein lysate preparation**

Mammalian cell lines were subjected to a short-term ligand stimulation and treatment with cancer therapeutics to study the dynamics of marker protein activation and inactivation in their protein lysates. A total cell number of  $7,5 \times 10^5$  cells per well were seeded on 6-well plates, allowed to attach to the plate surface, washed once in serum-free medium and serum starved overnight. The next day cells were exposed 45 min to serum-free medium containing variable doses of gefitinib and cetuximab under standard culturing conditions. Then cells were stimulated by directly adding EGF to the wells and again incubated for 10 min. Thereafter cells were harvested as described in section 2.2.3.1.1.

### **2.2.2.10 Detection of EGFR surface expression via fluorescence assisted cell sorting (FACS)**

FACS was employed to analyse the presence and determine the relative quantity of EGFR on the surface of mammalian cells. Cells were harvested from culture flasks, counted, pelleted by centrifugation, washed once with cold D-PBS and resuspended in a defined volume of ice-cold FACS wash buffer (1% BSA, 0,03% sodium azide in D-PBS) to adjust cell density in the suspension ( $1 \times 10^6$  cells/ml). A volume of 1 ml suspension was transferred to FACS tubes and washed again with FACS wash buffer. Cells were centrifuged and incubated with 10 µg/ml FITC-conjugated matuzumab (e.g. for EGFR expression analyses in NIH3T3 cells) or with 10 µg/ml PE-conjugated rat-anti-human EGFR antibody (e.g. for EGFR expression analyses in long-term-treated A431 cells) for 15 min on ice with repeated mixing. Cell pellets were washed three times with FACS wash buffer and resuspended in FACS wash buffer containing 100 µg/ml propidium iodide (PI) to discriminate dead from viable cells. When carrying out indirect stainings, cells were incubated with FITC-conjugated secondary antibody for 15 min on ice, washed three times and resuspended in FACS buffer containing PI. Cells were analyzed on a Becton Dickinson FACScalibur flow cytometer. For evaluation and quantification of the assay the median channel signal from every population was transformed by the help of Cell Quest software into absolute arbitrary units, in order to compare the signal intensity between distinct cell populations.

### **2.2.2.11 Internalization of radioactively labeled $^{125}\text{I}$ -cetuximab in A431 cell lines**

To study differences of A431 cells that long-term-treated with cancer therapeutics in the capacity internalize cetuximab, radioactively labeled cetuximab was used to track cellular uptake of this antibody. Cells were seeded in 24-well cell culture dishes and starved overnight in serum free medium. On the next day cells were washed in ice-cold serum free medium and incubated in ice-cold serum free medium containing 2nM  $^{125}\text{I}$ -cetuximab for 2 h to label surface EGFR. To start internalization the temperature was shifted to 37°C for variable durations (5 to 60 min) and thereafter cells were washed with ice-cold serum-free medium to remove unbound ligands. Bound ligands were dissociated from the cells by adding ice-cold stripping buffer and cells were again washed with ice-cold serum-free medium. The washing fraction was then combined with the stripping fraction to obtain all not-internalized ligands. Cells were lysed in 1M NaOH, wells were washed with medium and again both fractions were combined to obtain all internalized ligands. All quantifications of  $^{125}\text{I}$ -cetuximab were carried out as triplicates with a LKB Wallac 1277 Gammamaster counter.

### **2.2.2.12 In vivo pharmacology with murine tumor xenografts upon treatment with cancer therapeutics**

Drug sensitivity of certain cell lines to gefitinib and cetuximab was examined via xeno-transplantation of cells into mouse models, which were subsequently subjected to treatment. These in vivo studies are of particular interest since they may closely resemble the situation in human cancer patients. Female CD1 nu/nu mice (e.g. used for H292 and H1650 cell line xenografts) and BalbC nu/nu mice (e.g. used for H1975 and Calu6 cell line xenografts) were 4-5 weeks old when obtained from Charles River and allowed to accustom to the mouse facility for 1-2 weeks. NSCLC were harvested, resuspended in PBS and an equal volume of Matrigel and concomitantly injected subcutaneously into the left or right flank of the mice ( $5 \times 10^6$  cells in 100µl). At a tumor size of 70-80mm<sup>3</sup> mice were randomized and then treated twice per week i.p. with 15mg/kg cetuximab in 0,5 ml sterile PBS (0,5ml PBS vehicle) or daily p.o. with 40mg/kg gefitinib (1ml 0.5% Tween-80/physiol. NaCl). Each treatment group consisted of 10 mice and treatment periods varied depending on tumor growth as noted in the results section. Tumor sizes were determined via measurement of tumor width (w) and length (l) followed by calculation of the tumor volumes (length [mm] x

width [ $\text{mm}^2$ ]/2 = tumor volume [ $\text{mm}^3$ ]). After sacrifice of the mice, the tumors were carefully resected, directly frozen in liquid nitrogen and stored at  $-80^\circ\text{C}$ . Mouse husbandry and conduction of xenograft experiments was kindly performed by Mr. Gerhard Schuster and Mrs. Monika Schaefer in the laboratory of Dr. Christiane Amendt, TA Oncology, Merck.

## **2.2.3 Methods in protein analyses and biochemistry**

### **2.2.3.1 Preparation of protein lysates**

#### **2.2.3.1.1 Protein extraction from cell lines**

Protein lysates were prepared from cell lines grown on variable cell culture dish formats, depending on the experimental context. Two different buffers have been used for lysate preparation: RIPA buffer and Laemmli buffer (compositions are noted in section 2.1.9). The use of non-denaturing RIPA buffer allows quantification of the protein content in the lysate, which is of importance when the relative protein expression between different cell lines is examined. Denaturing Laemmli buffer was used for cell lysis when protein modification by phosphorylation was studied.

Prior to lysis cells were treated with growth factors or tumor therapeutics as indicated in the figure legends of the results section. Cells were transferred from the incubator on ice and immediately washed with ice-cold D-PBS. Cells were harvested after addition of lysate buffer (freshly supplemented with phosphatase inhibitor and protease inhibitor cocktails). Lysates were sonified on ice with a ultrasound homogenizator (permanent; 15 sec; 40% power) to shear genomic DNA and improve solubilization of proteins from subcellular membrane fractions. Centrifugation (30 min; 14000rpm;  $4^\circ\text{C}$ ) helped to clear lysates. The supernatant from RIPA lysates was subsequently subjected to quantification, while Laemmli buffer lysates were denaturated by boiling (10 min;  $95^\circ\text{C}$ ).

#### **2.2.3.1.2 Protein extraction from murine xenograft tumors**

Murine tumors from xenografts were carefully dissected on ice and representative pieces from the middle of the tumor were transferred to Precellys ceramic bead columns (1,4mm beads). An adequate volume of RIPA buffer (3x) was added and tumor tissue was destroyed by subjection to a Precellys 24 homogenizator (30 sec; 12000rpm;  $4^\circ\text{C}$ ). The ceramic beads were washed twice with cold sterile water and

combined with the 3x concentrated RIPA buffer. The combined lysate was subsequently treated as described for standard RIPA lysates.

### **2.2.3.2 Determination of protein concentrations**

Protein concentrations in RIPA buffer lysates were determined via the BCA (bicinchoninic acid) Protein Assay kit. To generate a standard curve dilutions of a BSA stock solution were made (concentrations were from 0 to 1000µg/ml). To determine the protein concentrations from a sample, two different dilutions were generated (1:4 and 1:12) and spotted on a flat bottom 96-well plate together with the standard samples (every data point was determined as duplicate). The assay was then performed as recommended by the manufacturer and evaluated via detection of the absorption at 550nm with a plate reader spectrometer. The concentration of RIPA lysates was adjusted according to the experimental purpose by diluting the samples with RIPA buffer, then XT reducing agent (20x) and XT loading buffer (4x) were added and samples were denatured as described above.

### **2.2.3.3 SDS-polyacrylamide-gelelectrophoresis (SDS-PAGE)**

Separation of proteins by their molecular weight was accomplished via sodium dodecyl sulphate polyacrylamide gelelectrophoresis (principle described in Laemmli et al., 1970). Criterion precast gels, MOPS running buffer (20x) and the Criterion Running Chamber system were used for SDS-PAGE separations as recommended by the manufacturer. Magic Mark and Sea Blue markers were loaded together with the protein samples as molecular size standards. The separation was performed at 100 to 150 Volt for variable durations, depending on the experimental context.

### **2.2.3.4 Transfer of proteins on nitrocellulose membranes**

Transfer and immobilization of proteins from gels onto nitrocellulose membranes was accomplished via electroblotting using a Criterion Blotter (principle described in Towbin et al., 1979). Transfer buffer was prepared freshly and it was used to generously soak all components of the blotting sandwich during assembly. Blotting was performed with a frigistor under stirring for 90 min at 0,8mA per cm<sup>2</sup> gel. Nitrocellulose membranes were stained with Ponceau Red solution and scanned after blotting to check and document proper transfer of proteins.

### 2.2.3.5 Immunoblot detection of proteins

Immunodetection of nitrocellulose bound proteins was performed after membrane blocking with immunoblot blocking buffer or Starting Block™ (PBS) blocking buffer for 30 min at RT on a shaker. Membranes were probed shaking with primary antibody overnight at 4°C, washed three times for 15 min with immunoblot washing buffer and incubated with horseradish-peroxidase (HRP)-coupled secondary antibody diluted in immunoblot washing buffer for 2 h at RT on a shaker. Immunoblots were again washed as described above before antigen-antibody complexes were detected by adding LumiLight® or LumiLight® Plus Western blotting substrate that produce chemoluminescence upon conversion by HRP. Luminescence was visualized via the Vers Doc immunoblot visualization and documentation system, pictures were processed with Quantity One software. All used antibodies and their dilution factors are listed in section 2.1.6.

### 2.2.3.6 Examination of receptor tyrosine kinase (RTK) activation levels using immunoblot arrays

Use of membrane arrays spotted with immobilized antibodies allows a paralleled identification of multiple antigens present in a single lysate. In this work a Proteome Profiler™ Array for human phospho-RTK detection was used to probe relative activation of 42 RTKs in long-term gefitinib or cetuximab-treated A431 cells.

A membrane spotted with duplicates of 42 RTK capture antibodies and 6 control antibodies is incubated with cell lysate which allows formation of specific antigen-antibody complexes. Unbound material is washed away and membranes are incubated with an HRP-coupled pan anti-phospho-tyrosine antibody and subsequent of activated receptors with detection of chemiluminescence by the Versa Doc documentation apparatus.

Preparation of lysis buffer was performed by the following protocol (in MiliQ water):

NP-40	1%
Tris, pH 8,0	20mM
NaCl	135mM
EDTA	2mM



*Added freshly:*

Sodium vanadate	1mM
Aprotinin	10µg/ml
Leupeptin	10µg/ml

Cells were harvested, lysates solubilized by rotation (30 min, 4°C) cleared by centrifugation (10 min, 14000rpm, 4°C) and protein content was quantified by BCA assay. After adjustment of protein concentrations, lysates were incubated with the array membranes overnight at 4°C and assay was developed as recommended by the manufacturer. Data analyses was performed with QuantityOne software by background subtraction, determination of average signal density from duplicates and normalization of values from long-term gefitinib or cetuximab-treated cell lysates against values from untreated control cell lysates of similar passage number, which were set 1. Assay development was kindly carried out by Mrs. Irina Onofrei in the laboratory of Dr. Andree Blaukat, TA Oncology, Merck.

### 3. Results

#### 3.1 *Impact of clinically relevant mutations in the EGFR kinase domain for EGFR-directed tumor therapy*

##### 3.1.1 Studies on stably transfected NIH3T3 cells

It was described earlier that stable transfection of murine fibroblastic NIH3T3 cells with human EGFR and parallel EGF supplementation of growth medium is sufficient to transform this cell line (Di Fiore et al., 1987). Due to this fact and the low endogenous expression of mouse EGFR in these cells (Velu et al., 1989; Helin and Beguinot, 1991), an unbiased and well-defined cellular model was available for studying the impact of EGFR kinase domain mutations.

##### 3.1.1.1 Validation of the cellular model system

After transfection and selection of stably transfected NIH3T3 cells, surface levels of human EGFR were assessed by FACS analyses with a human EGFR-specific antibody. EGFR is expressed in all tested cell lines, while no human EGFR could be detected on the surface of mock-transfected NIH3T3 cells (figure 10).

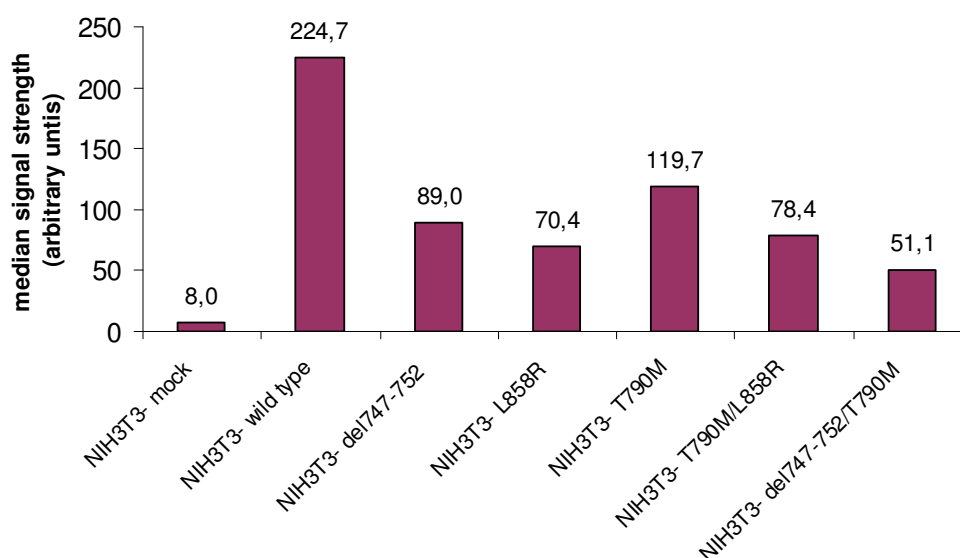


**Figure 10 Validation of EGFR expression in NIH3T3 cells stably transfected with EGFR variants.** NIH3T3 cells were stably transfected with plasmids coding for wild-type EGFR and kinase domain mutants as described in material and methods. Receptor surface expression was analyzed by FACS after staining of the cells with FITC-labeled cetuximab for 15 min. Median signal intensity from the fluorescence channel was calculated for every cell line and transformed to arbitrary units to compare relative expression levels between cell lines. Cells were analyzed on a Becton Dickinson FACScalibur flow cytometer.

The analyses showed above-average surface levels in the wild-type EGFR transfected cell line and comparable strong levels in the other five cell lines. As explained in the methods section, transfected plasmid DNA may only be integrated at a unique site in the genome of the used NIH3T3 cell line. Together with the observation from the FACS analyses (figure 10), this means that the effects observed for these cell lines are exclusively due to the respective EGFR mutation and are not caused by collateral genomic integration influences or variable expression levels between cell lines. On the other hand, the high EGFR levels in the cell line expressing wild type receptor need to be taken into consideration when comparing those data with these from the mutant cell lines.

#### **3.1.1.2 Examination of cellular signal transduction in NIH3T3 cells**

To study the effects the mutations have on EGFR-mediated signaling, cells were treated with EGF after serum starvation and exposure to either cetuximab or gefitinib and examined for activation of EGFR and downstream signaling cascades (figure 11).

Basal activation of EGFR and the downstream signaling marker Akt was high in cells expressing mutated receptor, but could hardly be detected in the cell line transfected with the wild-type receptor. Some activation of the Ras/Raf/Mek/MAPK signaling cascade, reflected by phosphorylation of MAPK, could be found in most cell lines, however a high activation was only seen in NIH3T3 cells expressing EGFR-del747-753-T790M.

Efficient blockage of EGF-induced activation of EGFR and downstream components by gefitinib was seen in NIH3T3 cells transfected with the classical EGFR kinase domain mutations, EGFR-del747-753 and EGFR-L858R. Some, less effective phosphorylation blockage of marker proteins by the TKI could be observed in cells with wild-type receptor. Yet, no significant signaling inhibition could be detected in cells expressing EGFR with a T790M amino-acid exchange mutation, either alone or in combination with one of the classical mutations.

Upon treatment of cells with the monoclonal antibody cetuximab, only moderate inhibition of protein phosphorylation was seen for all marker proteins in nearly all NIH3T3 cell lines, with the exception of NIH3T3-EGFR-del747-753-T790M cells. These did not show any change in this phosphoprotein analyses after challenge with cetuximab.

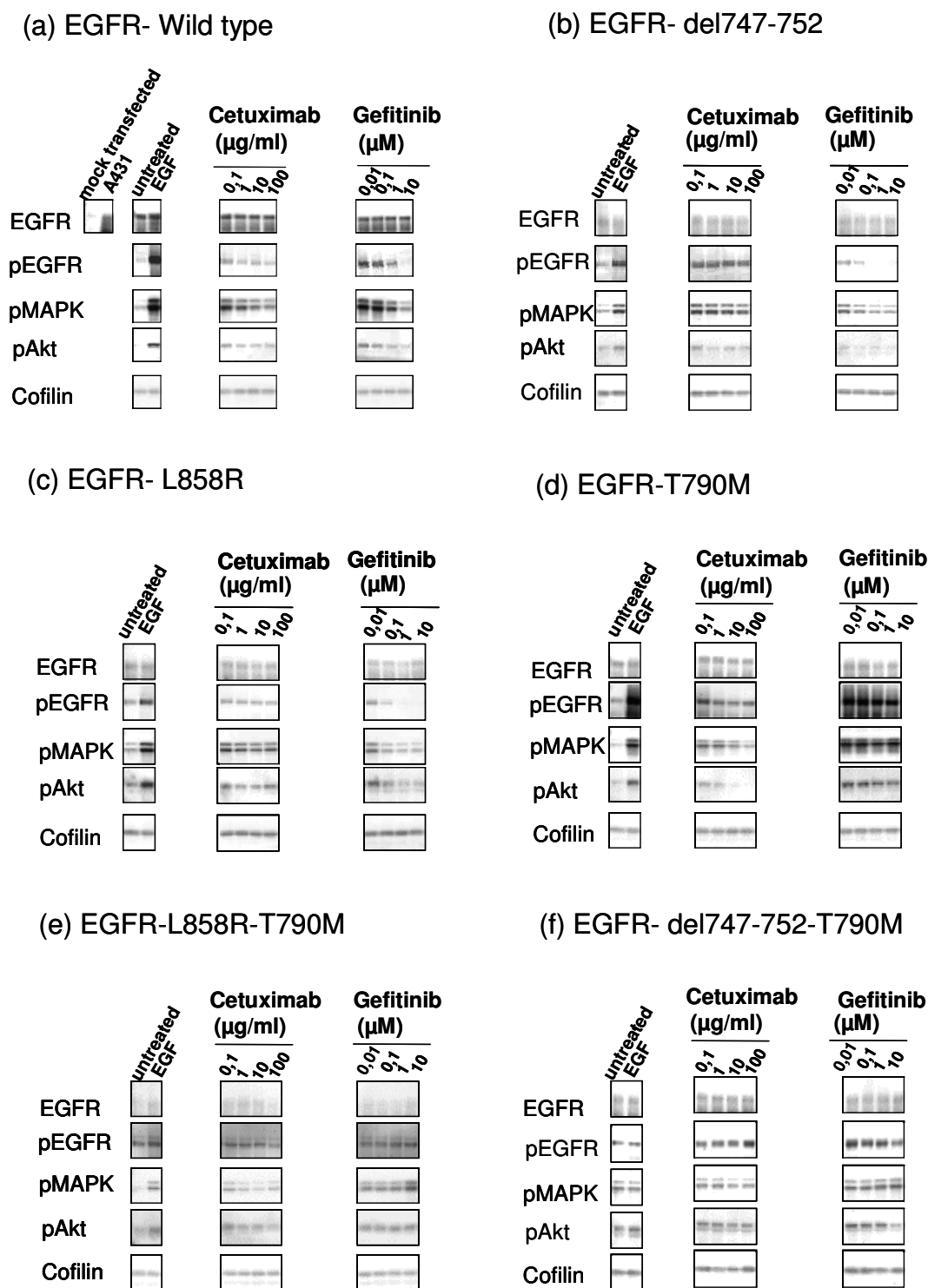


**Figure 11 Ligand activated NIH3T3 cells expressing EGFR mutants showed variable signaling responses upon treatment with cetuximab and gefitinib.** NIH3T3 cells were treated with variable doses of cetuximab [ $\mu\text{g/ml}$ ] or gefitinib [ $\mu\text{M}$ ] (45min) and stimulated with EGF (30ng/ml, 10min) after serum starvation. After lysis, total EGFR, phosphorylated EGFR (Tyr1068), phosphorylated MAPK (Tyr202/Tyr204) and phosphorylated Akt (Ser 473) were detected as marker proteins for EGFR-mediated signaling by immunoblotting. Membranes were probed with an anti-cofilin antibody as loading control. (a) Lysates of mock transfected NIH3T3 cells and A431 cells were probed for total EGFR content as negative and positive controls.

### 3.1.1.3 Cellular transformation by EGFR mutants

To test the paradigm that increased signaling activity correlates with cellular transformation, the colony formation capacity under external EGF supplementation was studied in a 3D soft-agar assay.

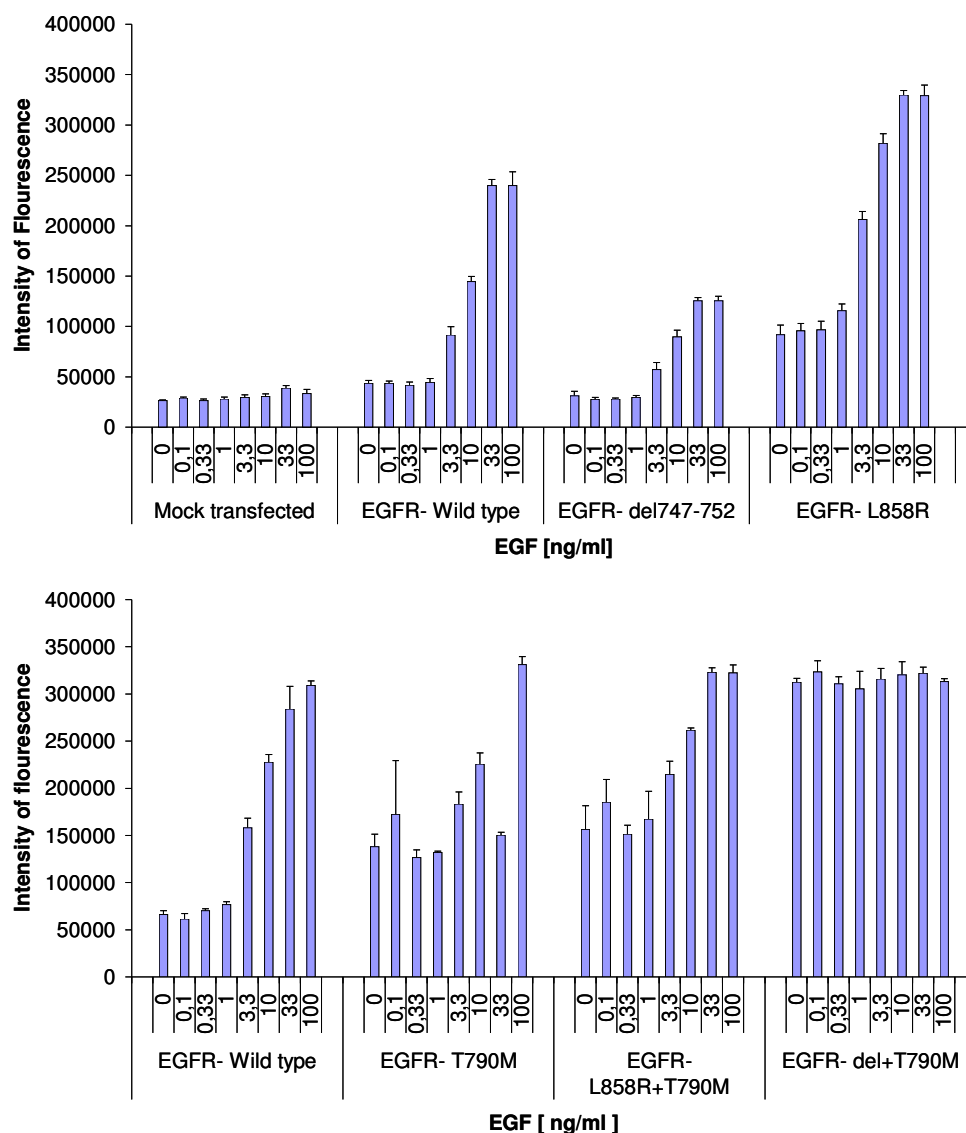


**Figure 12 NIH3T3 cells expressing EGFR mutants displayed variable growth patterns upon EGF stimulation in a soft-agar colony formation assay.** Stably transfected NIH3T3 cells, exogenously expressing wild-type and different variants of mutated receptor, were seeded in a soft agar matrix as described in material and methods and treated with serum-free medium containing variable doses of human EGF for 8 days. Fluorescence was detected after addition of Cell Titer Blue reagent, incubation (2 h) and concomitant detection of signals with a plate reader. Intensity of fluorescence is linearly correlated to the relative number of viable cells per well. Each bar is the average from triplicate values (mean +/- standard deviation).

As expected, wild-type (wt) EGFR transformed NIH3T3 cells only upon external supplementation with EGF. Figure 12 assembles data from two independent experiments with NIH3T3-EGFRwt cells as reference for the cell lines expressing mutated EGFR. Maximal saturation of wild-type receptor expressing cells is observed at a ligand concentration of 33ng/ml.

On the other hand, ligand independent growth was seen for all cell lines expressing mutant receptor, with NIH3T3-EGFR-del747-753 cells as an exception, which, like EGFRwt cells were strictly dependent on EGF supplementation. Yet, colony formation for all cells with mutated receptors, apart from NIH3T3-EGFR-del747-753-T790M, could further be increased by addition of external EGF. This cell line's ligand independent growth was paralleled by constitutive activation of EGFR, Akt and MAPK proteins as detected by immunoblot analyses (figure 11). Interestingly, the colony formation capacity of NIH3T3-EGFR-del747-753 cells, even under EGF stimulation, was lower than the growth potential of wild-type EGFR transfected cells, despite the basal activation of mutant receptor (figure 11).

#### **3.1.1.4 Growth inhibition of NIH3T3 cells under drug treatment in a 3D soft-agar matrix**

To examine the influence of EGFR mutations on gefitinib- or cetuximab-mediated growth inhibition of NIH3T3 cells, 3D soft-agar assays were performed under concomitant stimulation with 10ng/ml EGF. Ligand induced growth of NIH3T3 cells expressing wild-type EGFR is readily inhibited by concentrations higher than 0,1 $\mu$ M of gefitinib (figure 13). Compared with this, NIH3T3 expressing EGFR with classical mutations were hypersensitive to the TKI. As expected, colony formation of cells with EGFR variants containing a T790M amino-acid exchange mutation, did not respond to gefitinib. Growth inhibition at high concentrations (3,3 or 10  $\mu$ M) is probably due to off-target effects (Brehmer et al., 2005).

In contrast to this, cetuximab was capable of inhibiting colony formation in all cell lines, apart from NIH3T3-EGFR-del747-753-T790M. Notably, all other NIH3T3 cells with the T790M mutation were sensitive to cetuximab. The maximal inhibitory activity of the antibody, however, was not as marked as that observed for gefitinib (figure 13). These findings showed that the inhibitory effect of cetuximab is rather unaffected from mutations in the intracellular kinase domain of EGFR, while the T790M mutation confers resistance to gefitinib to otherwise sensitive cell lines.

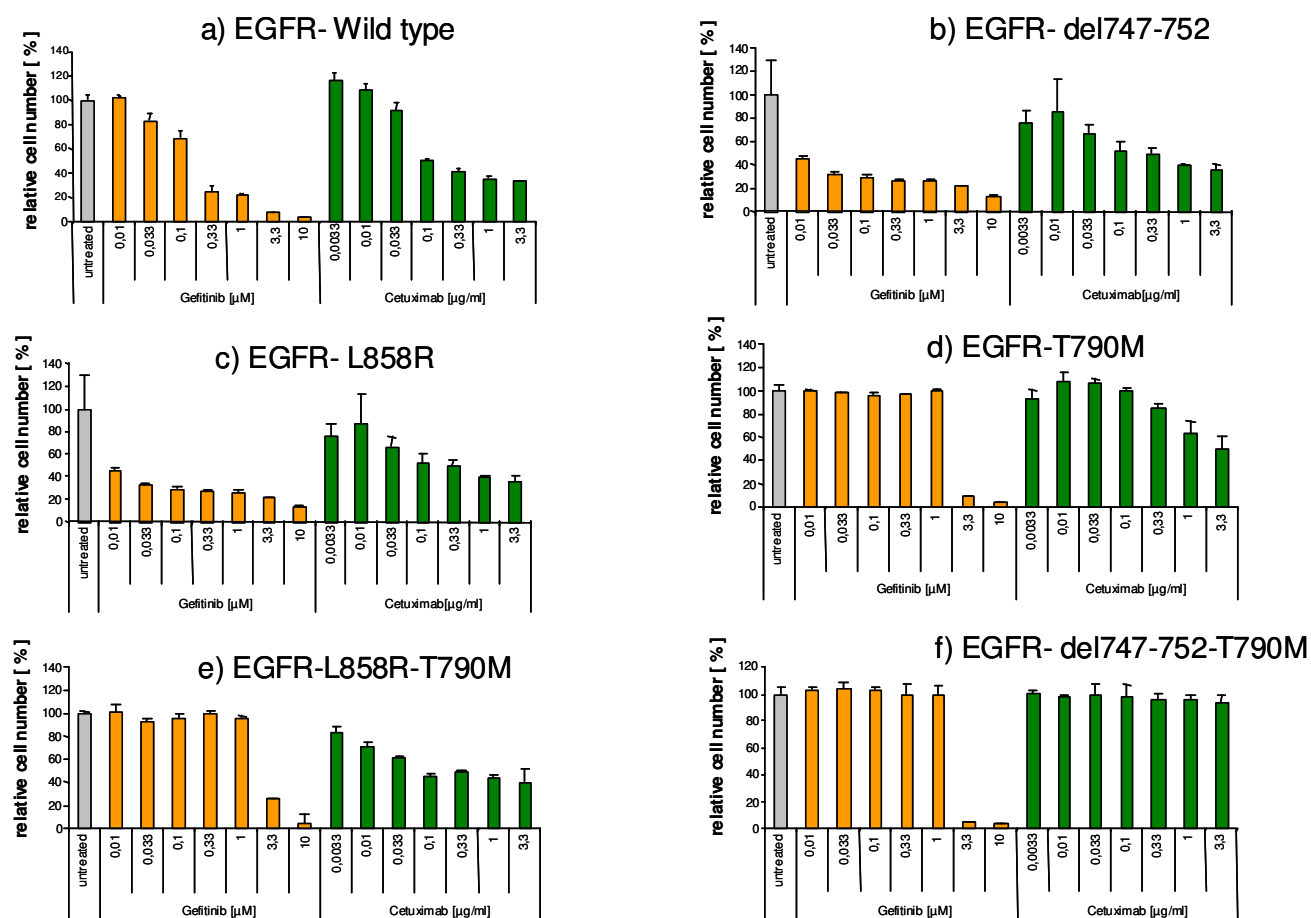


**Figure 13** NIH3T3 cells expressing EGFR mutants showed variable growth responses upon treatment with gefitinib and cetuximab. Stably transfected NIH3T3 cells, exogenously expressing wild-type and different variants of mutated receptor, were seeded in a soft agar matrix and treated in EGF supplemented (10 ng/ml) serum-free medium containing variable doses of cetuximab [0,003 - 3,3 µg/ml] or gefitinib [0,01 - 3,3 µM] for 8 days. Fluorescence intensity was detected by Cell Titer Blue reagent and read out with a plate reader. Relative cell numbers under treatment were calculated by signal normalization to medium-treated control cells. Each bar is the average from triplicate values. Bars for medium-treated control cells were determined as sextuplets (mean +/- standard deviation).

### 3.1.2 Examination of NSCLC cell lines endogenously expressing EGFR

#### 3.1.2.1 ErbB receptor and ligand expression levels in NSCLC cell lines

Studies in NSCLC cells that carry endogenous mutations can in general be considered of higher value than the analyses of the transfected NIH3T3 cell lines, since they should more closely reflect the pathological situation. In order to investigate the relevance of EGFR kinase domain mutations for determining response to cetuximab therapy a panel of twelve NSCLC cell lines was analyzed,

including all cell lines with mutant EGFR openly available for the scientific community. Previous work suggests that the levels of ErbB family members conjoint with the expression of their ligands may be important indicators for cellular response to gefitinib (Amann et al., 2005; Engelman et al., 2005; Fujimoto et al., 2005). Furthermore, it has been proposed that activating KRAS mutations are associated with resistance to TKIs (Pao et al., 2005b; Eberhard et al., 2005).

Table 1 summarizes the EGFR and KRAS mutation status in the NSCLC cell lines used in this thesis. Furthermore, mRNA expression levels of ErbB receptors and ErbB ligands in the respective cell lines were determined by Affymetrix cDNA expression profiling. The data show that the panel includes five cell lines with EGFR kinase domain mutations and eight cell lines with wild-type receptor. One of the cell lines (H1975) contains a T790M mutation, which has been shown to confer resistance to gefitinib (Pao et al., 2005a), in combination with a classical L858R mutation. Three cell lines carry mutated KRAS, which also was postulated to be responsible for non-response to EGFR-directed TKIs (Pao et al., 2005b). The frequency of KRAS mutations in this cell panel of 23% (3/13) is a little lower than the frequency of KRAS mutations observed in the clinic, where it was found to range from 26% to 39% in NSCLC patients (Jassem et al., 2004; Chong et al., 2007; Hirsch et al., 2007). Only the H1650 cell line is known to lack PTEN (8%; 1/13), yet not all cell lines in the panel have been profiled in this respect. This ratio is lower than the 20% to 46% patients with loss of PTEN observed in NSCLC patients (Tang et al., 2006; Capuzzo et al., 2006). Interestingly only two cell lines (H1781 and H460) have no or very low EGFR expression levels, while two cell lines over express EGFR (HCC2279 and HCC827). The other nine cell lines display medium EGFR mRNA expression levels. Expression of moderate and high levels of EGFR and its natural ligands is frequently observed in NSCLC and has been correlated with response to EGFR-targeting cancer therapy (Rusch et al., 1997; Fujimoto et al., 2005). Congruently, EGFR ligand expression was found in many NSCLC cell lines in the panel (table 1).



Cell line	EGFR expression level and mutation status *		KRAS status	No/low expression **	Medium expression **	High expression **	Additional characteristics
H1781	No/Low	Wild type	Wild type	AREG, BTC, EGF, ErbB4, EREG, HB-EGF, NRG1, NRG2	TGF $\alpha$	ErbB2, ErbB3	ErbB2-G776V mutation (Shigematsu et al., 2005)
H460		Wild type	Q61H mutation	AREG, BTC, ErbB2, ErbB3, ErbB4, EREG, NRG2, TGF $\alpha$	EGF, HB-EGF, NRG1		
A549	Medium	Wild type	G12S mutation	BTC, EGF, ErbB2, ErbB3, ErbB4, HB-EGF, NRG2	TGF $\alpha$	AREG, EREG, NRG1	
Calu-3		Wild type	Wild type	BTC, EGF, ErbB4, NRG2	HB-EGF	AREG, ErbB2, ErbB3, EREG, TGF $\alpha$ , NRG1	
Calu6		Wild type	Q61K	AREG, BTC, EGF, ErbB2, ErbB3, ErbB4, NRG1, NRG2	EREG, HB-EGF, TGF $\alpha$		
H1650		delE746-A750 mutation	Wild type	AREG, BTC, EGF, ErbB4, EREG, HB-EGF, NRG1, NRG2	ErbB2, ErbB3, TGF $\alpha$		Lack of PTEN (Janmaat et al., 2006)
H1666		Wild type	Wild type	BTC, EGF, ErbB2, ErbB3, ErbB4, NRG1, NRG2, TGF $\alpha$	EREG, HB-EGF	AREG	BRAF-V470F mutation (Toyooka et al., 2007)
H1975		L858R + T790M mutations	Wild type	BTC, EGF, ErbB4, NRG2	AREG, ErbB2, ErbB3, EREG, NRG1, TGF $\alpha$	HB-EGF	APC-T1556 frameshift (COSMIC database)
H292		Wild type	Wild type	BTC, EGF, ErbB4, EREG, NRG1, NRG2	AREG, ErbB2, ErbB3, TGF $\alpha$	HB-EGF	
H322		Wild type	Wild type	BTC, EGF, ErbB4, HB-EGF, NRG1, NRG2	AREG, ErbB2, ErbB3, EREG, TGF $\alpha$		p53 mutation (Zhang et al., 1994)
H4006		del746-750, S752V mutations	Wild type	BTC, ErbB4, EREG, NRG1, NRG2	AREG, EGF, ErbB2, HB-EGF, TGF $\alpha$	ErbB3	
HCC2279	High	del746-750 mutations	Wild type	BTC, EGF, ErbB2, ErbB3, ErbB4, NRG1, NRG2	AREG, EREG, TGF $\alpha$	HB-EGF	
HCC-827		delE746-A750 mutations	Wild type	BTC, EGF, ErbB4, HB-EGF, NRG2, TGF $\alpha$	AREG, ErbB2, ErbB3,	EREG, NRG1	

**Table 1 NSCLC cell lines characterized in this thesis and mRNA expression status of ErbB receptors and ligands.** (\*) EGFR mRNA, as well as (\*\*) ErbB receptor and ligand mRNA expression status has been determined with Affymetrics whole genome DNA chips as described in material and methods. Expression levels are indicated by grey scales (light grey = no/low expression, medium grey = medium expression, dark grey = high expression) and additional characteristics worth mentioning are noted.

### 3.1.2.2 Growth inhibition of NSCLC cells under drug treatment

The ability of gefitinib to cause growth inhibition in a pre-characterized panel of NSCLC cell lines was examined in order to confirm and extend current data available from the literature. In addition, the capacity of cetuximab to inhibit growth in this heterogeneous cell panel was determined, since not much is known about cellular sensitivity parameters for this therapeutic antibody.

Cell line	Gefitinib	Cetuximab	
	IC <sub>50</sub> [μM]	IC <sub>50</sub> [μg/ml]	Max. Inhibition [%]
A549	9,8	n.d.	0
Calu-3	1,9	0,27	21
Calu-6	26,4	n.d.	0
H1650	2,8	n.d.	0
H1666	11,1	0,39	23
H1781	10,9	n.d.	0
H1975	13,5	n.d.	0
H292	0,5	0,07	45
H322	4,9	0,72	73
H4006	0,02	n.d.	0
HCC2279	14,3	n.d.	0
HCC-827	0,003	0,084	25

**Table 2 Growth Inhibition of human NSCLC cell lines by gefitinib and cetuximab.** Monolayer growth - inhibition assays were performed as described in material and methods and evaluated using the Wst1 reagent by absorbance determination with a Mithras plate reader. EC<sub>50</sub> values were calculated as mean values from triplicates with Graph Pad Prism software. "Max. Inhibition" means growth inhibition in % at a maximal cetuximab concentration of 100μg/ml. Growth inhibition by gefitinib was 100% for all tested cell lines at the maximal treatment doses of 100μM. "n.d." means not determinable.

In monolayer growth assays, treatment with gefitinib showed variable effects on NSCLC cells expressing wild-type EGFR, e.g. H292 cells were sensitive to the TKI, while Calu6 and H1781 cells did not respond well, reflected by EC<sub>50</sub> values above 10μM (table 2). As reported earlier, H4006, HCC-827 and H1650 cell lines, which all carry EGFR mutations, responded well to gefitinib treatment with EC<sub>50</sub> values below 3μM. Interestingly, HCC2279 cells that do express mutant EGFR turned out to be rather resistant to gefitinib even at high doses resulting in an EC<sub>50</sub> of 14,3μM.

Cetuximab had only minor effects on the wild-type EGFR cells H1666, H292 and Calu3, except H322 that were particularly sensitive to cetuximab with an efficacy of 73% and an  $EC_{50}$  of 0,72 $\mu$ g/ml (table 2). Similarly, only one cell line expressing mutated EGF receptor (HCC827) was moderately inhibited by cetuximab.

To better reflect the pathophysiological situation, three-dimensional growth of the NSCLC cells in a soft-agar matrix was assessed. All cells in the panel were subsequently classified based on the  $EC_{50}$  value and efficacy of growth inhibition caused by gefitinib or cetuximab. The response to gefitinib in soft-agar assays was largely equivalent to that observed in monolayer assays (figure 14). In line with published results with EGFR-del746-750 expressing PC9 cells (Perez-Torres et al., 2006), an augmented response to gefitinib was seen in cell lines expressing mutant EGFR, such as H1650, H4006 or HCC827. While H1650 cells were classified sensitive, H4006 and HCC827 were classified very sensitive according to the categorization key specified in legend of figure 14. Contrary data were observed only for H1975, which carry the resistance conferring T790M mutation, as well as for the HCC2279 cell line. These cell lines were rated non-responsive (H1975) or moderately sensitive (H2279) reflected by efficacy values below 50% or 25%, respectively. The non-responsiveness of the latter cell line had been described earlier in a monolayer growth assay; however the underlying mechanism is still unclear (Fujimoto et al., 2005).

For cetuximab a different picture arose from three-dimensional growth assays, in contrast to the observations made in monolayer growth assays. The effects of cetuximab on several cell lines were more pronounced in the soft agar assay. While the growth of three cell lines expressing wild-type EGFR was efficiently inhibited by cetuximab (H292, H322 and A549), three others were not significantly affected (H1781, Calu3 and Calu6) (figure 14). Out of four NSCLC cell lines that express gefitinib-sensitizing EGFR mutations, colony formation of two was marginally impaired by cetuximab (H4006, H1650) and growth of one was strongly inhibited by cetuximab (HCC827). Interestingly, three-dimensional growth of the gefitinib-resistant cell line H1975 was inhibited by cetuximab while it was not affected in the monolayer assay. The same is true for A549 cells that carry an activating KRAS mutation.

Cell line	EGFR	KRAS	Gefitinib			Cetuximab		
			EC <sub>50</sub> value	Efficacy <sup>1</sup>	Categorization	EC <sub>50</sub> value	Efficacy <sup>2</sup>	Categorization
A549	wt	G12S			NC			Sens
Calu6	Wt	Q61K			Res			Res
H460	wt	Q61H			Res			Res
H1781	wt	wt			NC			Res
H292	wt	wt			Sens			Sens
H322	wt	wt			Sens			Sens
Calu3	wt	wt			Sens			Res
H1975	L858R/ T790M	wt			Res			Sens
H1650	delE746- A750	wt			Sens			Res
H4006	del746- 750	wt			Sens			Res
HCC2279	del746- 750	wt			Res			Res
HCC827	delE746- A750	wt			Sens			Sens

**Figure 14 Inhibition of colony formation in human NSCLC cell lines by gefitinib and cetuximab.** For soft-agar colony formation assays, cells were treated with variable doses of cetuximab and gefitinib in serum free medium for 8 days. Cell lines were categorized in relation to their sensitivity to either gefitinib or cetuximab. Cell lines were classified “very sensitive” (dark green) for an EC<sub>50</sub><0,01μM (Gefitinib) or an EC<sub>50</sub><0,1μg/ml (Cetuximab), respectively, and for an efficacy >75%. “Sensitive” (bright green) for 0,01μM< EC<sub>50</sub><0,1μM (Gefitinib) or 0,1μg/ml<EC<sub>50</sub><1μg/ml (Cetuximab), respectively, and for 50%<efficacy<75%. “Moderately sensitive” (orange) for 0,1μM< EC<sub>50</sub><1μM (Gefitinib) or 1μg/ml< EC<sub>50</sub><10μg/ml (Cetuximab), respectively, and for 25%<efficacy<50%. “Non-responsive” (red) for an EC<sub>50</sub>>1μM (Gefitinib) or EC<sub>50</sub>>10μg/ml (Cetuximab), respectively, and for an efficacy<25%. <sup>1</sup> Efficacy corresponds to % of cell number reduction at a concentration of 1μM gefitinib or 10μg/ml cetuximab as compared to untreated control.

From these data it appeared that colony formation assays were more appropriate to study the effects of cetuximab on cell growth than monolayer growth tests. Furthermore, with a single exception (HCC2279), a higher degree of sensitivity to gefitinib, reflected by lower EC<sub>50</sub> values, was observed in NSCLC carrying EGFR mutations. Cetuximab was able to inhibit growth of NSCLC cells expressing mutated

EGFR as well as of those expressing wild-type receptor. These data suggest that EGFR mutations do not have the same predictive value for cetuximab sensitivity as they do have for TKI. Based on the soft-agar assays growth responses gained, sensitivity categories were developed, which also refer to in the following sections (figure 14).

### **3.1.2.3 Examination of cellular signal transduction in NSCLC cells**

To better understand the observed growth responses to gefitinib and cetuximab, signaling cascades in the different NSCLC cell lines were extensively studied. All data sets are summarized in a heat plot graph in figure 15a and exemplary data for some cell lines are shown in figures 15b-d. The effect of the drugs on the phosphorylation of EGFR and on the EGF-induced activation of Akt and MAPK within the cell panel was compared with their inhibitory potential in the soft-agar assay.

In many cases an inhibition of EGFR phosphorylation by cetuximab was associated with sensitivity of the respective cell line in the three-dimensional growth assay. However, Calu6 and H1650 cells were non-responsive to cetuximab in the soft-agar assay, while EGFR phosphorylation was effectively inhibited by the antibody. On the other hand, phosphorylation of EGFR and downstream signaling in HCC-827 cells was not abolished by cetuximab, but the growth of cells was still very responsive to this drug.

Cell line	EGFR	KRAS	Gefitinib				Cetuximab			
			pEGFR	pAkt	pMAPK	Classification (*)	pEGFR	pAkt	pMAPK	Classification (*)
A549	wt	G12S				NC				Sens
Calu6	wt	Q61K				Res				Res
H1666	wt	wt				NG				NG
H1781	wt	wt				NC				Res
H292	wt	wt				Sens				Sens
H322	wt	wt				Sens				Sens
Calu3	wt	wt				Sens				Res
H1975	L858R/ T790M	wt				Res				Sens
H1650	delE746- A750	wt				Sens				Res
H4006	del746- 750	wt				Sens				Res
HCC2279	del746- 750	wt				Res				Res
HCC827	delE746- A750	wt				Sens				Sens

**Figure 15a Ligand activated NSCLC cells expressing wild-type and mutated EGFR showed variable signaling responses upon treatment with cetuximab and gefitinib.** Cells were treated with variable doses of cetuximab [ $\mu\text{g/ml}$ ] or gefitinib [ $\mu\text{M}$ ] (45min) and stimulated with EGF (30ng/ml, 10min) after serum starvation. After lysis, phosphorylated EGFR (Y1068), phosphorylated MAPK (Tyr202/Tyr204) and phosphorylated Akt (Ser 473) were detected as marker proteins for EGFR-mediated signaling by immunoblotting. Membranes were probed with a cofilin antibody as protein loading control. Cell lines were categorized with respect to the capability of gefitinib or cetuximab to inhibit EGF-mediated phosphorylation of target proteins. Cell lines were classified “Very sensitive” (dark green) for a 50% reduction of the phosphorylation signal at a concentration of 0,1 $\mu\text{M}$  (gefitinib) or 1 $\mu\text{g/ml}$  (cetuximab), respectively. “Sensitive” (bright green) for a 50% reduction of the phosphorylation signal at a concentration of 1 $\mu\text{M}$  (gefitinib) or 10 $\mu\text{g/ml}$  (cetuximab). “Moderately sensitive” (orange) for a 50% reduction of the phosphorylation signal at a concentration of 10 $\mu\text{M}$  (gefitinib) or 100 $\mu\text{g/ml}$  (cetuximab). “Non-responsive” (red) for a reduction of the phosphorylation signal at a concentration of 10 $\mu\text{M}$  (gefitinib) or 100 $\mu\text{g/ml}$  (cetuximab) that was lower than 50%.

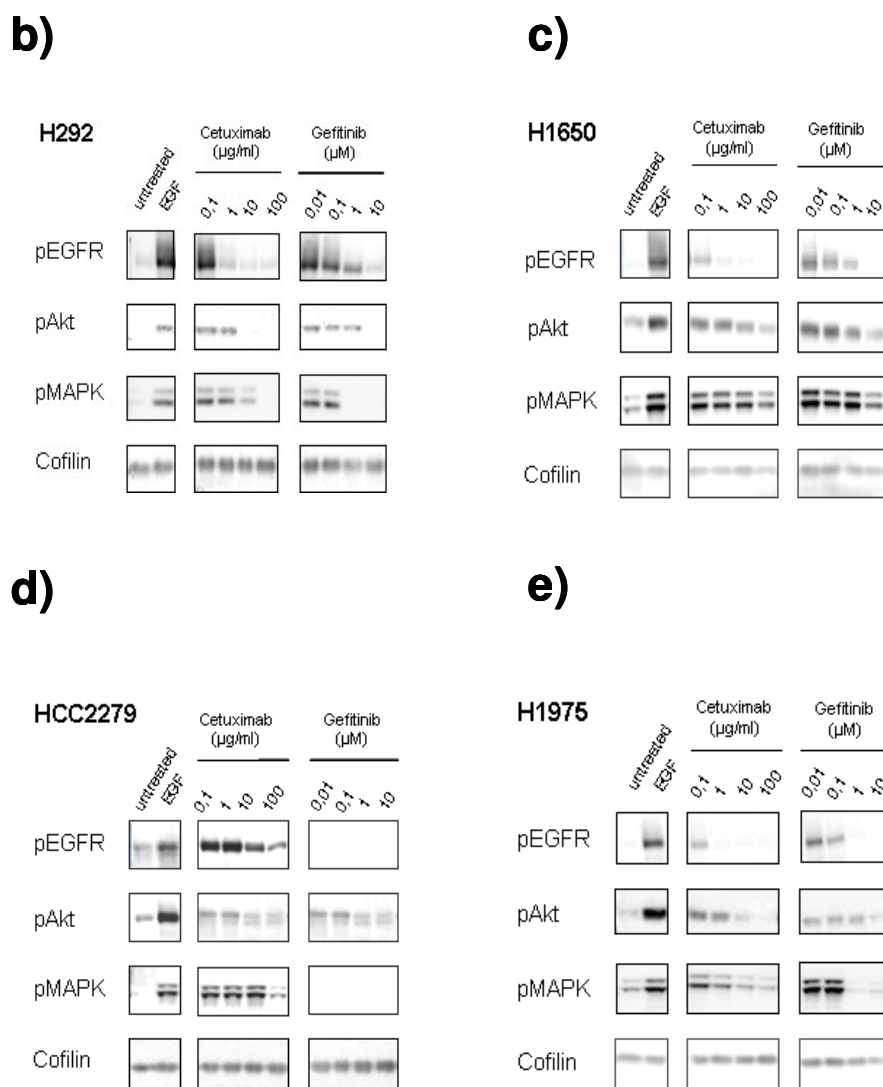


**Figure 15 b-d Ligand activated NSCLC cells expressing wild-type and mutated EGFR showed variable signaling responses upon treatment with cetuximab and gefitinib.** Exemplary immunoblots for (b) H292, (c) H1650, (d) H1975 and (e) HCC2279 cell lines are shown.

In summary, neither EGFR phosphorylation nor interference with MAPK or Akt activation appeared to be robust prognostic indicators for cetuximab induced growth inhibition in an agar matrix. Similar observations, e.g. only partial correlation of signaling and growth inhibition, were made for gefitinib, even in a cell line (H1650) bearing an EGFR mutation, which is particularly responsive to this TKI (figure 14).

### 3.1.2.4 Tumor regression of NSCLC cells under drug treatment in murine xenografts

To substantiate the data obtained in the three-dimensional growth assays and the signal transduction studies, murine tumor xenograft experiments in athymic mice with the panel of those NSCLC cell lines that developed subcutaneous tumors were applied. In perfect agreement with the in vitro data from soft-agar assays, H292 tumors responded very well to either i.p. to 15mg/kg or 50mg/kg cetuximab (twice a week) or p.o. to gefitinib (daily) leading to 95% (cetuximab) and 79% (gefitinib) reduction in tumor burden, respectively (figure 16c). A similar match of in vitro and in vivo response data was seen for H1975 tumors that were non-responsive to gefitinib but responsive to cetuximab resulting in 79% tumor burden decrease (figure 16b).

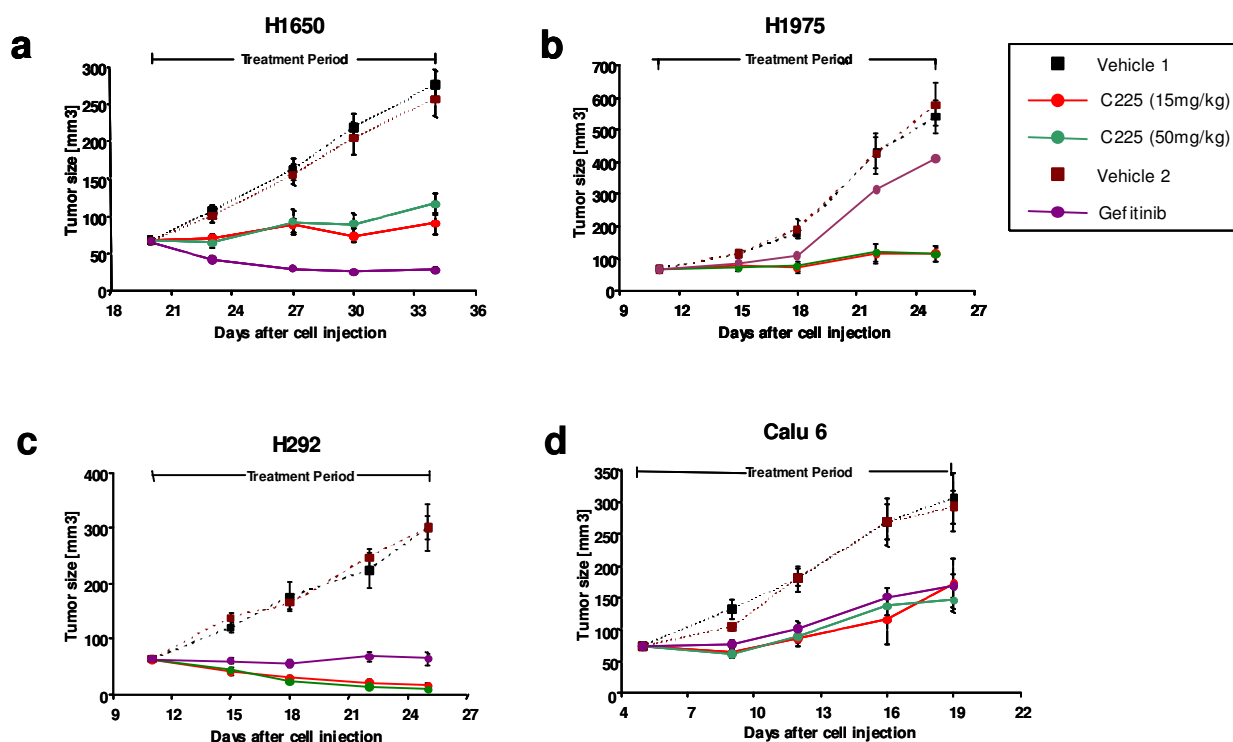


**Figure 16 Inhibitory effects of cetuximab or gefitinib on tumor formation of NSCLC cell lines in murine xenografts.** Murine xenograft experiments were performed with (a) H1650, (b) H1975, (c) H292 and (d) Calu6 cell lines as described in material and methods. Mice were treated daily with gefitinib (40mg/kg/d), twice a week with cetuximab (C225) (15mg/kg or 50mg/kg) or vehicle controls, after subcutaneous injection of cells, randomization and scheduling of treatment groups (n=10). Mouse husbandry and conduction of xenograft experiments was done by Mr. Schuster and Mrs. Schaefer in the laboratory of Dr. Amendt, Merck KGaA.



A discrepancy between in vivo and in vitro data was seen for H1650 cells that were effectively inhibited by both drugs in vivo (67% and 89% tumor burden decrease for cetuximab and gefitinib, respectively) (figure 16a), but were non-responsive to cetuximab in the colony formation assay (cf. figure 14). This finding is of particular interest, since H1650 lack expression of PTEN. Similarly, Calu-6 cells that carry an activating KRAS mutation were moderately affected by cetuximab and gefitinib in mouse xenografts (44% and 57% tumor burden reduction, respectively) (figure 16d), but completely resistant in vitro (cf. figure 14). These examinations showed that cetuximab displays in vivo efficacy in NSCLC cells with any genetic background, while expression of EGFR-T790M confers resistance to gefitinib.

To analyze whether the two drugs inhibited their target in vivo tumor tissues at the end of the treatment period was collected and EGFR phosphorylation, as well as MAPK and Akt activation was determined by immunoblotting using phospho-specific antibodies. A marked decrease of phospho-EGFR, phospho-Akt and phospho-MAPK signals was found after cetuximab treatment in H1650 xenografts (figure 17a), while only a slight (pEGFR, pAkt) and no pharmacodynamic effect (pMAPK) was observed in H1975 xenografts (figure 17b). Congruent with the lack of xenograft growth inhibition of H1975 cells upon gefitinib treatment, corresponding tumors showed only modestly reduced levels of phospho-EGFR and phosphoMAPK and no reduction of pAkt (figure 17b). Yet a clear reduction of phospho-EGFR, phospho-Akt and phospho-MAPK was observed in H1650 xenografts upon gefitinib treatment (figure 17a).

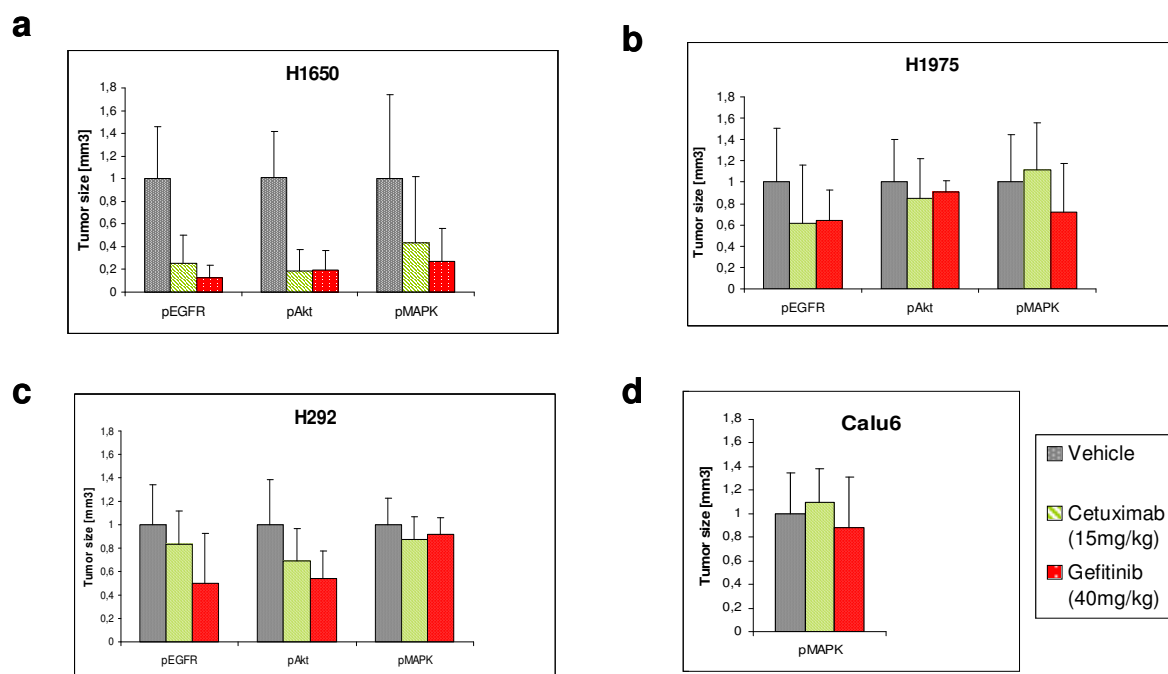


**Figure 17 Inhibitory effects of cetuximab or gefitinib on EGFR-mediated signaling of NSCLC cell lines in murine xenografts.** At the day of scarifice, mice from xenograft experiments were treated with the respective drug concentrations two h prior to resection. Tumors were removed, processed and protein lysates were analyzed for phosphorylation levels of EGFR, MAPK and Akt with immunoblots. Chemiluminescence signals were detected and quantified with BioRad Quantity One® software. Each bar is the average from five to ten tumor lysates (mean +/- standard deviation).

A modest reduction of Akt activation was observed for cetuximab-treated H292 tumors, but interestingly no decrease in phosphorylation of EGFR or MAPK was seen in the same tumors. However, a minor gefitinib-mediated decrease in phospho-EGFR and phospho-Akt, was found in H292 tumors (figure 17c). This is striking, as H292 tumors respond well to either drug (cf. figure 16c). For murine tumors originating from transplanted Calu6 cells, neither phospho-EGFR, nor phospho-Akt could be detected via immunoblotting. Activated MAPK could be detected in these tissues; however, for this marker no alteration was found (figure 17d). It can be inferred from these examinations that inhibition of neither EGFR nor Akt or MAPK activation with cetuximab or gefitinib is clearly correlated to tumor sensitivity to either drug.

### **3.1.2.5 Identification of response predicting marker genes through gene expression profiling in drug sensitive and resistant NSCLC cell lines**

Because interference with EGFR signaling pathways in vitro did not correlate well with cellular growth inhibition in response to gefitinib or cetuximab, an unbiased global gene expression profiling approach was carried out to identify candidate genes or a signature associated with response of NSCLC cell line to EGFR inhibitors. Based on the in vitro sensitivity classification in the colony formation assay (cf. figure 14) cell lines were classified for each drug into a “resistant” and a “sensitive” group. Due to the intermediate and therefore not clearly classifiable responses gained for A549 and H1781 cells upon gefitinib treatment, these were not included in the analyses for gefitinib.

A statistical comparison between gefitinib-resistant and sensitive cell lines was performed for 9002 Affymetrix probe sets fulfilling global filtering criteria (see Materials and Methods). Based on this analyses 56 probe sets representing 46 known genes showed significantly differential expression with an unadjusted  $p < 0,001$ , corresponding to a false discovery rate of 0,16 (table 3). Interestingly, from these 46 candidates, 17 (37%) had been identified in a recently published study that also examined expression profiling with NSCLC cell lines based on their response to gefitinib in a monolayer assay. This includes tumor-associated calcium signal transducer 2 (TACSTD2) and E-cadherin (CDH1), whose overexpression in gefitinib sensitive NSCLC cells has already been validated on the protein level (Coldren et al., 2006). Furthermore, the analyses confirmed 8 (17%) candidate genes that were identified in an examination with NSCLC cells profiled for their sensitivity against erlotinib (Yauch et al., 2005). Seven of these genes were also identified in the gefitinib response analyses from Coldren and two of them (TACSTD2 and CDS1) were additionally found in another expression profiling study with NSCLC cells and tumor samples to identify response predictors for erlotinib (Balko et al., 2006).

GeneSymbol	Gene Name	ratio **	p.value	FDR	Literature
ELOVL7	ELOVL family member 7, elongation of long chain fatty acids	9,52	1,3E-06	0,01152	
ALDH1A3	aldehyde dehydrogenase 1 family, member A3	16,5	1,2E-05	0,04607	1,3
C1orf106	chromosome 1 open reading frame 106	9,81	1,8E-05	0,04607	
C20orf100	chromosome 20 open reading frame 100	0,11	2,2E-05	0,04607	
MOBK2B	Mps One Binder kinase activator-like 2B	5,81	2,6E-05	0,04607	
FGFBP1	Fibroblast growth factor-binding protein 1	4,57	6,7E-05	0,08249	
TSPAN1	tetraspanin 1	9,02	0,00007	0,08249	1,3,6
KCNK1 *	potassium channel, subfamily K, member 1	5,96	7,3E-05	0,08249	1
TACSTD2	tumor-associated calcium signal transducer 2	38,5	8,4E-05	0,08416	1
ST14 *	suppression of tumorigenicity 14	8,37	0,00011	0,0911	1,3
DMKN	dermokine	6,92	0,00011	0,0911	
CLDN7	Claudin-7	7,94	0,00013	0,0911	1,3
ELF3	E74-like factor 3	7,66	0,00014	0,0911	1
RAB25	RAB25, member RAS oncogene family	16,1	0,00016	0,0911	
RBM35A *	RNA binding motif protein 35A	14,3	0,00019	0,0911	
VGLL1	vestigial like 1	21,9	0,00019	0,0911	
VGLL3	vestigial like 3	10,8	0,00019	0,0911	
MAL2	T-cell differentiation protein 2	26,6	0,0002	0,0911	1,3
CDH1 *	E-cadherin	26,3	0,0002	0,0911	1
TRIM22	tripartite motif-containing 22	12,4	0,00025	0,1016	
MOBK2B	MOB1, Mps One Binder kinase activator-like 2B	3,78	0,00026	0,1016	
GPR110	G protein-coupled receptor 110	9,05	0,00027	0,1016	1
SPINT1	serine peptidase inhibitor, Kunitz type 1	9,36	0,00031	0,1016	1,3
HPCAL1 *	Hippocalcin-like protein 1	0,24	0,00027	0,1016	
COL6A1	Collagen alpha-1(VI) chain	0,14	0,00029	0,1016	
HERC6	HECT domain and RCC1-like domain-containing protein 6	4,91	0,00034	0,10451	
SAMD9	sterile alpha motif domain containing 9	6,54	0,00035	0,1048	
FXYD3	FXYD domain containing ion transport regulator 3	12,1	0,00036	0,1048	1
ANXA6	Annexin A6	0,27	0,00042	0,11189	3
CENTD1	Centaurin-delta 1	3,77	0,00042	0,11189	1
KLF5	Kruppel-like factor 5	5,13	0,00044	0,11189	
FKBP11 *	FK506-binding protein 11	0,16	0,00043	0,11189	
EPS8L2	Epidermal growth factor receptor kinase substrate 8-like protein 2	3,88	0,00045	0,11323	1
EDG2	Lysophosphatidic acid receptor 1	4,84	0,00048	0,11425	
LIMA1	LIM domain and actin-binding protein 1	3,53	0,00054	0,12181	
TNNC1	troponin C type 1 (slow)	6	0,00055	0,12181	
SLC44A3	Choline transporter-like protein 3	3,82	0,00062	0,13273	
TIMP4	Metalloproteinase inhibitor 4	0,3	0,0008	0,15761	
SH2B3	SH2B adapter protein 3	0,22	0,00082	0,15761	
CA12 *	Carbonic anhydrase 12	0,21	0,00084	0,15761	
TMEM30B	transmembrane protein 30B	11,7	0,00087	0,15761	
ECHDC2	Enoyl coenzyme A hydratase domain-containing protein 2	3,1	0,0009	0,15761	
CXCL16	chemokine (C-X-C motif) ligand 16	4,4	0,00093	0,15761	
SHROOM3	Shroom3	4,08	0,00095	0,15761	
STARD10	START domain containing 10	4,07	0,00095	0,15761	1
FLJ20920	hypothetical protein FLJ20920	3,26	0,00096	0,15761	
CDH11	Cadherin-11 (Osteoblast-cadherin)	0,06	0,00096	0,15761	

**Table 3 Gene expression profiling for the identification of candidates predicting growth response to gefitinib.** Whole genome expression profiling was performed as described in section material and methods. (\*) Indicates that the respective gene found to be differentially regulated (p-value <0,001) by more than one probe in a panel of ten NSCLC cell lines. The figure lists the probe with the lowest p-value. (\*\*) Depicts the quotient between mean Affymetrix signals of the cells that were classified sensitive and signal of cells classified resistant to gefitinib (mean signal<sub>sensitive</sub> / mean signal<sub>resistant</sub>). "Literature" Indicates that the corresponding gene has been found to be putatively predictive by other authors (Coldren et al., 2006 (1); Balko et al., 2006 (2); Yauch et al., 2005 (3)).

Among the new identified candidates associated with gefitinib response, were genes that are possibly involved in controlling expression of distinct target mRNAs (C20orf100, RBM35A, VGLL1, KLF5), in regulating activity of specific signal transduction components (MOBKL2B, ZD52F10, EDG2, SH2B3, CXCL16), as well as in managing cellular invasion or tumor homeostasis (COL6A, LIMA1, TNNC1, CA12, TIMP4, SHROOM3, CDH11), cellular proliferation (TRIM22, SAMD9) or balancing of calcium or other ion levels (KCNK1, HPCAL1, CA12, CXCL16).

A similar analyses for the identification of genes predictive for in vitro response to cetuximab revealed only one candidate (TRIM6) with an unadjusted  $p < 0,001$  (table 4). However, choosing a p-value cutoff of 0,02 leads to 33 genes that could be associated with response to cetuximab (table 4). Several of these candidates have been linked with cellular signal transduction processes (SDC2, RGS20, TMEM46, AMFR, JAG2, TSPAN8, TGFB1, SOCS2, DUSP6, CD109), with cellular adhesion and migration (SDC2, RGMB, AMFR, SRGAP1, MMP2) and protein trafficking (TMEM46, LPHN1, CPNE3, SPG20, ANXA8), but the list also includes transcription factors (TRIM6, PLAGL1) and proteins associated with balancing of calcium levels (STOM, ANXA8, CADPS2). Though statistically questionable the identified gene candidates promise potential biological significance and warrant further examination.

GeneSymbol	Gene Name	ratio **	p.value
TRIM6	tripartite motif-containing 6	4,4	0,00096
ALDH3B1 *	aldehyde dehydrogenase 3 family, member B1	3,24	0,0026
SUSD2	sushi domain containing 2	2,43	0,0035
SDC2 *	syndecan 2	0,16	0,0036
RGS20	regulator of G-protein signalling 20	3,3	0,0042
KIAA1609	KIAA1609	2,42	0,0044
PLAGL1 *	pleiomorphic adenoma gene-like 1	0,29	0,0053
RGMB	RGM domain family, member B	0,39	0,0068
STOM	stomatin	2,83	0,007
LOC400566	hypothetical gene supported by AK128660	2,29	0,009
TMEM46	transmembrane protein 46	0,26	0,01
GPR172A	G- protein coupled receptor 172A	0,43	0,011
TACC2 *	transforming, acidic coiled-coil containing protein 2	2,12	0,012
AMFR	autocrine motility factor receptor	0,46	0,012
CCT5	chaperonin containing TCP1, subunit 5	0,44	0,013
PLAGL1	pleiomorphic adenoma gene-like 1	0,36	0,013
HYLS1	hydroletharus syndrome 1	2,31	0,014
JAG2 *	jagged 2	2,09	0,014
TGFB1	transforming growth factor, beta 1	0,4	0,014
TSPAN8	tetraspanin 8	0,16	0,014
LPHN1	latrophilin 1	0,44	0,015
CPNE3	copine III	2,03	0,015
SOCS2 *	suppressor of cytokine signaling 2	2,72	0,017
C16orf74	chromosome 16 open reading frame 74	1,83	0,017
MMP2	matrix metalloproteinase 2	0,3	0,017
SRGAP1	SLIT-ROBO Rho GTPase activating protein 1	1,99	0,017
CADPS2	Ca <sup>2+</sup> -dependent activator protein for secretion 2	0,31	0,017
DUSP6 *	dual specificity phosphatase 6	0,34	0,017
BRP44L	brain protein 44-like	0,49	0,018
ANXA8	Annexin A8 (Annexin VIII)	3,93	0,018
AGPAT1	1-acylglycerol-3-phosphate O-acyltransferase 1	0,53	0,018
SEZ6L2	seizure related 6 homolog (mouse)-like 2	0,41	0,018
SLC1A4	solute carrier family 1, member 4	0,46	0,019
SPG20	spastic paraplegia 20, spartin	3,63	0,02
H2AFX	H2A histone family, member X	2,08	0,02
RNF144	Ring finger protein 144	0,45	0,02
C5orf13	chromosome 5 open reading frame 13	0,34	0,02
H2AFX	H2A histone family, member X	2,06	0,02
BTBD11	BTB (POZ) domain containing 11	2,91	0,02

**Table 4 Gene expression profiling for the identification of candidates predicting growth response to cetuximab.** Whole genome expression profiling was performed as described. (\*) Indicates that the respective gene was found to be differentially regulated (p-value <0,02) by more than one probe in a panel of twelve NSCLC cell lines. The figure lists the probe with the lowest p-value. (\*\*) Depicts the quotient between mean Affymetrix signals of the cells that were classified sensitive and these classified resistant to gefitinib (mean signal<sub>sensitive</sub> / mean signal<sub>resistant</sub>).

### **3.2 *Establishment and characterization of cancer cell lines treated long-term with EGFR-directed cancer drugs***

An appropriate pre-selection of cancer patients for EGFR-directed cancer therapy is important in order to achieve significant clinical outcomes. Aside from EGFR kinase domain mutations, which are highly predictive for clinical and in vitro response to gefitinib, but not for antibody therapy, reliable biomarkers with prognostic value for cetuximab have not yet been identified. Furthermore, as can be seen from clinical and laboratory studies, mutations in kinase domain are neither exclusive nor stringently predictive for sensitivity to gefitinib (Irmer et al., 2007a). In addition, tumors with primary sensitivity to gefitinib do often relapse and gain resistance against TKI treatment. The same holds also true for therapy with therapeutic antibodies, such as cetuximab (Italiano, 2006).

Thus, four cancer cell lines, two with primary sensitivity and two with primary resistance, were exposed to either cetuximab or gefitinib for a period of several months in order to study long-term effects of different EGFR-directed therapies in a cell culture model.

#### **3.2.1 Identification and selection of cancer cell lines with primary drug resistance and sensitivity**

Four cell lines were selected on the basis of preceding examinations. Difi is a colorectal cancer cell line that was derived from a familial adenomatous polyposis patient (Gross et al. 1991). A431 is an epidermoid carcinoma cell line (Krupp et al., 1982). Both cell lines express high levels of EGFR and are sensitive to EGFR-targeting cancer therapeutics (Wu et al., 1995; Janmaat et al., 2003). In contrast, the lung cancer cell line H460 and colorectal cell line SW707 express moderate or very low levels of EGFR and are not responsive to gefitinib or cetuximab. In order to substantiate these observations and to directly compare cellular responsivity, the four cell lines were subjected to growth inhibition by cetuximab and gefitinib.

Diffi cells were highly sensitive to cetuximab in a monolayer growth assay ( $EC_{50} < 0,1 \mu\text{g/ml}$ ) and moderate effects were observed for A431 cells, while H460 as well as SW707 cell lines did not show any growth inhibition, even at high doses of cetuximab.

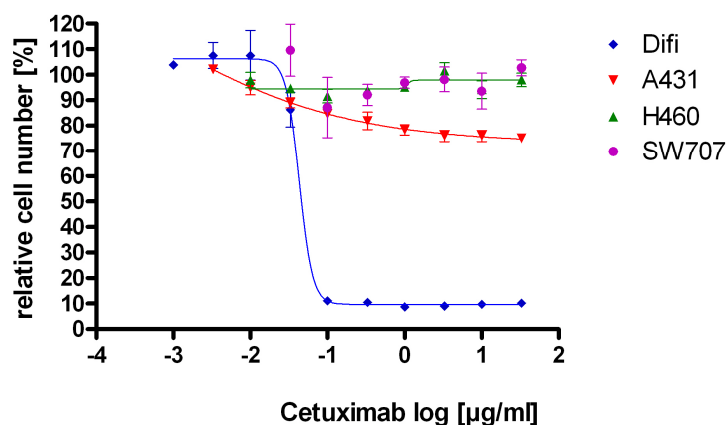


**Figure 18** Difi cells were found to be sensitive to cetuximab in a monolayer growth assay. Monolayer growth inhibition assays with A431, Difi, H460 and SW707 cells were performed under treatment with variable doses of cetuximab. Assay evaluation with Wst1 reagent by absorbance measurement on a plate reader and data processing with Graph Pad Prism software were performed as described.

As expected from the studies with NSCLC cell lines (table 2 and figure 14), 3D growth in softagar was more sensitive to EGFR inhibition. Under these conditions growth of A431 cells was markedly inhibited by cetuximab ( $EC_{50} < 1 \mu\text{g/ml}$ ). Difi cells again responded very well ( $EC_{50} < 1 \mu\text{g/ml}$ ), while colony formation of H460 and SW707 cells was not influenced by cetuximab (figure 19).

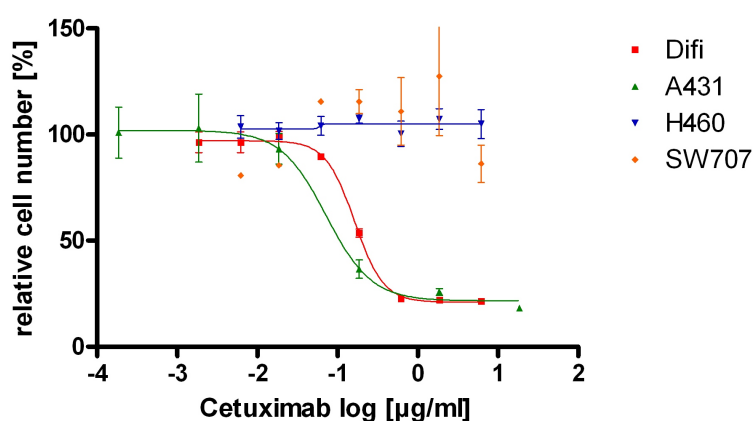


**Figure 19** Difi and A431 cells were found to be sensitive to cetuximab in a soft agar colony formation assay. Soft-agar assays with A431, Difi, H460 and SW707 cells were performed under treatment with variable doses of cetuximab, evaluated with Cell Titer Blue reagent by fluorescence measurement on a plate reader and data were processed with Graph Pad Prism software.



The sensitivity profiles of the four cell lines towards gefitinib were validated likewise. In a monolayer growth assay Difi cells were hypersensitive to gefitinib ( $EC_{50} < 0,1 \mu\text{g/ml}$ ) and also A431 ( $EC_{50} < 1 \mu\text{g/ml}$ ) are responsive to this drug. As expected from the preceding screens H460 and SW707 cells were found to be resistant to the TKI ( $EC_{50} > 10 \mu\text{g/ml}$ ) (figure 20). Growth effects observed at higher doses were probably due to off-target effects of the TKI.

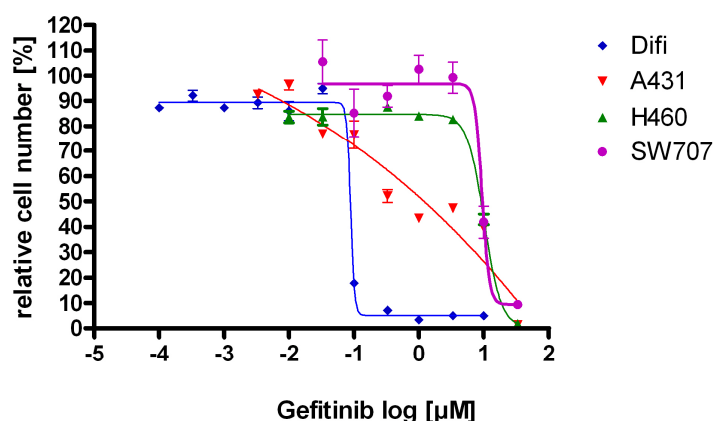


**Figure 20** Difi and A431 cells were found to be sensitive to gefitinib in a monolayer growth assay.

Monolayer growth inhibition assays with A431, Difi, H460 and SW707 cells were performed under treatment with variable doses of gefitinib, evaluated with Wst1 reagent by absorbance measurement on a plate reader and processed with Graph Pad Prism software.

### 3.2.2 Examination of sensitivity and cross-sensitivity of long-term-treated A431 cells

In order to examine A431 cells that had been treated for fifteen months with either gefitinib or cetuximab for acquisition of resistance to the respective drug, growth properties in soft-agar assays were studied. Further it was investigated, if long-term exposure of cells to either drug led to cross-resistance against the other drug. This question is of special interest, since it may have implications for the therapy of cancer patients that e.g. relapse from gefitinib therapy. In this case frequently observed in the clinic, it would be important to know if these patients could profit from subsequent cetuximab regimen.

Before being able to address this question, it was important to remove the drugs from A431 cells after long-term exposure to ensure comparability between the different

populations. Cetuximab exposed A431 cells were washed for variable time points with full medium lacking the antibody and were subjected to FACS analyses to determine residual antibodies on cell surfaces.

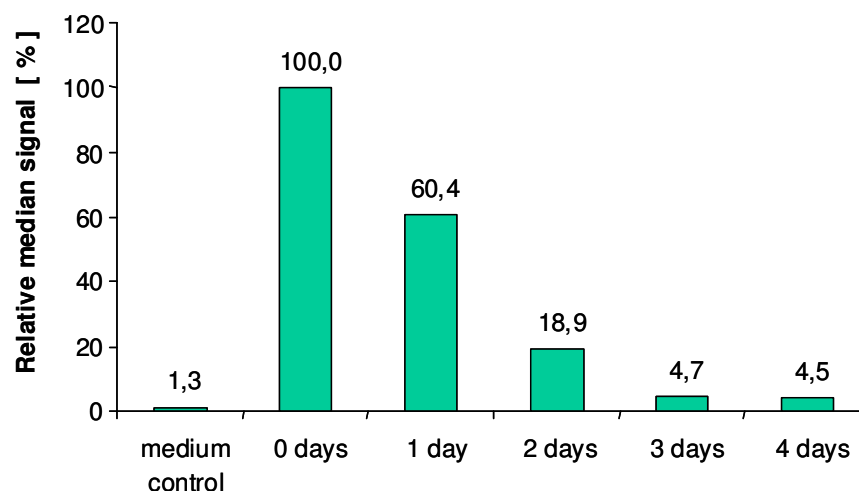


**Figure 21 Washing cetuximab long-term treated A431 cells with medium for three days cleared the cellular surface from antibody.** A431 cells long-term-treated with cetuximab were washed for variable durations (0-4 days) with full medium three times per day. Cetuximab remaining at the cellular surface was detected with a mouse IgG specific FITC conjugated antibody followed by analyses on a Becton Dickinson FACScalibur flow cytometer. Median signal intensity from the fluorescence channel was calculated for every condition and transformed to arbitrary units. Median signal intensities from washed cells were normalized to median signal intensity for unwashed cells (0 days), which were fully covered with cetuximab. Medium-treated A431 cells of similar passage number were used as negative control.

Washing long-term cetuximab-treated A431 cells for three days (three times per day) removed the majority of the antibody from the system (figure 21). A431 cells treated long-term with gefitinib were also washed for three days (three times per day) before they were used for further experiments.

A431 cells that were long-term incubated with gefitinib displayed a significant resistance against this drug in monolayer growth assays, as compared to A431 cells of similar passage number that were cultured in parallel in regular growth medium (untreated control) (figure 22). This was reflected by an  $EC_{50}$  value that is roughly 20 fold higher as the value of the reference population (45 $\mu$ M vs. 2 $\mu$ M). Interestingly, A431 cells that were exposed to cetuximab for 15 months (long-term cetuximab) also displayed a significantly reduced response towards the TKI ( $EC_{50}$  = 24 $\mu$ M). However

this gain is lower than the resistance observed for A431 cells long-term exposed to gefitinib.

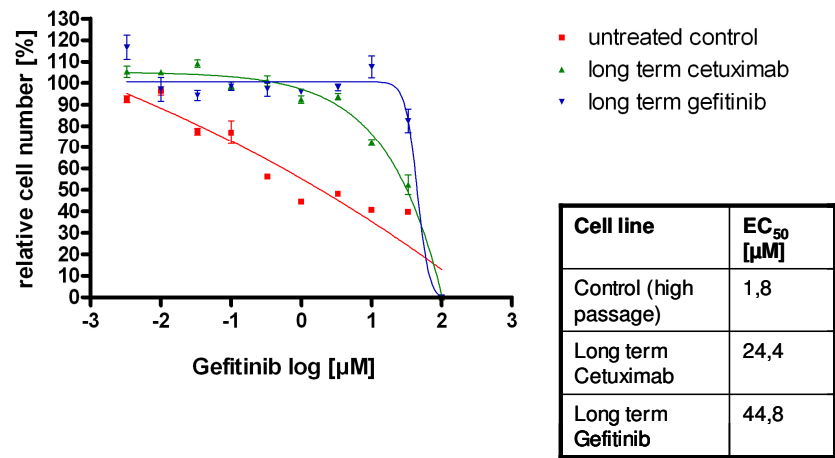


**Figure 22 A431 cells long-term treated with gefitinib or cetuximab showed reduced growth inhibition by gefitinib in a monolayer assay.** A431 cells that were long-term treated with gefitinib or cetuximab were washed for two or three days (three times per day), respectively, with full medium before start of experiment. Together with medium-treated A431 cells of similar passage (untreated control), they were subjected to a monolayer growth assay and treated with variable doses of gefitinib. EC<sub>50</sub> values were calculated as mean values from triplicates using the Graph Pad Prism software. Relative cell numbers under treatment were calculated by signal normalization to medium-treated cells. Each data point is the average from quadruplet values (mean +/- standard deviation).

In addition, soft agar colony formation assays were applied to confirm the data generated with the monolayer growth assays (figure 23).

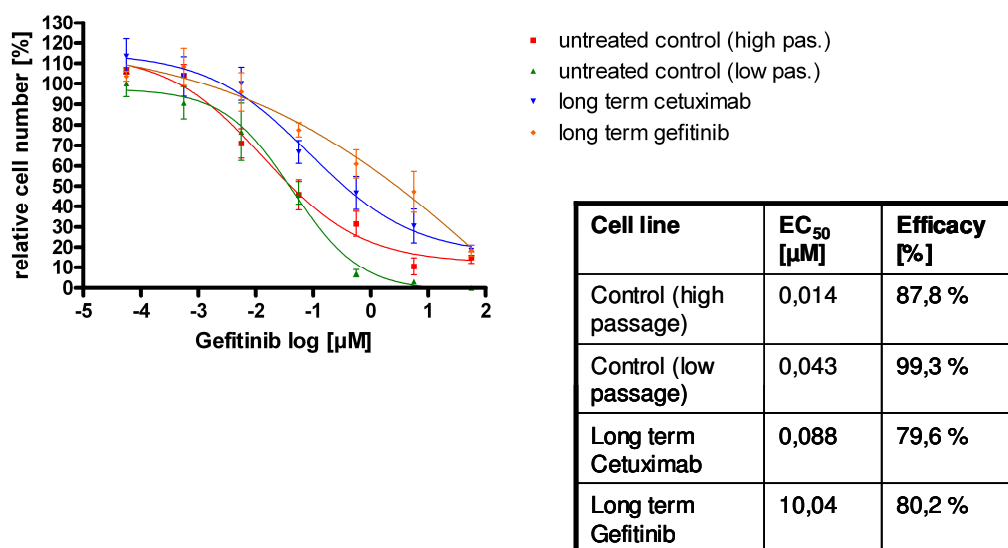


**Figure 23 A431 cells long-term treated with gefitinib or cetuximab showed reduced growth inhibition by gefitinib in a soft-agar assay.** A431 cells that were long-term treated with gefitinib or cetuximab were washed for two or three days (three times per day), respectively, with full medium before start of experiment. Together with medium-treated A431 cells of similar passage (untreated control), they were subjected to a soft-agar colony formation assay and treated with variable doses of gefitinib. EC<sub>50</sub> values were calculated as mean values from triplicates with Graph Pad Prism software. Relative cell numbers under treatment were calculated by signal normalization to medium-treated cells. Each data point is the average from triplicate values (mean +/- standard deviation).

Gefitinib resistance of A431 cells that were long-term exposed to this drug was confirmed in soft-agar assays. Resistance of these cells was reflected by an EC<sub>50</sub> value that was roughly 700 fold higher than the EC<sub>50</sub> value from medium cultured cells of similar passage number (control - high passage) and roughly 200 fold higher than the EC<sub>50</sub> measured for the A431 starting population (control - low passage) (figure 23). A431 cells that were long-term exposed to cetuximab displayed only a moderate gain of resistance to gefitinib, reflected by an EC<sub>50</sub> value that was roughly 4 fold increased over the value of control cells with similar passage number (figure 23). This finding for cetuximab was in contrast to the observation from monolayer growth assays, where A431 cells displayed significant resistance to gefitinib after long-term treatment with cetuximab (figure 22).

The analysis was also performed to test cetuximab-mediated growth inhibition in the long-term cultured A431 cells. As expected from previous analyses growth inhibitory effects of the antibody were only very moderate in a monolayer growth assay.

As figure 24 shows there was still a decent inhibition of the medium-treated control cells of high passage number. However, cell numbers were only very moderately reduced by cetuximab in A431 cells after long-term exposure to cetuximab or gefitinib. Yet, inhibitory effects were too weak to allow calculation of EC<sub>50</sub> values for any of the tested populations.

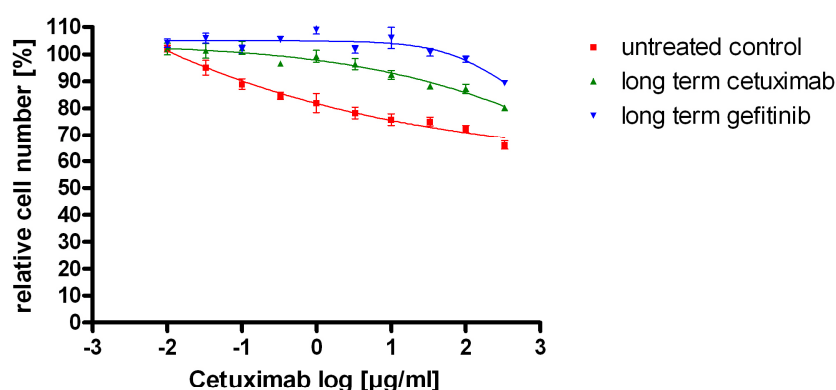


**Figure 24** A431 cells long-term treated with gefitinib or cetuximab showed poor growth inhibition by cetuximab in a monolayer assay. A431 cells that were long-term treated with gefitinib or cetuximab were washed for two or three days (three times per day), respectively, with full medium before start of experiment. Together with medium-treated A431 cells of similar passage (untreated control), they were subjected to a monolayer growth assay and treated with variable doses of cetuximab. EC<sub>50</sub> values were calculated as mean values from triplicates with Graph Pad Prism software. Relative cell numbers under treatment were calculated by signal normalization to medium-treated cells. Each data point is the average from quadruplet values (mean +/- standard deviation).

Due to the relative resistance of monolayer cell growth to cetuximab, soft-agar colony formation assays were carried out to determine the sensitivity and cross-sensitivity of long-term-treated A431 cell populations.

Interestingly, long-term exposure of A431 cells to cetuximab under standard cell culture condition did not appear to render these cells resistant to the antibody in a soft-agar growth assay (figure 25). In contrast, it even appeared that this population was rather sensitized, when comparing the EC<sub>50</sub> value to those of medium-treated control cells (0,008µg/ml vs. 0,04µg/ml and 0,054µg/ml, respectively). Yet, the

efficacy of growth-inhibition for cetuximab long-term treated cells by cetuximab was somewhat lower than for medium-treated A431 cells with similar passage number (high passage) (67% vs. 87%).

Surprisingly, A431 cells resistant to gefitinib after long-term exposure to this drug still responded very well to cetuximab. The extent of cetuximab caused growth inhibition was comparable to medium-treated control cells ( $EC_{50}$  0,014 $\mu$ g/ml vs. 0,04 $\mu$ g/ml and 0,054 $\mu$ g/ml, respectively) and the same was true for the efficacies of growth inhibition (76% vs. 87% and 78%, respectively).

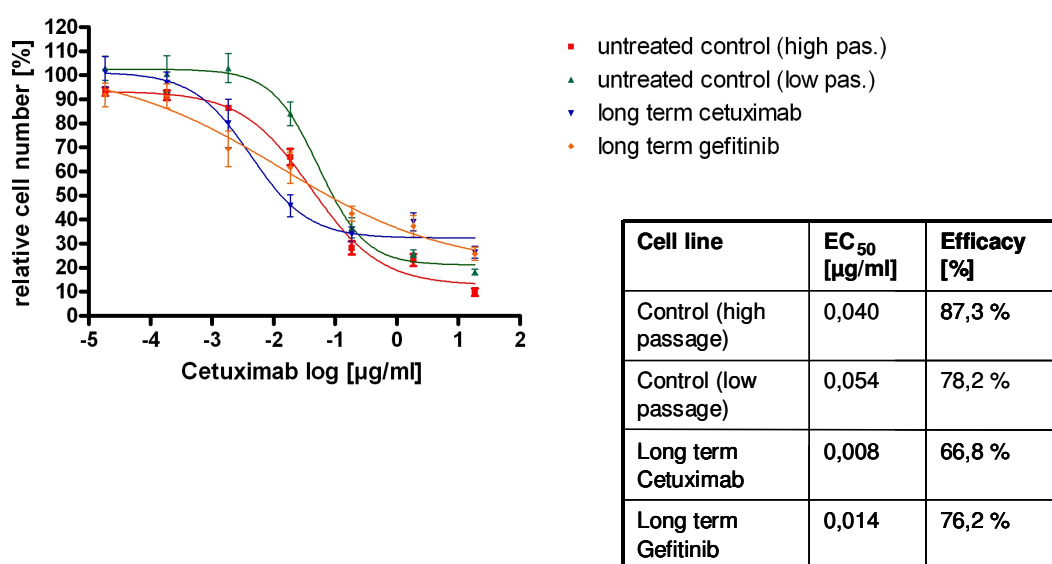


**Figure 25 A431 cells long-term treated with gefitinib or cetuximab did not show reduced growth inhibition by cetuximab in a soft-agar assay.** A431 cells that were long-term treated with gefitinib or cetuximab were washed for two or three days (three times per day), respectively, with full medium before start of experiment. Together with medium-treated A431 cells of similar passage (untreated control), they were subjected to a soft-agar colony formation assay and treated with variable doses of cetuximab.  $EC_{50}$  values were calculated as mean values from triplicates with Graph Pad Prism software. Relative cell numbers under treatment were calculated by signal normalization to medium-treated cells. Each data point is the average from triplicate values (mean  $\pm$  standard deviation).

### 3.2.3 Morphological changes in cell lines with primary drug sensitivity

During the cultivation of the different A431 cells, it became obvious that the populations were subject to significant morphological changes. Phenotypical alterations were first observed after two to three months of cetuximab treatment. While the concentration of cetuximab was kept constant (33 $\mu$ g/ml), doses were steadily increased in the gefitinib-treated population. Here, the starting concentration

was 0,5 $\mu$ M (corresponding to the EC<sub>50</sub> in a monolayer growth assay), which significantly reduced cell numbers in culture and caused a longer period of growth stasis in the viable cells. After two to three months cells resumed growth and from this point, gefitinib concentrations were increased in steps of dose doublings (0,5 $\mu$ M; 1 $\mu$ M; 2 $\mu$ M; 5 $\mu$ M; 10  $\mu$ M). The morphology of A431 was documented fifteen months after the start of treatments (figure 26).

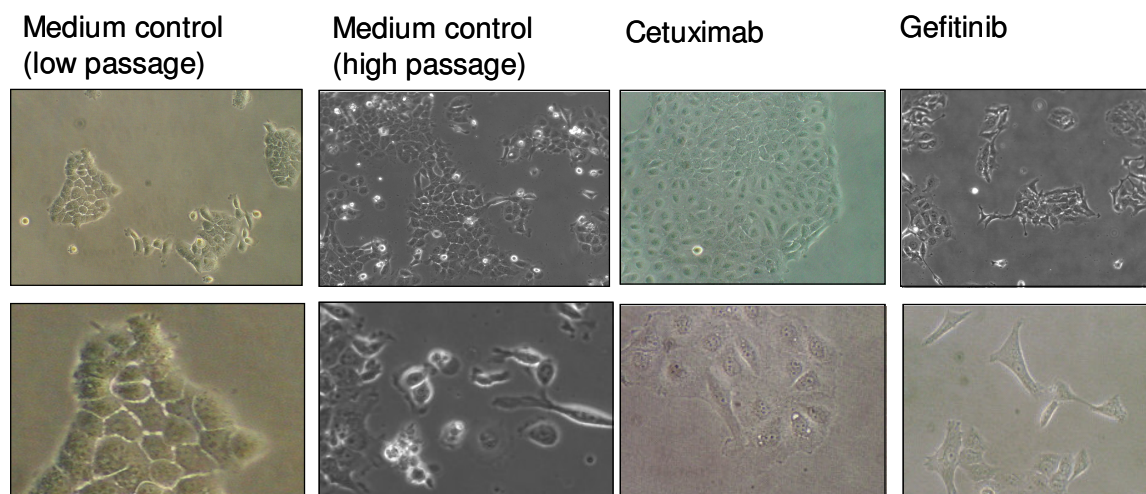


**Figure 26** A431 cells showed distinct morphological alterations upon long-term treatment with cetuximab, gefitinib or long-term cultivation in full medium. A431 cells treated with cetuximab or gefitinib for 15 months, as well as medium-treated control cells of similar passage number (high passage) and medium-treated cells from the starting population (low passage) were seeded and photographed under 40 fold (up) and 400 fold (down) magnifications with a light microscope.

The A431 cell line is widely used as a model for cancer cells that display typical epithelial features. Epithelial cells are closely attached to each other through tight cell-cell contacts and are mainly assembled in compact colonies in cell culture. The A431 starting population (medium control, low passage) was a classic example for that (figure 26). In contrast, A431 cells showed a completely different morphology after a long-term cultivation in regular growth medium (medium control - high passage). In this population most cells had a longitudinal cell shape and a fibroblastic morphology with many cell extensions. Cell-cell contacts were loose and colonies were mainly broken up with single cells or small aggregates spreaded over the surface of the culture dish. This population displayed typical features of mesenchymal cell lines. Obviously, cultivation of A431 cells under standard cell

culture conditions for a period of fifteen months provoked morphological changes, which have been described as epithelial-mesenchymal transition (EMT).

The population that had been long-term exposed to cetuximab also showed morphological alterations in comparison to the starting population (low passage). In proportion, cells from the cetuximab-treated population were slightly bigger, appeared flattened and contained a more prominent nucleus than cells from the starting population. Also these features pointed towards a more mesenchymal phenotype. However, the cetuximab-treated population still displayed fundamental epithelial characteristics, including tight cell-cell contacts and development of organized, defined colonies.

In contrast, the morphology of A431 cells that were treated with gefitinib appeared very similar to that from long-term untreated A431 cells with similar passage number (medium control – high passage). Cell extensions protruding from gefitinib-resistant A431 cells were even a little more pronounced than in the high passage reference cells, possibly indicating an increased migratory activity within this population (figure 26).

In parallel to A431 cells, Difi cells were as well long-term exposed to cetuximab and gefitinib. Since these cells are hypersensitive to either drug under monolayer growth conditions, treatment doses were increased for cetuximab (from a starting concentration of 0,2µg/ml to a maximal dose of 5µg/ml) and gefitinib (from a starting concentration of 75nM to a maximal dose of 1,5µM). The starting doses were chosen to be close to the calculated  $EC_{50}$  value for each drug. Both therapeutics significantly reduced cell numbers in culture and caused a long period of growth stasis in the living cells. Even after 15 months of drug exposure, cetuximab and gefitinib-treated Difi cells still grew slowly as compared to medium-treated reference cells.



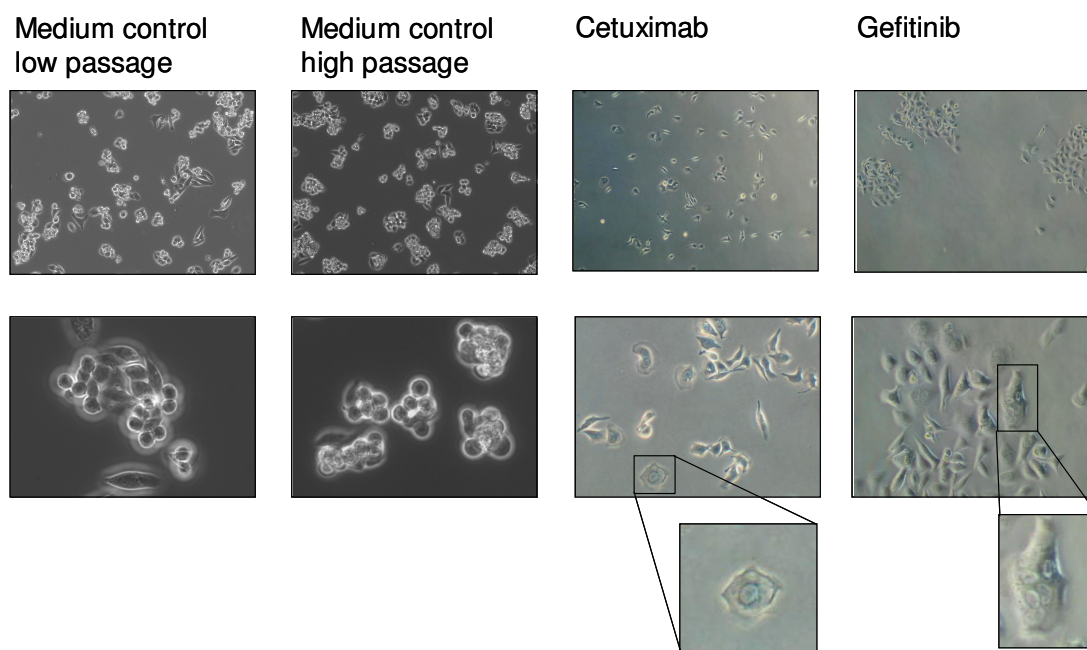


**Figure 27** Difi cells showed distinct morphological alterations upon long-term treatment with cetuximab and gefitinib. Difi cells treated with cetuximab or gefitinib for 15 months, as well as medium-treated control cells of similar passage number (high passage) and medium-treated cells from the starting population (low passage) were seeded and photographed under 40 fold (up) and 400 fold (down) magnifications with a light microscope.

Plain cultivation of Difi cells under standard cell culture conditions did not confer any significant change with regard to the cell population's morphology, as it had been observed for A431 cells (figures 26 and 27). On the other hand, higher magnifications of Difi populations that were exposed to gefitinib or cetuximab revealed considerable alterations. Especially cetuximab-treated cells showing a diffuse morphology and unorganized colony formation and some cells show an enlarged hyperchromatic nucleus (figure 27). Notably, gefitinib-treated Difi cells displayed an unusual colony formation pattern and single cell morphology. Figure 27 exemplarily highlights one gefitinib-treated cell with five nuclei. Along with multinucleated cells in the gefitinib-treated population, a high ratio of Difi cells with two nuclei was found after exposure to either drug. This may point towards impaired cellular cytokinesis.

Similarly, H460 lung cancer and SW707 colon cancer cell lines were long-term treated with cetuximab and gefitinib for 12 months and 8 months, respectively. Drug concentrations were kept constant for cetuximab (33 $\mu$ g/ml) and gefitinib (10 $\mu$ M), since no growth inhibition was seen for cetuximab at variable doses and the EC<sub>50</sub> for monolayer growth inhibition by gefitinib was around 10 $\mu$ M in these cell lines.

In contrast to the cell lines with primary sensitivity for gefitinib and cetuximab, A431 and Difi, no morphological changes were observed between medium-treated control populations and cells that were exposed for several months to either drug (figure 28). This implied that the morphological changes seen for A431 and Difi cells upon drug exposure were primarily due to effects of both drugs on EGFR and not on cellular off-targets.

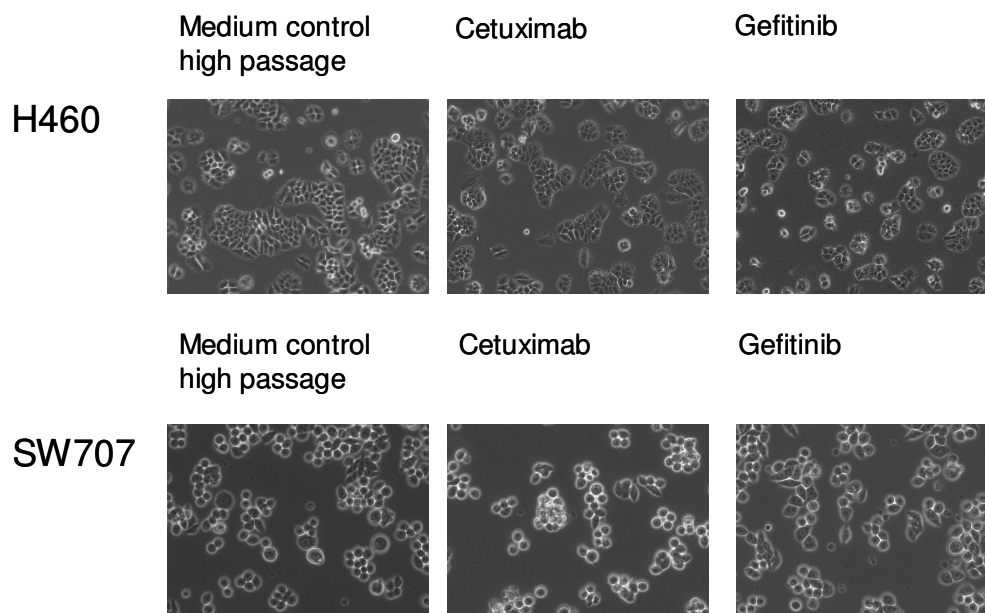


**Figure 28** H460 and SW707 cells did not show morphological alterations upon long-term treatment with cetuximab or gefitinib. H460 and SW707 cells treated with cetuximab or gefitinib for 12 months or 8 months, respectively, as well as medium-treated control cells of similar passage number (high passage) were seeded and photographed under 40 fold magnification with a light microscope.

### 3.2.4 Characterization of biological and biochemical changes in long-term-treated A431 cells

#### 3.2.4.1 Examination of EGFR levels and dynamics in A431 cells

The significant morphological changes observed for A431 cells implied major molecular alterations underlying and causing the rendered phenotypes. To start with a detailed examination of biochemical and biological changes in A431 cells, the surface levels of EGFR were determined via FACS analyses.

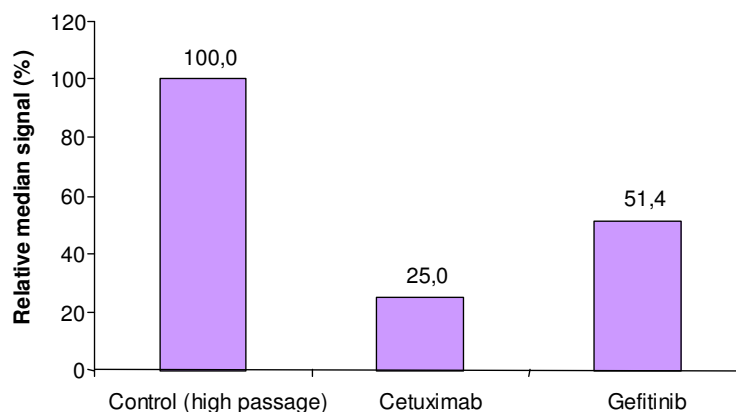


**Figure 29 A431 cells showed reduced EGFR surface levels after long-term treatment with cetuximab and gefitinib.** A431 cells long-term treated with cetuximab or gefitinib were washed for two or three days, respectively, with full medium three times per day. EGFR on these and medium-treated control cells of similar passage number (high passage) was detected with an EGFR-specific FITC conjugated antibody, which has been shown to bind another epitope than cetuximab (Jürgen Schmidt, TA Oncology, Merck KGaA, personal communication), followed by analyses on a Becton Dickinson FACScalibur flow cytometer. Median signal intensity from the fluorescence channel was calculated for every condition and transformed to arbitrary units. Median signal intensities from cells treated with cancer therapeutics were normalized against median signal intensity of medium-treated control cells of similar passage number.

Long-term exposure of A431 cells to cetuximab, led to a fourfold reduction of the surface EGFR. As also apparent from figure 29, gefitinib-resistant A431 cells displayed twofold reduced surface levels of EGFR, as compared to medium-treated control cells of similar passage number.

It has been reported that pancreas cancer cells, which are resistant to cetuximab in murine xenografts, displayed reduced cetuximab-mediated receptor internalization, as compared to pancreas cancer cells that are sensitive to the antibody (Arnoletti et al., 2005). This finding could also be reproduced for six NSCLC cell lines selected from the panel characterized above (Irmer et al., 2007b). To access the cetuximab associated dynamics of EGFR in long-term-treated A431 cells, they were incubated with radioactively labeled antibody for 30 min followed by measuring intracellular and extracellular portions of radiation.

As evident from figure 30, medium-treated control cells of high or low passage number showed efficient cetuximab induced EGFR internalization after a 30-min exposure to  $^{125}\text{I}$ -labeled cetuximab (41% and 46% internalization, respectively). On the other hand A431 cells that were long-term treated with cetuximab and cleared

from the antibody prior to the experiment (cf. figure 21), showed a slightly reduced capacity for cetuximab induced receptor turnover. Gefitinib-resistant A431 cells, however, had a markedly decreased ability for EGFR internalization upon exposure with cetuximab. Noteworthy, these gefitinib-resistant A431 cells do show a slightly decreased response to cetuximab in a soft-agar colony formation assay, in regard to their  $EC_{50}$  value, as compared to medium-treated control cell lines (figure 25).

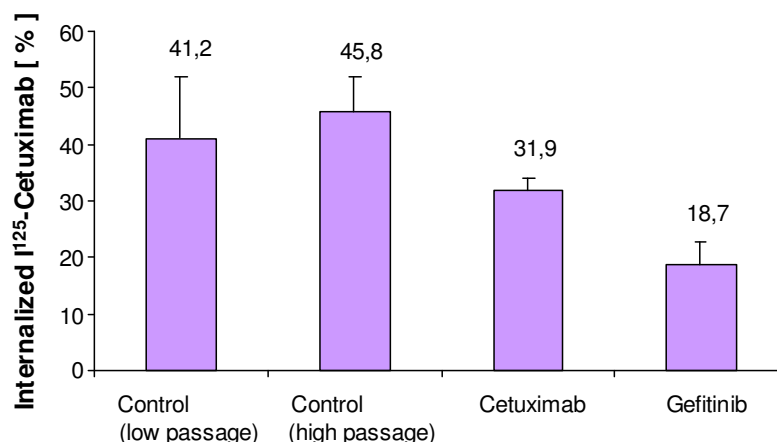


**Figure 30 A431 cells showed reduced EGFR internalization after long-term treatment with cetuximab or gefitinib.** Internalization of  $^{125}\text{I}$ -cetuximab was examined 30 min after incubation of A431 cells with 2nM radioactively labeled antibody under serum starving conditions. The internalization rate is indicated as fraction of  $^{125}\text{I}$ -cetuximab that was found in cell lysates in relation to total  $^{125}\text{I}$ -cetuximab deployed in the experiment. Antibody internalization of A431 cells long-term treated with cetuximab or gefitinib and washed with medium for three or two days, was compared with internalization of medium-treated control cells of similar passage number (high passage) or from the starting population (low passage).

In the next step, total expression of EGFR and other ErbB receptors in the different A431 populations was determined via immunoblot analyses of cell lysates. As depicted in figure 31, expression of EGFR was comparable between the long-term cultured populations, yet gefitinib-resistant A431 cells showed a roughly two-fold decreased expression of the receptor. In contrast A431 cells from the starting population showed moderately higher levels of total EGFR. Together with the results from the FACS analyses (figure 29) this indicated that gefitinib-resistant A431 cells had a roughly two fold reduced level of total cellular EGFR, as compared to medium-treated control cells of similar passage number (medium control; fifteen months). On the other hand, A431 cells that were exposed long-term to cetuximab had markedly reduced surface levels of receptor; however, cellular levels of total EGFR were

comparable to the levels in medium-treated control cells of similar passage. This would mean that in long-term cetuximab-treated cells roughly fourfold more EGFR was localized within the cell as compared to medium-treated cells of similar passage number.

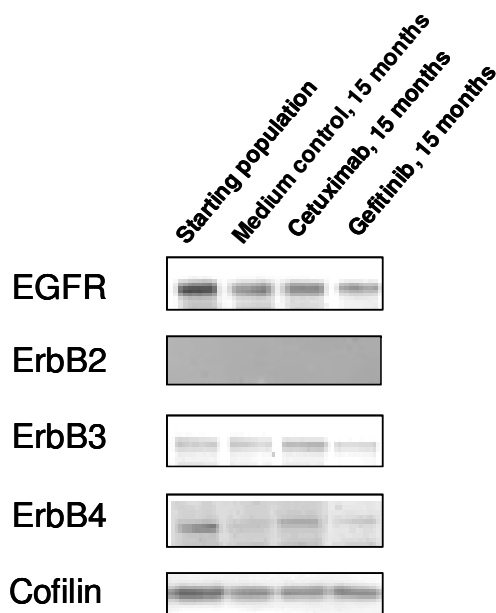


**Figure 31 Expression of ErbB receptors moderately differed between long-term gefitinib or cetuximab-treated A431 cells and reference A431 cells.** ErbB receptor expression in A431 cells treated 15 months with gefitinib or cetuximab was compared with expression in medium-treated controls cells of similar passage number and expression in the starting population. Cellular lysates were normalized after protein quantification by BCA assay and probed by immunoblotting. Expression of cofilin has been determined as a loading control.

While ErbB2 could not be detected in either population, ErbB3 expression was similar in all populations and slightly higher in cetuximab-treated cells. Expression of the ErbB4 receptor was moderately higher in A431 cells from the starting population and cetuximab-exposed cells as compared to the gefitinib-resistant population and medium-treated cells of similar passage number.

#### 3.2.4.2 Analyses of molecular markers for epithelial-mesenchymal transition (EMT) in A431 cells

In order to further characterize the morphological changes observed within the different A431 cell populations, cellular lysates were probed for the expression of EMT marker proteins (figure 32).

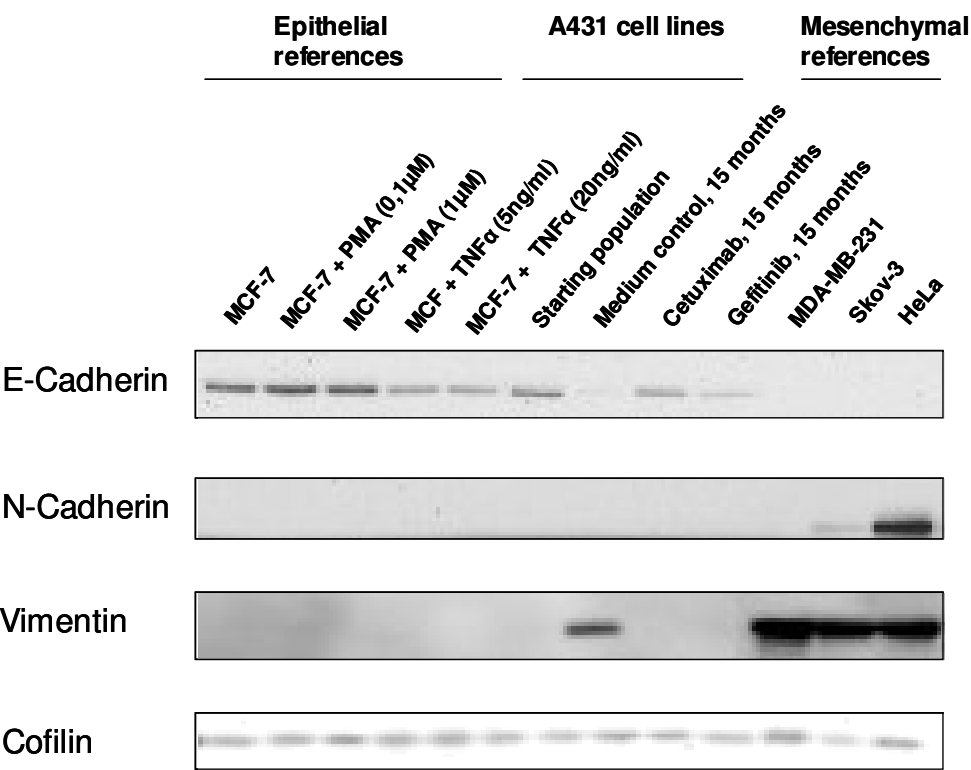


**Figure 32** Long-term incubation of epithelial A431 cells with cetuximab or gefitinib, but not long-term cultivation in medium, prevented expression of mesenchymal cell-like marker proteins. EMT marker protein expression in A431 cells long-term treated with gefitinib or cetuximab and in medium-treated control cells of similar passage number was determined and compared with EMT marker expression in typically epithelial (MCF7, A431 starting population) and mesenchymal (MDA-MB-231, Skov-3, HeLa) reference cell lines. Cellular lysates were normalized after protein quantification by BCA assay and probed by immunoblotting. Expression of cofilin has been determined as a loading control.

MCF-7 and A431 cells from the starting population are typical epithelial cells and served as references. On the other hand, MDA-MB-231, Skov-3 and HeLa cells were included as typical mesenchymal references. Other controls were MCF-7 cells, treated with Phorbol 12-myristate 13-acetate (PMA) (8 h; 0,1 µM or 1 µM, respectively) or with tumor necrosis factor alpha (TNFα) (48 h; 5ng/nl or 20ng/ml, respectively). It was expected that treatment of MCF cells with PMA would reduce cellular levels of E-Cadherin (Kuroda et al., 1998; Li et al., 2005a); yet this could not be reproduced here. Treatment with TNFα has been shown to initiate EMT in MCF-7 cells (Dong et al., 2007), which was reflected by a moderate decrease in E-Cadherin expression (figure 32).

The expression profile of untreated MCF-7 and A431 cells from the start population was typically epithelial (figure 32): these cells showed a high expression of E-cadherin, but lacked expression of mesenchymal markers N-cadherin and vimentin. This expression profile was also shared by A431 cells after long-term exposure to cetuximab or gefitinib. In contrast, medium-treated A431 of similar passage number lost E-cadherin expression and had high levels of vimentin. This profile was also shared by the mesenchymal reference cell lines MDA-MB-231, Skov-3 and Hela. The latter two cell lines also expressed low or high levels of N-cadherin, respectively. While TNFa treatment moderately diminished the E-cadherin levels of MCF-7 cells, exposure with PMA did not have any effect on the expression of EMT marker proteins. Interestingly, gefitinib-resistant cells did express markedly less E-cadherin than A431 cells that were long-term exposed to cetuximab, which correlated with the reduction of cell-cell contacts (cf. figure 26).

#### **3.2.4.3 Identification of scavenger pathways compensating for EGFR blockade in A431 cells**

It has been reported that gefitinib or cetuximab mediated blockage of EGFR may be compensated by an increased action of other RTK-mediated signaling pathways (Liu et al., 2001; Chakravarti et al., 2002). In order to identify RTKs, which are turned on upon long-term treatment of A431 cells with EGFR-directed drugs, lysates from the different populations were probed with a human phospho-RTK array. This array allowed simultaneous assessment of the relative activation of 42 different RTKs.

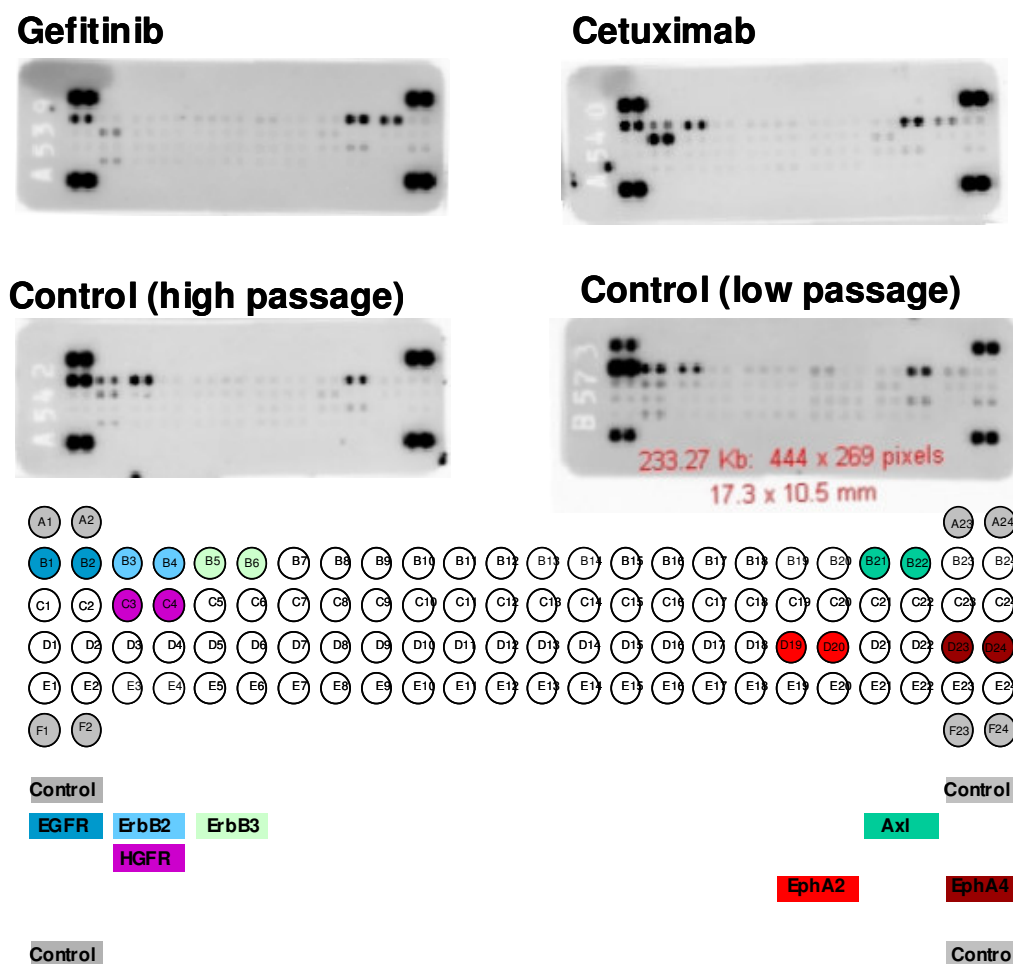
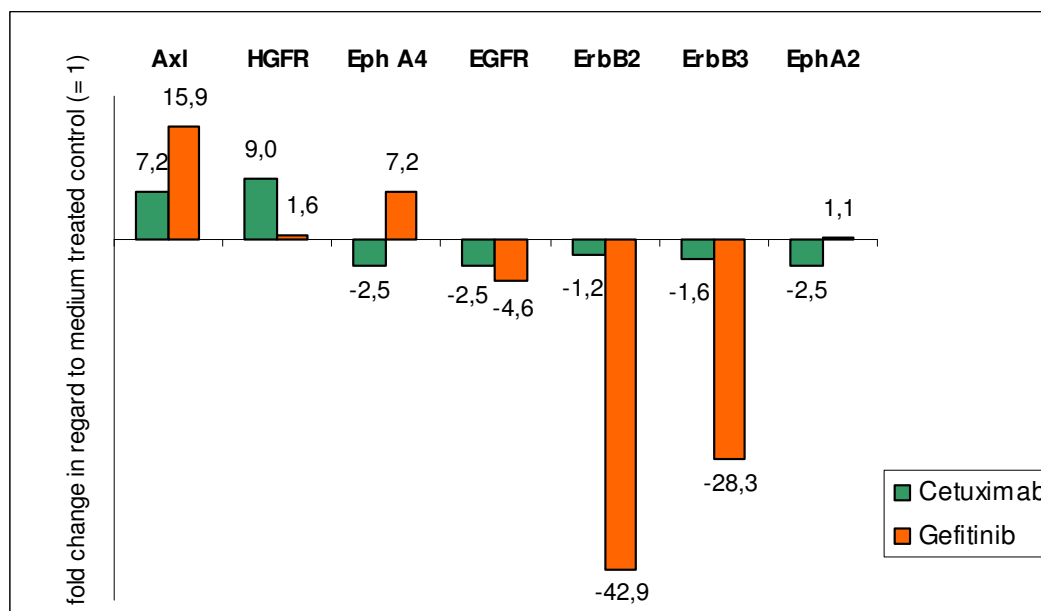


**Figure 33 Differential activation of RTKs in A431 cells under long-term treatment with cetuximab or gefitinib.** Proteome Profiler™ Array membranes spotted with capture antibodies for human RTKs were probed with cellular lysates from A431 long-term treated with cancer therapeutics and medium-treated control cells of similar passage number (high passage) or from starting population (low passage) as described in material and methods. Phosphorylation of captured RTKs was visualized with a HRP-coupled anti-phospho-tyrosine antibody followed by chemiluminescence detection with the Versa Doc documentation system. Kinases with significant differences of activation between cell lines are highlighted in color. The array used for lysates from the starting population (low passage), was from another production charge as the other arrays.

The signal intensities from the immunoblots were quantified and relative phosphorylation levels of significant differently regulated RTKs were summarized (figure 34). There was a high activation of HGFR and Axl in A431 cells long-term treated with cetuximab as compared to medium-treated cells of similar passage number. Axl phosphorylation was also markedly upregulated in gefitinib-resistant A431 cells, which was also true for EphA4. On the other hand, phosphorylation of ErbB2 and ErbB3 was significantly downregulated in gefitinib-resistant A431 cells,



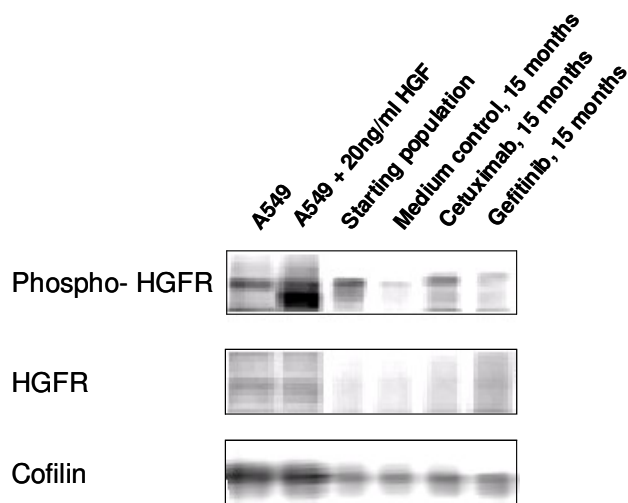
but not in cells that were long-term exposed to cetuximab. Further, phosphorylation of EGFR was fivefold downregulated in gefitinib-resistant cells, but only moderately decreased in A431 cells after a fifteen months exposure to cetuximab. In addition, a moderate decrease of EphA2 phosphorylation was observed in the latter cell population, which could be a secondary effect caused by EGFR inhibition through cetuximab (Larsen et al., 2007).



**Figure 34 Differential activation of Axl, HGFR, EphA4, EGFR, ErbB2, ErbB3 and EphA2 was observed in A431 cells after long-term incubation with cetuximab or gefitinib.** Chemiluminescence signals were quantified and data processing with QuantityOne software was done by background subtraction, determination of average signal density from duplicate values and normalization of values from long-term cetuximab or gefitinib-treated cell lysates against values from untreated control cell lysates of similar passage number (high passage), which were set 1.

To verify HGFR activation in long-term cetuximab-treated cells further immunoblot analyses with specific phospho-HGFR antibodies were carried out. A549 lung cancer cells treated with 20ng/ml HGF for 5 min were used as a positive control. Cetuximab long-term treated A431 cells showed markedly increased levels of activated HGFR and moderately increased levels of total HGFR as compared to medium treated cells with a similar passage number (medium control; fifteen months) (figure 35). Gefitinib-resistant A431 cells showed only moderately increased levels of activated HGFR and markedly increased expression of total HGFR. Interestingly, A431 cells from the starting population showed a comparable expression of HGFR as cells from the long-

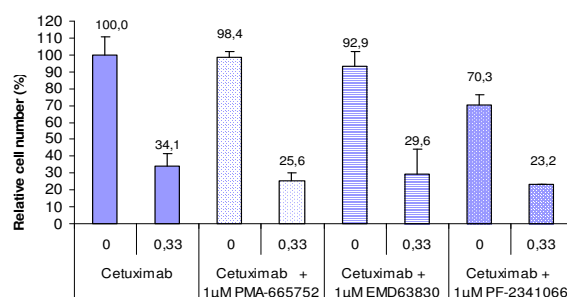
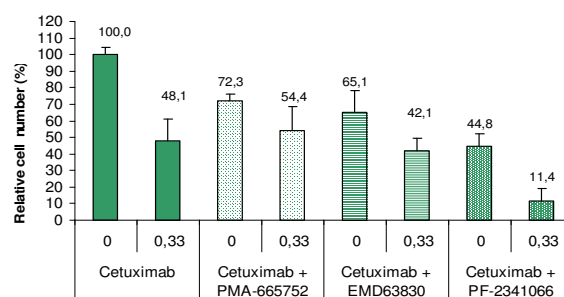
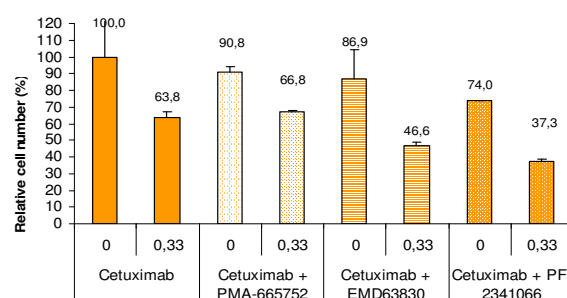
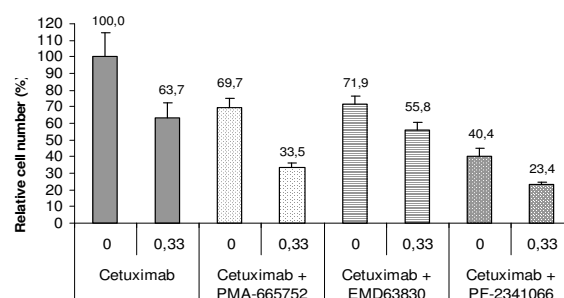
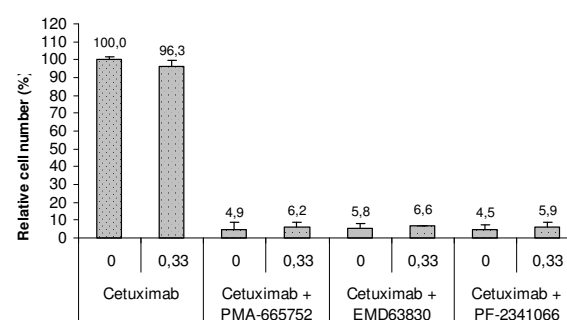
term medium-treated population, but a significantly increased activation of this receptor.



**Figure 35 High activation of HGFR was seen in long-term cetuximab-treated A431 cells.** Activation and expression of HGFR in A431 cells long-term treated with gefitinib or cetuximab and in medium-treated control cells of similar passage number was determined and compared an compared with levels in A431 cells from the starting population. Cellular lysates were normalized after protein quantification by BCA assay and probed by immunoblotting. Expression of cofilin has been determined as a loading control.

Thus, the ratio of activated receptor over total receptor was the highest in A431 cells from the starting population, followed by cetuximab long-term treated A431 cells. Gefitinib-resistant A431 cells displayed an increased HGFR expression, but a low ratio of activated receptor. In contrast, medium-treated control cells of high passage number showed a low expression combined with a low activation of HGFR, which may imply a decreased importance of this signaling component for cellular growth.

To test whether high activation of HGFR in long-term cetuximab-treated cells and cells from the start population correlated with increased sensitivity of these populations to HGFR-directed TKIs, soft-agar colony formation assays under treatment with cetuximab and/or HGFR-TKIs were performed. PHA-665752 (SUGEN/Pfizer) (Christensen et al., 2003), PF-2341066 (Pfizer) (Zou et al., 2007) and EMD638330 (Merck KGaA) are HGFR specific ATP-competitors designed for cancer therapy. SNU-5 cells that are hypersensitive to HGFR-specific TKIs were used as a positive control for treatments (figure 36).

**(a) Long term cultured (high passage)****(b) Long term Cetuximab treated****(c) Long term Gefitinib treated****(d) Short term cultured (low passage)****(e) Snu5 cells**

**Figure 36** Growth of cetuximab long-term treated A431 cells was more efficiently blocked by HGFR inhibitors than growth of gefitinib-resistant or medium-treated cells of similar passage number. A431 cells were treated with 1µM of HGFR specific tyrosine kinase inhibitors PHA-665752, EMD63830 or PF-2341066 in combination with or without 0,33µg/ml cetuximab in a soft-agar colony formation assay. Evaluation was performed through fluorescence detection by Cell Titer Blue reagent and read-out with a plate reader after 10 days of cultivation. Relative cell numbers (%) were calculated by subtraction of pharmacological background and signal normalization to medium-treated samples. Each bar is the average from triplicate values. Bars for medium-treated control cells were calculated from sextuplets (mean +/- standard deviation). Pharmacological background was determined by treatment of cells with 100µM paclitaxel, which efficiently kills all cells. (d) A431 cells from the starting population (low passage) and (e) SNU-5 cells were used as controls.

A431 cells from the starting population (short term cultured; low passage) and long-term cetuximab-treated cells were most efficiently inhibited by single treatment with 1 $\mu$ M of different HGFR inhibitors, as reflected by the efficacies of inhibition (decrease of cell number compared to medium-treated cells) (figure 36). Both populations were partially inhibited by PHA-665752 (28% efficacy for long-term cetuximab-treated and 30% efficacy for the starting population) and EMD638330 (35% and 28%, respectively), while they were markedly inhibited by PF-2341066 (55% and 60%, respectively). In addition, these data show that growth of both populations could be further repressed by combining HGFR inhibitors with cetuximab.

In contrast, medium-treated A431 cells with a high passage number (long-term cultured; figure 36a) were not particularly responsive to single treatment with HGFR TKIs, as reflected by the efficacies of inhibition (1% for PHA-665752, 7% for EMD638330 and 30% for PF-2341066). Yet, this population was highly sensitive to cetuximab in this experiment.

Gefitinib-resistant A431 cells were also only slightly responsive to the HGFR inhibitors as displayed by the efficacies of inhibition (9% for PHA-665752, 13% for EMD638330 and 26% for PF-2341066) (figure 36c). This again was in line with the relatively low level of HGFR expression in this population (figure 35). Combining HGFR TKIs with the EGFR-targeting antibody cetuximab efficiently blocked soft-agar growth of gefitinib-resistant cells. However, the combination of HGFR TKIs with cetuximab seemed to be additive and not synergistic in any cell population.

### **3.2.5 Examination of differential gene expression in cancer cell lines upon long-term treatment with EGFR-specific cancer drugs**

The morphological alterations that were observed after long-term treatment in gefitinib and cetuximab sensitive cell lines, A431 and Difi, but not in primary resistant cell lines, H460 and SW707 cells, underlined that the fundamental phenotypical changes which occurred can be expected due to specific EGFR blockage. Since significant molecular alterations, reflected by differential expression of mRNA entities, could underlie this rendered morphology, differential gene expression patterns in the various populations were examined.

A candidate-based approach with Taqman<sup>®</sup> low density arrays was performed to reveal differentially expressed candidates between the different populations and cell

lines. This approach aimed at the identification of factors that were differently expressed in primary sensitive cell lines (A431 and Difi) after long-term exposure to either drug, but whose expression was not altered in primary resistant cell lines (H460 and SW707). The detection of such factors could help to identify mechanisms, which are responsible for the development of an acquired resistance to gefitinib or cetuximab in primary sensitive cells. In this regard, H460 and SW707 cell lines were considered as negative controls.

Table 5 summarizes the data from 25 selected candidate genes that were derived from a global expression analysis, which were classified due to their regulation in primary sensitive or resistant cell lines after long-term exposure to cetuximab.

Eight candidate genes were differentially regulated in long-term cetuximab-treated Difi and A431 cells, but their expression was unaltered in long-term-treated H460 and SW707 cell lines, as compared to medium-treated control cells of similar passage number. Notably, CCL5 (chemokine ligand 5) expression was not detected in SW707 cells and EREG was not expressed in H460 cells. Interestingly, expression of the ErbB ligands EGF and BTC was upregulated, while expression of the ligands EREG and HB-EGF was downregulated in primary sensitive cancer cells after long-term exposure to cetuximab as compared to medium-treated cells of similar passage number. Furthermore, A431 and Difi cells showed stronger expression of complement factor 3 (C3) and CCL5, and lower expression levels of TIMP1 (TIMP metalloproteinase inhibitor 1) and EGFR after long-term cetuximab treatment.

Primary sensitive (A431, Difi)	Fold change >2 or <0,5 in regard to control for <u>both</u> cell lines with same trend			BTC (+), C3 (+), CCL5* (+), EGF (+), EGFR (-), EREG* (-), HB-EGF (-), TIMP1 (-),
	Fold change >2 or <0,5 in regard to control for <u>one</u> cell line		Same trend in different groups: ErbB4 (-), IGFBP (-), MMP-7 (-)	AREG (-), CXCL1 (+), CXCL6 (+), ErbB2 (+), IL8 (+), IL-1 (-), Lumican (-), MIG-6 (-), PTHLH (-)
	No differential expression in regard to control in either cell line		ACE2 (-), TGFa (+)	CXCL10, ErbB3, PTHLH
		Fold change >2 or <0,5 in regard to control for <u>both</u> cell lines with same trend	Fold change >2 or <0,5 in regard to control for <u>one</u> cell line	No differential expression in regard to control in either cell line
Primary resistant group (H460, SW707)				

**Table 5 Differential mRNA expression in human cancer cell lines long-term treated with cetuximab.** Two cell lines with primary cetuximab sensitivity (Difi, A431) and two cell lines with primary cetuximab resistance (H460, SW707) were long-term treated with cetuximab and differential candidate gene expression was determined in comparison to long-term medium cells of similar passage number. A differential candidate gene expression of >2 or <0,5 after long-term cetuximab treatment in both cell lines within one group (e.g. the primary sensitive group), connected with no respective differential expression after cetuximab treatment in the other group (e.g. the primary resistant group), was considered to be of particular interest, e.g. HB-EGF (green). A differential candidate gene expression of >2 or <0,5 after long-term cetuximab treatment in only one cell line within one group, connected with no strong change in the other group, was considered to be marginally interesting, e.g. TGFa or AREG (orange). A differential candidate gene expression of >2 or <0,5 after long-term cetuximab treatment in one or two cell lines within one group, connected with a respective change for one or two cell lines in the other group, was considered uninteresting when the change followed the same trend for both groups, e.g. ErbB4 (red). (+) Indicates up-regulation of the respective candidate in cetuximab long-term-treated cells as compared to medium-treated control cells with similar passage number, (-) indicates down-regulation. Gene expression of some candidate genes could not be detected in one (\*) of the four cell lines. The evaluation of data probed via Taqman<sup>®</sup> LDAs was performed by Mr. Baumgärtner in the laboratory of Mr. Haas, Merck KGaA.

The following chart shows the calculated fold changes of C3, EGF, HB-EGF and CCL-5 mRNA expression levels in long-term cetuximab-treated cell lines, as compared to medium-treated cells of similar passage number (figure 37).

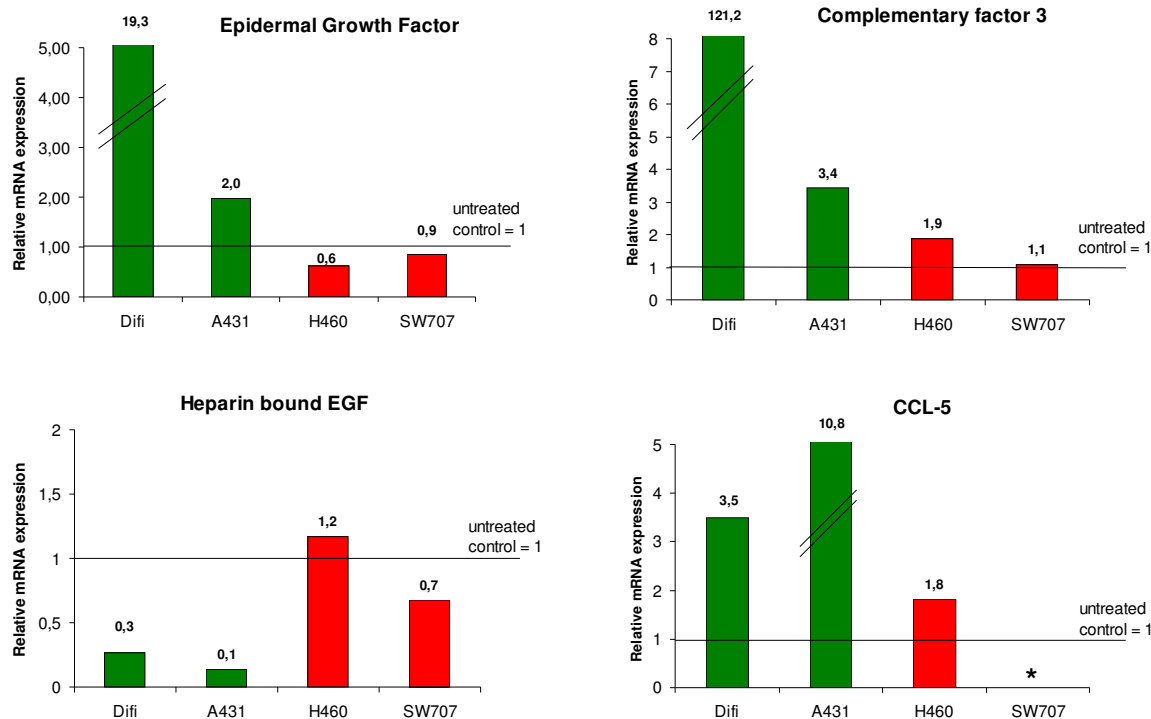


**Figure 37** Complementary factor 3, CCL-5 and natural ligands of EGFR were differentially expressed in human cancer cell lines after long-term treatment with cetuximab. Real-time PCR analyses (with Taqman® low density Arrays) was performed with mRNA from Difi and A431 cells (primary sensitive to cetuximab; green bars) and H460 and SW707 cells (primary resistant to cetuximab, red bars). Relative expression of mRNA from cell lines after long-term treatment with cetuximab to mRNA of medium-treated control cell lines of similar passage number was calculated as described in material and methods. Relative expression of a candidate gene is indicated as fold change in relation to the medium treated control (control = 1). (\*) No expression of CCL-5 mRNA could be detected in SW707 cells.

The same analyses were performed with the gefitinib-treated cancer cell lines. Again, 25 candidate genes were classified due to their regulation pattern in primary sensitive or primary resistant cell lines after long-term exposure to gefitinib (table 6).

Primary sensitive (A431, Difi)	Fold change >2 or <0,5 in regard to control for <u>both</u> cell lines with same trend		Same trend in different groups: AREG (-), HBEGF (-), IL8 (-), PTHLH (+)	CXCL6* (+), EREG* (-)
	Fold change >2 or <0,5 in regard to control for <u>one</u> cell line	Same trend in different groups: IGFBP3 (-)	Same trend in different groups: BTC (-), C3 (+), ErbB4 (+), MIG6 (-), MMP-7 (-)  Different trend in different groups: IL-1** [sensitive (-), resistant (+)]	CXCL10 (+), EGFR (-), Lumican (+), TIMP1(-), VEGF (-)
	No differential expression in regard to control in either cell line			ACE2, CXCL1, EGF, ErbB2, ErbB3, TNFSF, PDZK
Primary resistant group (H460, SW707)				
		Fold change >2 or <0,5 in regard to control for <u>both</u> cell lines with same trend	Fold change >2 or <0,5 in regard to control for <u>one</u> cell line	No differential expression in regard to control in either cell line

**Table 6 Differential mRNA expression in human cancer cell lines long-term treated with gefitinib.** Two cell lines with primary cetuximab sensitivity (Difi, A431) and two cell lines with primary cetuximab resistance (H460, SW707) were long-term treated with gefitinib and differential candidate gene expression was determined in comparison to long-term medium cells of similar passage number. A differential candidate gene expression of >2 or <0,5 after long-term gefitinib treatment in both cell lines within one group (e.g. the primary sensitive group), connected with no respective differential expression after gefitinib treatment in the other group (e.g. the primary resistant group), was considered to be of particular interest, e.g. EREG (green). Candidates showing different trends over different groups were also considered to be interesting, e.g. IL1a (green). A differential candidate gene expression of >2 or <0,5 after long-term gefitinib treatment in only one cell line within one group, connected with no strong change in the other group, was considered marginally interesting, e.g. CXCL-10 (orange). A differential candidate gene expression of >2 or <0,5 after long-term gefitinib treatment in one or two cell lines within one group, connected with a respective change for one or two cell lines in the other group, was considered uninteresting when the change followed the same trend for both groups, e.g. AREG (red). (+) Indicates up-regulation of the respective candidate over in long-term treated cells as compared to medium-treated control cells with similar passage number, (-) indicates down-regulation. Gene expression of some candidate genes could not be detected in one (\*) or two (\*\*) of the four cell lines. The evaluation of data probed via Taqman® LDAs was performed by Mr. Baumgärtner in the laboratory of Mr. Haas, Merck KGaA.

As compiled in table 6, EREG mRNA was found to be downregulated in gefitinib-resistant Difi and A431 cell lines. On the other hand CXCL-6 (chemokine ligand 6) mRNA was upregulated in both cell lines that acquired resistance to gefitinib. Both genes were unaltered in long-term gefitinib-treated SW707 cells and could not be detected in H460 cells. Expression of another candidate gene, interleukine 1 (IL1),



was downregulated in A431 cells that acquired resistance to gefitinib, while IL1 expression increased in long-term gefitinib-treated H460 cells, which are primary resistant to the TKI. Other candidate genes (BTC, C3, ErbB4, Mig6 and MMP-7) were not considered interesting as putative factors determining response to gefitinib, since their expression was altered with the same trend in primary sensitive, as well as in primary resistant cell lines.

Calculated fold changes of EREG, CXCL-6 and IL1 mRNA expression levels in long-term gefitinib-treated cell lines, as compared to medium-treated cells of similar passage number are shown in figure 38.

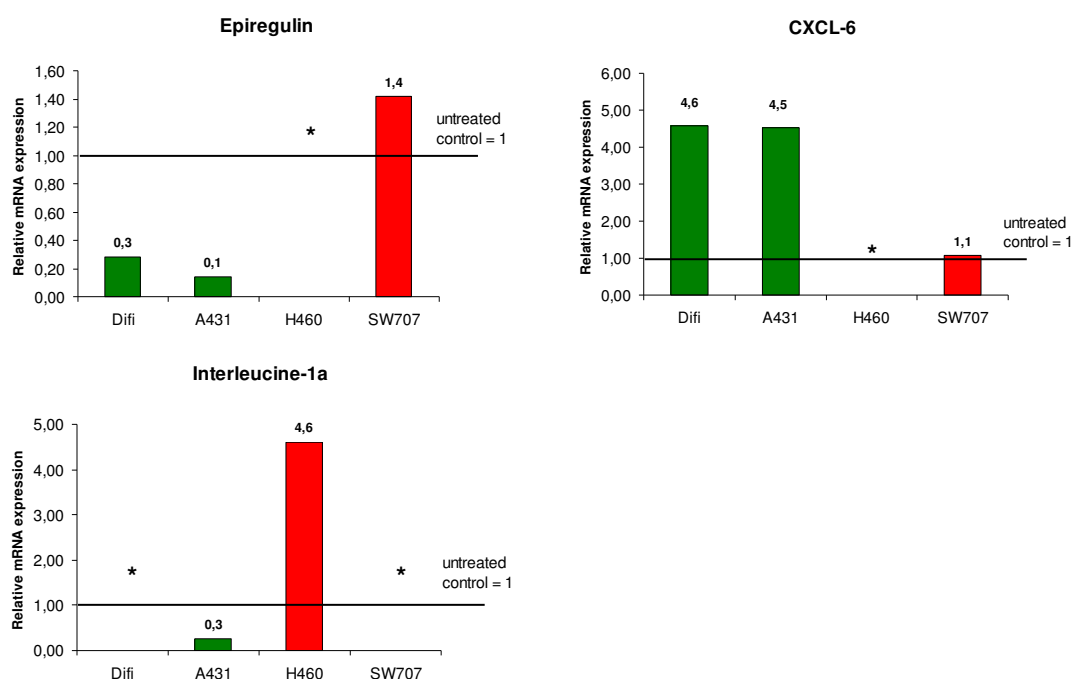


**Figure 38 Epiregulin and CXCL-6 were differentially expressed in human cancer cell lines after long-term treatment with gefitinib.** Real-time PCR analyses (with Taqman® low density arrays) was performed with mRNA from Difi and A431 cells (primary sensitive to gefitinib; green bars) and H460 and SW707 cells (primary resistant to gefitinib; red bars). Relative expression of mRNA from cell lines after long-term treatment with gefitinib to mRNA of medium-treated control cell lines of similar passage number was calculated as described in material and methods. Relative expression of a candidate gene is indicated as fold change in relation to the medium treated control (control = 1) (\*) No expression of Epiregulin and CXCL-6 mRNA could be detected in H460 cells. (\*\*) Interleukine-1a expression could not be detected in Difi and SW707 cells.

## 4. Discussion

Innovative cancer treatment strategies focus on the specific inhibition of target structures that are either unique or overrepresented in cancer cells. Since the onset of apprehending EGFR as a suitable drug target (Sato et al., 1983), a variety of specific cancer therapeutics has been developed, with gefitinib and cetuximab being the compounds with the broadest clinical use (Johnston et al., 2006). Since cancer patient response rates to these therapeutics are found to be sometimes unsatisfying, it is necessary to identify patient subpopulations that may profit best from the respective regimen.

This study evaluated existing marker proteins proposed to impart sensitivity to EGFR-targeting therapy and further postulates new candidate factors with predictive value. In addition, this work revealed new insights in the mode of action of the therapeutic antibody cetuximab and the tyrosine kinase inhibitor (TKI) gefitinib.

### **4.1 Response to gefitinib is neither exclusively nor strictly determined by presence of EGFR kinase mutations**

EGFR kinase domain mutations have been associated with clinical response of NSCLC patients to treatment with gefitinib (Lynch et al., 2004; Paez et al., 2004). And meanwhile these findings were reproduced in different laboratory examinations (Amann et al., 2005; Sordella et al., 2005). A little later a secondary mutation, T790M, appearing in combination with sensitizing mutations was found to confer resistance to gefitinib (Kobayashi et al., 2005; Pao et al., 2005a). In this work, two consecutive approaches have been chosen to evaluate the impact of EGFR kinase domain mutations for gefitinib therapy: the generation of NIH3T3 cells exogenously expressing different EGFR variants and the characterization of a panel of NSCLC cell lines endogenously expressing EGFR variants.

In soft-agar colony formation assays it could be demonstrated that murine NIH3T3 cells expressing human EGFR with classical kinase domain mutations (L858R and a short deletion mutation encompassing the LREA motive) were hypersensitive to gefitinib. This is in line with another study using the same cell model (Greulich et al., 2005). In addition, it was verified that colony formation of cells with EGFR variants

containing a T790M amino-acid exchange mutation was unaffected by gefitinib (figure 13).

The study on a panel of NSCLC supported the notion that sensitivity of NSCLC cell lines to gefitinib treatment in a soft-agar matrix growth assay is frequently, however not exclusively, seen in cells that carry EGFR kinase domain mutations. Notably, a NSCLC cell line, HCC2279, was identified that has an EGFR mutation, yet is resistant to gefitinib (cf. figure 14). This is in line with in vitro data from others (Fujimoto et al., 2005) and underlines the findings from various clinical trials where also patients with wild-type EGFR responded very well to TKI treatments (as summarized in Irmer et al., 2007a). It was suggested that EGFR kinase mutations and KRAS mutations are mutually exclusive and that activating mutations in KRAS confer resistance to gefitinib (Pao et al., 2005b; Eberhard et al., 2005). The data presented in this work also supported this notion, which is reflected by the growth responses observed for Calu6 and H460 cell lines that both carry KRAS mutations. On the other hand, A549 cells, which also express mutant KRAS, were moderately responsive to gefitinib and were not clearly assignable in the two-armed classification approach.

In summary, these in vitro examinations provide verification that response to gefitinib is neither exclusively nor strictly determined by the presence of EGFR kinase mutations. Obviously, cellular factors other than EGFR-T790M or KRAS mutations, which occur in parallel to kinase domain mutations, may specify cellular resistance to gefitinib. These factors may not come into play in the genetically engineered NIH3T3 cells, which are growth dependent on EGFR. While inhibition of EGFR signaling in NIH3T3 cells strictly paralleled the growth inhibition (figures 11 and 13), this was not the case for NSCLC cell lines (figures 14 and 15). This also points toward the increased level of complexity when studying tumor cells transformed by multiple cancerogenic factors.

#### **4.2 Cellular sensitivity to cetuximab is determined by factors other than EGFR kinase domain mutations**

Scarce clinical examinations indicate that response to cetuximab in NSCLC does not appear to correlate with the presence of EGFR mutations (Lynch et al., 2004,

Mukohara et al., 2005, Tsuchihashi et al., 2005). Apart from a report which shows that one cell line (PC9), carrying an EGFR mutation, is growth inhibited by cetuximab in a soft-agar assay (Perez-Torres et al., 2006), no systematic in vitro examinations have been published in that respect.

Here, a panel of twelve NSCLC cell lines was characterized concerning their growth response under treatment with cetuximab. From these examinations it was evident that EGFR kinase mutations in NSCLC do not have any predictive value for cetuximab in vitro response. A recent study with 30 colorectal cancer patients showed that KRAS mutations are associated with resistance to cetuximab therapy (Lievre et al., 2006). Interestingly, cetuximab inhibited growth of A549 cells in a soft-agar matrix, which may be indicative for its basic potential to repress proliferation of cells with KRAS mutations. However, this sensitivity was only classified moderate and two other cell lines with an equivalent activating KRAS mutation, Calu6 and H460, did not respond to cetuximab under the applied assay conditions. Yet, in vivo tumor growth of Calu-6 cells could be delayed by treatment with cetuximab and gefitinib in murine xenografts (figure 16), suggesting again that KRAS mutations are not necessarily associated with resistance to cetuximab.

Furthermore, it could be shown that the antibody effectively inhibits in vitro growth of gefitinib-sensitive H1650 cells, which lack the tumor suppressor PTEN in addition to having an EGFR kinase domain mutation. Lack of PTEN, which negatively regulates activity of Akt by dephosphorylating phosphatidylinositol triphosphate (PI3P), was suggested to be a prognostic marker for gefitinib resistance (She et al., 2003). While the presence of the EGFR mutation might be predominant over the lack of PTEN when explaining the observed sensitivity of the cell line towards gefitinib, the data from the xenograft experiment suggested that lack of PTEN is not necessarily predictive for resistance to cetuximab in NSCLC (cf. figure 16).

Taken together, sensitivity of NSCLC cell lines to cetuximab was independent of EGFR kinase domain mutations. In addition, these observations suggest that lack of PTEN is not causative for resistance to cetuximab. In addition, the postulated value of KRAS mutations for explaining resistance to EGFR-targeting drugs can be put into question according to results of the investigations performed in this study. In summary, it can be inferred from the in vivo examinations that cetuximab may block or at least delay growth of any NSCLC cell lines studied, independent from the genetic background. The inconsistency of some results from in vitro and in vivo

experiments observed for cetuximab underlines the necessity to perform in vivo and clinical examinations in order to cover all aspects of the complex functionality of this drug.

#### **4.3 Basal expression profiling of NSCLC cells identifies candidate genes putatively predicting response to EGFR-targeting therapy**

Three global gene expression profiling approaches have already been conducted to identify candidate genes or signatures associated with response of NSCLC cell lines to EGFR-targeting TKIs (Yauch et al., 2005; Balko et al., 2006; Coldren et al., 2006). In this study an Affymetrix whole genome chip based expression analyses identified 46 genes that show a significantly differential expression between gefitinib sensitive and resistant cell lines with an unadjusted  $p < 0,001$  (table 3). This includes 15 candidates (32,6%) that were also found in at least one of the other three analyses. Furthermore this study revealed novel genes whose expression levels may affect outcome of a gefitinib therapy. These include lysophosphatidic acid receptor 1 (EDG1), which is capable to transactivate EGFR via the release of HB-EGF, a natural ligand of EGFR and ErbB4 (Liu and Armant, 2004). A fivefold higher expression of EDG1 was found in gefitinib sensitive cell lines may suggest that dependence of cells to transactivation of EGFR via EDG1 could confer an enhanced sensitivity to gefitinib.

This work provides the first report that uses whole genome expression profiling to correlate cetuximab in vitro responsiveness of cancer cell lines with their relative gene expression. A number of potentially relevant candidate genes with differential expression between cetuximab-resistant and sensitive NSCLC cells were identified, that despite not reaching strict statistical significance fit well in a biological context (cf. table 4). The analyses showed syndecan 2 (SDC2) to be six-fold higher expressed in cetuximab-resistant cell lines. Syndecan 2 is a member of the heparine sulphate proteoglycane (HSPG) family and is known to be implicated in cellular adhesion and signaling, as well as in cancer progression and angiogenesis (Essner et al., 2006). Interestingly, syndecan 1, which is also a member of the HSPG family, has been shown to bind certain ErbB ligands in multiple myeloma cells, such as HB-EGF and AREG, and is suggested to facilitate ErbB activation via concentrating ligands at the cell membrane (Mahtouk et al., 2006). Interestingly, tetraspanin 8 (TSPAN8) was found to be roughly six-fold higher expressed in cetuximab-resistant cells. Members

of the tetraspanine family of membrane-associated proteins were found to be associated, together with HSPGs, in mediating AREG-driven proliferation (Piepkorn et al., 1998). High expression of tetraspanin 8 has been found in NSCLC tumor tissues (Remmelink et al., 2005) and was combined with increased invasion and metastasis of colorectal cancers (Le Naour et al., 2006). The identification of syndecan 2 and tetraspanine 8 as putative markers predicting cellular resistance against cetuximab provoke the general hypothesis that membrane associated scaffold proteins that concentrate and present natural ligands to EGF receptors may provide an alternative mechanism in receptor activation, which cannot be effectively blocked by the antibody.

Of course, the identified candidate genes of interest await validation by immunoblot or FACS analyses. Furthermore, it will be interesting to see whether the postulated candidates can be confirmed in functional assays. These questions are currently subject of an ongoing project that is part of another PhD thesis.

#### **4.4 Long-term exposure of A431 cells to gefitinib, but not to cetuximab, causes gain of resistance to EGFR-directed drugs**

A couple of studies on cancer cell lines that were long-term treated with EGFR-targeting TKIs have been conducted in the past. In all cases, acquisition of resistance was observed after several months of drug exposure and recurrent dose escalation (Perez-Soler et al., 2003; Kwak et al., 2005; Ando et al., 2005; Kokubo et al., 2005; Engelman et al., 2006). In this study A431 cells were treated with gefitinib for 15 months and acquired resistance to this TKI, as diagnosed by monolayer and soft-agar growth assays (figures 22 and 23). Furthermore, this work showed that gefitinib-resistant A431 cells still respond effectively to cetuximab in a soft-agar colony formation assay. Growth response of these cells was comparable to medium-treated control cells of similar passage number (figure 25). This finding is of high interest as it may imply that resistance mechanisms to the TKI gefitinib are fundamentally different from those that specify response to cetuximab. Even though it is problematic to draw conclusions from laboratory examinations for the clinic, this could indicate that patients that relapse from gefitinib can still profit from a cetuximab regimen.

Apart from this work, a cancer cell line was generated that resumed growth after xeno-transplantation into mice and long-term exposure to cetuximab. Interestingly,

this cell population retained normal in vitro sensitivity to cetuximab as compared to the parental cell line. Yet, cells isolated from the relapsed xenograft showed increased in vivo resistance to cetuximab (Viloria-Petit et al., 2001). Even though in this work cells were exposed to cetuximab under standard cell culture conditions that study is the only published reference. Notably, also long-term cetuximab-treated A431 from this work did not acquire resistance to the antibody, as assessed by soft-agar colony formation assays (figure 25). Interestingly, A431 cells that were long-term exposed to cetuximab showed a considerably decreased response to gefitinib, as reflected by monolayer growth assays (figure 22) and also by soft agar colony formation assays (figure 23). Inferring from these results, cetuximab long-term treatment appears to alter A431 cells in regard to their response to gefitinib, yet this is not mirrored by altered in vitro sensitivity towards the antibody itself. This implies that long-term exposure of A431 cells to cetuximab causes alterations that also affect the mode of EGFR activity or accessibility to gefitinib.

#### **4.5 Cetuximab and gefitinib long-term-treated A431 cells show moderately altered expression patterns and different dynamics of EGFR**

Studies on cell lines with acquired resistance to EGFR-specific TKIs consistently indicate down regulation of EGFR expression (Perez-Soler et al., 2003; Ando et al., 2005). In line with these observations, this examination proved decreased EGFR protein expression and equally reduced surface levels in gefitinib-resistant A431 cells (cf. figures 31 and 29). One study finds an increased ligand-induced internalization of EGFR in a gefitinib-resistant lung cancer cell line (Kwak et al., 2005). This work revealed a decreased cetuximab-induced internalization of the receptor in gefitinib-resistant A431 cells (figure 30) that correlated to their modestly decreased response to cetuximab in a soft-agar colony formation assay as compared with medium-treated control cells of similar passage number (figure 25). In summary, long-term treatment of A431 cells with gefitinib caused reduced expression of EGFR and putatively diminished receptor dynamics, as reflected by retarded EGFR turnover through cetuximab.

A six-week exposure of a cetuximab-sensitive pancreas cancer cell line to the antibody has been reported to cause a reduction of EGFR surface levels (Huang et al., 2003). In agreement with that observation, A431 cells displayed markedly

reduced surface levels of EGFR after long-term exposure to cetuximab (figure 29). However, total cellular levels of EGFR in these cells were comparable to the levels in medium-treated control cells of similar passage number (figure 31) suggesting that in long-term cetuximab-treated cells the majority of EGFR are localized within the cell. Since only full-length receptor was accounted for immunoblot signals, intracellular EGFR molecules complexed with cetuximab may not be subjected to a rapid degradation mechanism. The perception that a multitude of antibody-receptor complexes were accumulated within the cell may also help to explain the observation that long-term cetuximab-exposed cells showed reduced capacity for antibody-mediated receptor internalization (figure 30).

Another notion of this study is that long-term cetuximab-treated-A431 cells, but not gefitinib-resistant cells, displayed increased protein levels of ErbB3 and ErbB4 receptors, as compared to medium-treated cells of similar passage number (figure 31). The significance of this observation is not clear, yet it eventually points towards compensatory signaling via ErbB3 and ErbB4 receptors. However, expression of the highly signaling competent receptor ErbB2 cannot be detected in any A431 cell population (figure 31).

#### **4.6 Cetuximab and to a minor extent gefitinib, block epithelial-mesenchymal transition (EMT) in long-term cultured A431 cells**

A role for EGFR in triggering EMT in breast cancer cells has been described in vitro (Lo et al., 2005; Lee et al., 2006b). Furthermore, ectopic expression of the constitutively active EGFRvIII receptor in ovary cancer cells caused EMT (Zeineldin et al., 2006). These data point towards a general significance of EGFR in the induction of this de-differentiation process.

In this study EMT was observed in the epidermoid cell line A431 after long-term culture, as reflected by loss of E-cadherin expression, gain of vimentin expression (figure 32) and characteristic morphological alterations (figure 26). In addition, it was shown that long-term exposure to cetuximab blocked EMT in this cell line and arrested cells in a typically epithelial state (figures 26 and 32). This also appeared to hold true for gefitinib, however this population displayed somewhat diminished levels of E-cadherin and cellular morphology was rather metastable with more mesenchymal features (figures 26 and 32).



Complex formation of EGFR with E-cadherin in basolateral areas of epithelial cells has been demonstrated to modulate EGFR kinase activity and downstream signaling (Pece et al., 1999; Pece et al., 2000; Qian et al., 2004). Furthermore, long-term incubation of A431 cells with EGF causes endocytosis and degradation of E-cadherin, which is paralleled by induction of the transcription factor Snail, a hallmark for EMT (Lu et al., 2003). Therefore a potential explanation of the cetuximab-mediated blockade of EMT lies in the capacity of the antibody to compete with EGF for binding sites on the receptor, thereby inhibiting the effects conferred by the ligand. Since A431 can activate EGFR through autocrine secretion of ligands (Van de Vijver et al., 1991) it can be expected that this drives long-term cultured A431 cells into EMT.

Interestingly, EMT was found to be implicated in explaining cellular growth response to EGFR-targeting TKIs. NSCLC cells with epithelial characteristics display an increased grade of sensitivity as compared to mesenchymal NSCLC cells (Thomson et al., 2005; Yauch et al., 2005; Witta et al., 2006). The observed capacity of cetuximab to arrest cancer cells in an epithelial state together with the notion that epithelial cells are more responsive to EGFR-targeting TKIs may also explain the finding that combined treatment of A431 cells with cetuximab and gefitinib provokes cellular responses that are superior to single agent treatments (Matar et al., 2004).

#### **4.7 Activation of HGFR may compensate for cetuximab-mediated blockage of EGFR**

Overexpression of HGFR was recently reported in a primarily gefitinib sensitive NSCLC cell line, which has acquired resistance to this TKI due to long-term exposure. Furthermore, this study found HGFR amplification in 22% of NSCLC tumors that relapsed on EGFR-targeting TKIs (Engelman et al., 2007). In this work, a screen on the activation level of RTKs in A431 cells after long-term exposure to EGFR-targeting drugs, identified HGFR as being hyper-activated in cetuximab, but not in gefitinib-treated cell populations (cf. figures 33 and 34). Evaluation by immunoblot found a marked increase of HGFR expression in gefitinib-resistant A431 cells, which however was not accompanied by a significant activation of HGFR (figure 35). In contrast, cetuximab long-term-treated cells displayed only a moderate rise in total HGFR expression, but exhibited a substantial increase in receptor phosphorylation (figure 35). These observations are in line with the results reported

by others and further indicate for the first time a role for HGFR in compensating blockage of EGFR by cetuximab.

In addition, this work could show that HGFR-specific TKIs cause an appreciable growth inhibition in A431 cells that were long-term treated with cetuximab, but not in the gefitinib-resistant population or medium-treated A431 cells of similar passage number (figure 36). Interestingly, elevated activation of HGFR and sensitivity to HGFR TKIs was also observed in A431 cells from the starting population (figures 35 and 36). As already mentioned, these cells and the population that was long-term exposed to cetuximab, showed molecular and morphological features that are typical for epithelial cells. The importance of activated HGFR in mediating EMT has been well described (Jiang et al., 1999; Comoglio and Boccaccio, 2001). Notably, it is known that HGFR may associate with EGFR in cancer cells and that this interaction allows ligand-independent activation of HGFR. Yet exposure of cells to an EGFR inhibiting antibody reversed HGFR phosphorylation (Jo et al., 2000). From these data it can be hypothesized that EGFR-dependent activation of HGFR may be necessary for enabling HGFR-mediated onset of EMT. Blockage of EGFR by cetuximab thus may impede complex formation between both receptors due to sterical hindrance, causing epithelial arrest of cells. The fact that high activation of HGFR, as observed in long-term cetuximab exposed A431 cells, alone was not sufficient for eliciting EMT, may indicate that the EGFR-HGFR interaction provides a particular signaling output which is not stimulated by regular activation of HGFR. Though highly speculative on the basis of the data provided in this work, these considerations may provide a novel mechanistic insight to RTK-mediated EMT initiation.

#### **4.8 Cell lines with primary resistance or sensitivity to EGFR-targeting drugs show differential basal expression patterns after long-term exposure to cancer therapeutics**

A candidate-based expression analyses with cell lines long-term treated with EGFR specific drugs has been performed in this work. The examination served to identify factors that were differently expressed in primary sensitive cell lines (A431 and Difi) after long-term exposure to either gefitinib or cetuximab, but whose expression was not altered in primary resistant cell lines (H460 and SW707).

Eight candidate genes were found to be differentially regulated in long-term cetuximab-treated Difi and A431 cells, but unaltered in long-term-treated H460 and SW707 cell lines. Namely, CCL5 was up-regulated in cetuximab-sensitive, but not resistant cell lines after long-term exposure to this drug (figure 37). Expression of the chemokine CCL5 is controlled by TNF $\alpha$  and is part of the inflammatory response system, whose components serve as chemoattractants for immune cells. It has been shown that impairment of EGFR activity causes increased expression of CCL5 (Pastore et al., 2005). Even though the role for this in cetuximab caused immune response cannot be acknowledged in vitro, it may possess relevance for the clinic. Interestingly, also expression of complement component C3 was triggered in cetuximab sensitive cell lines (figure 37). This finding may provide another valuable insight in the mode of cetuximab-triggered killing of tumor cells through antibody-mediated complement-dependent cytotoxicity (CDC). Deposition of processed C3 on the surface of tumor cells allows binding of cytotoxic T-cells carrying the C3 receptor, which is the initial step for activation of the complement system (Gelderman et al., 2004). The up-regulation of immunogenic factors in cetuximab sensitive cells, though in vitro, calls into attention the versatility of antibody-mediated tumor inhibition. In addition, both candidates may be favourable due to their unproblematic clinical accessibility, since detection of these proteins should be possible from patient's serum. Interestingly, another inflammatory factor (CXCL6) was found to be up-regulated in cells with acquired resistance to gefitinib, yet not in cells with primary resistance to that TKI (figure 38).

Furthermore, four ErbB ligands were found to be either up- (BTC, EGF) or down-regulated (EREG, HB-EGF) in cetuximab-sensitive cells after long-term treatment with the antibody (table 5). Notably, both ligands that were up-regulated in cetuximab-treated cells (BTC and EGF) bind exclusively to EGFR, while the ligands that are down-regulated (EREG and HB-EGF) may bind to EGFR as well as to ErbB4 receptors (Elenius et al., 1997; Komurasaki et al., 2000). It is unclear, whether ligand binding sites or competition with cetuximab corresponds to the observed gene expression pattern.

#### 4.9 Perspectives

Against the background of the clinical significance of EGFR-driven cancerogenesis it is at hand that a better understanding on the functionality of EGFR-targeting cancer

drugs is needed. Firstly, identification of cellular factors that predict resistance or sensitivity to EGFR-targeting therapeutics allows for exclusion or selection of patients for these regimens. Secondly, understanding the mode of action of EGFR-targeting TKIs and monoclonal antibodies provides also valuable insight to cancer drugs that aim at other cellular targets with tumorigenic potency and therefore allows refining therapy strategies. Thirdly, elucidation of factors that predict resistance to EGFR-specific therapy may suggest combination therapies that could be superior to single drug treatment.

In terms of preclinical examinations it will therefore be helpful to collect and evaluate additional data from mRNA basal expression analyses in patients or cell lines with differential response to EGFR-targeting drugs. The new candidates suggested in this work to be possibly predictive for cellular response to cetuximab or gefitinib in NSCLC will need to be validated on the protein level, followed by retrospective clinical examinations. Initial growth-inhibitory in vitro experiments and the availability of specific inhibitors against resistance-conferring factors will point out the perspectives and limits of combination therapy in the respective tumor context. However, in addition to plain analyses of mRNA or protein expression, more detailed studies focusing on post-translational modifications by phosphate residues or ubiquitin, as well as on subcellular localization of EGFR and other proteins will be necessary to better understand the mechanisms of cellular drug response. Moreover, the efficacy of cetuximab to block receptor homo- or heterodimerization could further be studied by BRET (bioluminescence resonance energy transfer) analyses; however, this technique did not yield satisfying results when applied in conjunction with this work.

In-depth characterization of the cellular resistance models established in this work will shed light on the causes of primary and secondary resistance to EGFR-targeting drugs. Since cetuximab was found to block an epithelial cell line from going through EMT, it will be interesting to see if this observation translates into general mode of action for this therapeutic antibody. If so, this might have important implications for a preferred cetuximab treatment of early, non-invasive tumor stages. For studying sensitivity and cross-sensitivity to EGFR-specific cancer therapeutics in the long-term drug exposed cell lines, xenograft models will provide additional cognitions in the clinical context.

## 5. Summary

This study characterized a panel of NSCLC cell lines as well as a stably transfected cell model expressing wild-type and mutated EGFR variants in terms of response to the EGFR-targeting drugs, gefitinib and cetuximab. The examinations support the notion that response to gefitinib is neither exclusive nor strictly determined by the presence of EGFR kinase mutations. Yet, cells expressing EGFR kinase domain mutations tended to generally respond better to treatments with gefitinib compared to those with wild-type EGFR. On the other hand, preliminary studies suggesting that cellular sensitivity to cetuximab is determined by factors other than EGFR kinase domain mutations could be substantiated through a robust set of data. Moreover, several promising candidate genes differentially expressed in gefitinib sensitive and resistant NSCLC cell lines were revealed by a global mRNA expression analyses. In addition, though statistically questionable, several biologically interesting genes that are possibly involved in determining in vitro response of NSCLC cells to cetuximab have been postulated.

In this work, four cancer cell models, which are long-term exposed to gefitinib or cetuximab were established and characterized in terms of gain-of-resistance towards EGFR-targeting compounds, as well as in regard to biological and molecular alterations caused by long-term treatments. It was found that gefitinib long-term treatment of primary sensitive A431 cells conferred growth-resistance to this TKI, but not to cetuximab. This observation may have clinical implications for patients that relapsed on gefitinib as it suggests that they might still profit from cetuximab therapy. On the other hand long-term exposure of A431 cells to cetuximab did not render cells resistant to neither the antibody nor gefitinib in regard to in vitro growth-inhibition. Furthermore, it appeared that long-term gefitinib-treated A431 cells downregulate overall EGFR levels, while long-term cetuximab exposed cells displayed decreased EGFR surface levels but constant overall expression. In addition, a candidate-based approach identified genes that are differentially expressed in cancer cells with primary or secondary resistance to gefitinib or cetuximab.

Finally, this study for the first time provided evidence that cetuximab may block metastasis-facilitating epithelial-mesenchymal-transition (EMT) in an epithelial cell line. Moreover, it was suggested that activation of the HGFR may compensate for cetuximab-mediated blockage of EGFR. This was also reflected by an increased response of this population towards treatment with HGFR inhibitors.

## 5. Zusammenfassung

Im Rahmen dieser Arbeit wurden eine Reihe von NSCLC-Zelllinien, sowie eine mit verschiedenen EGFR-Varianten stabil transfizierte Modellzelllinie hinsichtlich ihrer Responsivität gegenüber den EGFR-spezifischen Tumorthérapeutika Gefitinib und Cetuximab untersucht. Dabei wurde festgestellt, dass Mutationen in der EGFR-Kinasedomäne weder hinreichend noch notwendig für eine zelluläre Sensitivität gegenüber Gefitinib sind. Dennoch war zu beobachten, dass Mutationen in der EGFR-Kinasedomäne für eine allgemein erhöhte Sensitivität gegenüber Gefitinib verantwortlich sind. Auf der anderen Seite wurde gezeigt, dass die Sensitivität von NSCLC-Zellen gegenüber Cetuximab nicht von Mutationen der EGFR-Kinasedomäne determiniert wird sondern von anderen Faktoren abhängt. Darüber hinaus konnten im Rahmen einer globalen Expressionsanalyse eine Reihe von Kandidatengenen identifiziert werden, welche in Gefitinib-sensitiven und -resistenten Zelllinien differentiell exprimiert sind. Entsprechend konnten auch biologisch interessante Gene identifiziert werden, welche möglicherweise prognostische Bedeutung für die Sensitivität von NSCLC-Zellen gegenüber Cetuximab besitzen.

Zudem wurden in dieser Arbeit vier mit Gefitinib oder Cetuximab langzeitbehandelte Krebszelllinien etabliert und charakterisiert. Es konnte festgestellt werden, dass die langzeit mit Gefitinib behandelte epitheliale Zelllinie A431 eine Resistenz gegenüber Gefitinib, nicht aber gegenüber Cetuximab erwirbt. Diese Beobachtung besitzt möglicherweise klinische Relevanz, da sie impliziert, dass Patienten welche nicht mehr auf Gefitinib ansprechen durchaus noch auf Cetuximab respondieren können. Auf der anderen Seite konnte für Cetuximab-langzeitbehandelte A431 Zellen im Wachstumsinhibitions-Assay weder eine Resistenz gegenüber Cetuximab noch gegenüber Gefitinib festgestellt werden. Zudem wurde gezeigt, dass Gefitinib-resistente A431 Zellen eine Verminderung der zellulären EGFR-Proteinexpression aufweisen. Demgegenüber war in Cetuximab-langzeitbehandelten A431 Zellen eine verminderte Lokalisation von EGFR auf der Zelloberfläche zu sehen, während die Proteinexpression insgesamt unverändert blieb.

Diese Arbeit zeigte erstmalig, dass Cetuximab den Prozess der epithelialen-mesenchymalen-Transition (EMT) in A431 Zellen blockieren kann; EMT wurde klinisch mit der Metastasierung von Tumoren assoziiert. Zudem war die Aktivität von HGFR in Cetuximab-langzeitbehandelten A431 Zellen deutlich erhöht, was sich auch in einer erhöhten Sensitivität gegenüber HGFR-Inhibitoren widerspiegelte.

## 6. References

Adjei,A.A. (2006). Novel combinations based on epidermal growth factor receptor inhibition. *Clin. Cancer Res.* 12, 4446s-4450s.

Adnane,J., Gaudray,P., Dionne,C.A., Crumley,G., Jaye,M., Schlessinger,J., Jeanteur,P., Birnbaum,D., and Theillet,C. (1991). BEK and FLG, two receptors to members of the FGF family, are amplified in subsets of human breast cancers. *Oncogene* 6, 659-663.

Albanell,J., Rojo,F., Averbuch,S., Feyereislova,A., Mascaro,J.M., Herbst,R., LoRusso,P., Rischin,D., Sauleda,S., Gee,J., Nicholson,R.I., and Baselga,J. (2002). Pharmacodynamic studies of the epidermal growth factor receptor inhibitor ZD1839 in skin from cancer patients: histopathologic and molecular consequences of receptor inhibition. *J. Clin. Oncol.* 20, 110-124.

Allan,D.G. (2005). Nimotuzumab: evidence of clinical benefit without rash. *Oncologist.* 10, 760-761.

Amann,J., Kalyankrishna,S., Massion,P.P., Ohm,J.E., Girard,L., Shigematsu,H., Peyton,M., Juroske,D., Huang,Y., Stuart,S.J., Kim,Y.H., Pollack,J.R., Yanagisawa,K., Gazdar,A., Minna,J.D., Kurie,J.M., and Carbone,D.P. (2005). Aberrant epidermal growth factor receptor signaling and enhanced sensitivity to EGFR inhibitors in lung cancer. *Cancer Res.* 65, 226-235.

Ando,K., Ohmori,T., Inoue,F., Kadofuku,T., Hosaka,T., Ishida,H., Shirai,T., Okuda,K., Hirose,T., Horichi,N., Nishio,K., Saijo,N., Adachi,M., and Kuroki,T. (2005). Enhancement of sensitivity to tumor necrosis factor alpha in non-small cell lung cancer cells with acquired resistance to gefitinib. *Clin. Cancer Res.* 11, 8872-8879.

Arnoletti,J.P., Upson,J., Babb,J.S., Bellacosa,A., and Watson,J.C. (2005). Differential stromal and epithelial localization of cyclooxygenase-2 (COX-2) during colorectal tumorigenesis. *J. Exp. Clin. Cancer Res.* 24, 279-287.

Asahina,H., Yamazaki,K., Kinoshita,I., Sukoh,N., Harada,M., Yokouchi,H., Ishida,T., Ogura,S., Kojima,T., Okamoto,Y., Fujita,Y., aka-Akita,H., Isobe,H., and Nishimura,M. (2006). A phase II trial of gefitinib as first-line therapy for advanced non-small cell

lung cancer with epidermal growth factor receptor mutations. *Br. J. Cancer* 95, 998-1004.

Balko,J.M., Potti,A., Saunders,C., Stromberg,A., Haura,E.B., and Black,E.P. (2006). Gene expression patterns that predict sensitivity to epidermal growth factor receptor tyrosine kinase inhibitors in lung cancer cell lines and human lung tumors. *BMC. Genomics* 7, 289.

Barber,T.D., Vogelstein,B., Kinzler,K.W., and Velculescu,V.E. (2004). Somatic mutations of EGFR in colorectal cancers and glioblastomas. *N. Engl. J. Med.* 351, 2883.

Bartlett,J.M., Langdon,S.P., Simpson,B.J., Stewart,M., Katsaros,D., Sismondi,P., Love,S., Scott,W.N., Williams,A.R., Lessells,A.M., Macleod,K.G., Smyth,J.F., and Miller,W.R. (1996). The prognostic value of epidermal growth factor receptor mRNA expression in primary ovarian cancer. *Br. J. Cancer* 73, 301-306.

Baselga,J., Rischin,D., Ranson,M., Calvert,H., Raymond,E., Kieback,D.G., Kaye,S.B., Gianni,L., Harris,A., Bjork,T., Averbuch,S.D., Feyereislova,A., Swaisland,H., Rojo,F., and Albanell,J. (2002). Phase I safety, pharmacokinetic, and pharmacodynamic trial of ZD1839, a selective oral epidermal growth factor receptor tyrosine kinase inhibitor, in patients with five selected solid tumor types. *J. Clin. Oncol.* 20, 4292-4302.

Baselga,J., Albanell,J., Ruiz,A., Lluch,A., Gascon,P., Guillem,V., Gonzalez,S., Sauleda,S., Marimon,I., Tabernero,J.M., Koehler,M.T., and Rojo,F. (2005). Phase II and tumor pharmacodynamic study of gefitinib in patients with advanced breast cancer. *J. Clin. Oncol.* 23, 5323-5333.

Battle,E., Sancho,E., Franci,C., Dominguez,D., Monfar,M., Baulida,J., and Garcia De,H.A. (2000). The transcription factor snail is a repressor of E-cadherin gene expression in epithelial tumor cells. *Nat. Cell Biol.* 2, 84-89.

Bianco,R., Shin,I., Ritter,C.A., Yakes,F.M., Basso,A., Rosen,N., Tsurutani,J., Dennis,P.A., Mills,G.B., and Arteaga,C.L. (2003). Loss of PTEN/MMAC1/TEP in EGF receptor-expressing tumor cells counteracts the antitumor action of EGFR tyrosine kinase inhibitors. *Oncogene* 22, 2812-2822.



Blume-Jensen,P. and Hunter,T. (2001). Oncogenic kinase signaling. *Nature* 411, 355-365.

Brehmer,D., Greff,Z., Godl,K., Blencke,S., Kurtenbach,A., Weber,M., Muller,S., Klebl,B., Cotten,M., Keri,G., Wissing,J., and Daub,H. (2005). Cellular targets of gefitinib. *Cancer Res.* 65, 379-382.

Calvo,E. and Baselga,J. (2006). Ethnic differences in response to epidermal growth factor receptor tyrosine kinase inhibitors. *J. Clin. Oncol.* 24, 2158-2163.

Cano,A., Perez-Moreno,M.A., Rodrigo,I., Locascio,A., Blanco,M.J., del Barrio,M.G., Portillo,F., and Nieto,M.A. (2000). The transcription factor snail controls epithelial-mesenchymal transitions by repressing E-cadherin expression. *Nat. Cell Biol.* 2, 76-83.

Caponigro,F. (2004). Rationale and clinical validation of epidermal growth factor receptor as a target in the treatment of head and neck cancer. *Anticancer Drugs* 15, 311-320.

Cappuzzo,F., Magrini,E., Ceresoli,G.L., Bartolini,S., Rossi,E., Ludovini,V., Gregorc,V., Ligorio,C., Cancellieri,A., Damiani,S., Spreafico,A., Paties,C.T., Lombardo,L., Calandri,C., Bellezza,G., Tonato,M., and Crino,L. (2004). Akt phosphorylation and gefitinib efficacy in patients with advanced non-small-cell lung cancer. *J. Natl. Cancer Inst.* 96, 1133-1141.

Cappuzzo,F., Hirsch,F.R., Rossi,E., Bartolini,S., Ceresoli,G.L., Bemis,L., Haney,J., Witta,S., Danenberg,K., Domenichini,I., Ludovini,V., Magrini,E., Gregorc,V., Doglioni,C., Sidoni,A., Tonato,M., Franklin,W.A., Crino,L., Bunn,P.A., Jr., and Varella-Garcia,M. (2005). Epidermal growth factor receptor gene and protein and gefitinib sensitivity in non-small-cell lung cancer. *J. Natl. Cancer Inst.* 97, 643-655.

Cappuzzo,F., Toschi,L., Tallini,G., Ceresoli,G.L., Domenichini,I., Bartolini,S., Finocchiaro,G., Magrini,E., Metro,G., Cancellieri,A., Trisolini,R., Crino,L., Bunn,P.A., Santoro,A., Franklin,W.A., Varella-Garcia,M., Hirsch,F.R. (2006) Insulin-like growth factor receptor 1 (IGFR-1) is significantly associated with longer survival in non-small-cell lung cancer patients treated with gefitinib. *Ann Oncol*, 17, 1120-1127.

- Chakravarti,A., Loeffler,J.S., and Dyson,N.J. (2002). Insulin-like growth factor receptor I mediates resistance to anti-epidermal growth factor receptor therapy in primary human glioblastoma cells through continued activation of phosphoinositide 3-kinase signaling. *Cancer Res.* 62, 200-207.
- Choong,N.W., Dietrich,S., Seiwert,T.Y., Tretiakova,M.S., Nallasura,V., Davies,G.C., Lipkowitz,S., Husain,A.N., Salgia,R., and Ma,P.C. (2006). Gefitinib response of erlotinib-refractory lung cancer involving meninges--role of EGFR mutation. *Nat. Clin. Pract. Oncol.* 3, 50-57.
- Chong,I.W., Chang,M.Y., Sheu,C.C., Wang,C.Y., Hwang,J.J., Huang,M.S., Lin,S.R. (2007). Detection of activated K-ras in non-small cell lung cancer by membrane array: a comparison with direct sequencing. *Oncol Rep*, 18, 17-24.
- Christensen,J.G., Schreck,R., Burrows,J., Kuruganti,P., Chan,E., Le,P., Chen,J., Wang,X., Ruslim,L., Blake,R., Lipson,K.E., Ramphal,J., Do,S., Cui,J.J., Cherrington,J.M., and Mendel,D.B. (2003). A selective small molecule inhibitor of c-Met kinase inhibits c-Met-dependent phenotypes in vitro and exhibits cytoreductive antitumor activity in vivo. *Cancer Res.* 63, 7345-7355.
- Christensen,J.G., Burrows,J., and Salgia,R. (2005). c-Met as a target for human cancer and characterization of inhibitors for therapeutic intervention. *Cancer Lett.* 225, 1-26.
- Cohen,E.E., Rosen,F., Stadler,W.M., Recant,W., Stenson,K., Huo,D., and Vokes,E.E. (2003). Phase II trial of ZD1839 in recurrent or metastatic squamous cell carcinoma of the head and neck. *J. Clin. Oncol.* 21, 1980-1987.
- Cohen,M.H., Williams,G.A., Sridhara,R., Chen,G., McGuinn,W.D., Jr., Morse,D., Abraham,S., Rahman,A., Liang,C., Lostritto,R., Baird,A., and Pazdur,R. (2004). United States Food and Drug Administration Drug Approval summary: Gefitinib (ZD1839; Iressa) tablets. *Clin. Cancer Res.* 10, 1212-1218.
- Cohen,P. (2002). Protein kinases--the major drug targets of the twenty-first century? *Nat. Rev. Drug Discov.* 1, 309-315.
- Coldren,C.D., Helfrich,B.A., Witta,S.E., Sugita,M., Lapadat,R., Zeng,C., Baron,A., Franklin,W.A., Hirsch,F.R., Geraci,M.W., and Bunn,P.A., Jr. (2006). Baseline gene

expression predicts sensitivity to gefitinib in non-small cell lung cancer cell lines. *Mol. Cancer Res.* 4, 521-528.

Comoglio,P.M. and Boccaccio,C. (2001). Scatter factors and invasive growth. *Semin. Cancer Biol.* 11, 153-165.

Cunningham,D., Humblet,Y., Siena,S., Khayat,D., Bleiberg,H., Santoro,A., Bets,D., Mueser,M., Harstrick,A., Verslype,C., Chau,I., and Van,C.E. (2004). Cetuximab monotherapy and cetuximab plus irinotecan in irinotecan-refractory metastatic colorectal cancer. *N. Engl. J. Med.* 351, 337-345.

Damstrup,L., Wandahl,P.M., Bastholm,L., Elling,F., and Skovgaard,P.H. (2002). Epidermal growth factor receptor mutation type III transfected into a small cell lung cancer cell line is predominantly localized at the cell surface and enhances the malignant phenotype. *Int. J. Cancer* 97, 7-14.

Dancey,J. and Sausville,E.A. (2003). Issues and progress with protein kinase inhibitors for cancer treatment. *Nat. Rev. Drug Discov.* 2, 296-313.

Datta,S.R., Dudek,H., Tao,X., Masters,S., Fu,H., Gotoh,Y., and Greenberg,M.E. (1997). Akt phosphorylation of BAD couples survival signals to the cell-intrinsic death machinery. *Cell* 91, 231-241.

Davis,C.G., Gallo,M.L., and Corvalan,J.R. (1999). Transgenic mice as a source of fully human antibodies for the treatment of cancer. *Cancer Metastasis Rev.* 18, 421-425.

de Bono,J.S. and Rowinsky,E.K. (2002). The ErbB receptor family: a therapeutic target for cancer. *Trends Mol. Med.* 8, S19-S26.

Di Fiore,P.P., Pierce,J.H., Fleming,T.P., Hazan,R., Ullrich,A., King,C.R., Schlessinger,J., and Aaronson,S.A. (1987). Overexpression of the human EGF receptor confers an EGF-dependent transformed phenotype to NIH 3T3 cells. *Cell* 51, 1063-1070.

Dong,R., Wang,Q., He,X.L., Chu,Y.K., Lu,J.G., and Ma,Q.J. (2007). Role of nuclear factor kappa B and reactive oxygen species in the tumor necrosis factor- $\alpha$ -induced

epithelial-mesenchymal transition of MCF-7 cells. *Braz. J. Med. Biol. Res.* 40, 1071-1078.

Douglass,E.C. (2003). Development of ZD1839 in colorectal cancer. *Semin. Oncol.* 30, 17-22.

Eberhard,D.A., Johnson,B.E., Amler,L.C., Goddard,A.D., Heldens,S.L., Herbst,R.S., Ince,W.L., Janne,P.A., Januario,T., Johnson,D.H., Klein,P., Miller,V.A., Ostland,M.A., Ramies,D.A., Sebisanoovic,D., Stinson,J.A., Zhang,Y.R., Seshagiri,S., and Hillan,K.J. (2005). Mutations in the epidermal growth factor receptor and in KRAS are predictive and prognostic indicators in patients with non-small-cell lung cancer treated with chemotherapy alone and in combination with erlotinib. *J. Clin. Oncol.* 23, 5900-5909.

Ekstrand,A.J., James,C.D., Cavenee,W.K., Seliger,B., Pettersson,R.F., and Collins,V.P. (1991). Genes for epidermal growth factor receptor, transforming growth factor alpha, and epidermal growth factor and their expression in human gliomas in vivo. *Cancer Res.* 51, 2164-2172.

Elenius,K., Paul,S., Allison,G., Sun,J., and Klagsbrun,M. (1997). Activation of HER4 by heparin-binding EGF-like growth factor stimulates chemotaxis but not proliferation. *EMBO J.* 16, 1268-1278.

Engelman,J.A., Janne,P.A., Mermel,C., Pearlberg,J., Mukohara,T., Fleet,C., Cichowski,K., Johnson,B.E., and Cantley,L.C. (2005). ErbB-3 mediates phosphoinositide 3-kinase activity in gefitinib-sensitive non-small cell lung cancer cell lines. *Proc. Natl. Acad. Sci. U. S. A* 102, 3788-3793.

Engelman,J.A., Mukohara,T., Zejnullahu,K., Lifshits,E., Borrás,A.M., Gale,C.M., Naumov,G.N., Yeap,B.Y., Jarrell,E., Sun,J., Tracy,S., Zhao,X., Heymach,J.V., Johnson,B.E., Cantley,L.C., and Janne,P.A. (2006). Allelic dilution obscures detection of a biologically significant resistance mutation in EGFR-amplified lung cancer. *J. Clin. Invest* 116, 2695-2706.

Engelman,J.A., Zejnullahu,K., Mitsudomi,T., Song,Y., Hyland,C., Park,J.O., Lindeman,N., Gale,C.M., Zhao,X., Christensen,J., Kosaka,T., Holmes,A.J., Rogers,A.M., Cappuzzo,F., Mok,T., Lee,C., Johnson,B.E., Cantley,L.C., and

Janne,P.A. (2007). MET amplification leads to gefitinib resistance in lung cancer by activating ERBB3 signaling. *Science* 316, 1039-1043.

Essner,J.J., Chen,E., and Ekker,S.C. (2006). Syndecan-2. *Int. J. Biochem. Cell Biol.* 38, 152-156.

Fabian,M.A., Biggs,W.H., III, Treiber,D.K., Atteridge,C.E., Azimioara,M.D., Benedetti,M.G., Carter,T.A., Ciceri,P., Edeen,P.T., Floyd,M., Ford,J.M., Galvin,M., Gerlach,J.L., Grotzfeld,R.M., Herrgard,S., Insko,D.E., Insko,M.A., Lai,A.G., Lelias,J.M., Mehta,S.A., Milanov,Z.V., Velasco,A.M., Wodicka,L.M., Patel,H.K., Zarrinkar,P.P., and Lockhart,D.J. (2005). A small molecule-kinase interaction map for clinical kinase inhibitors. *Nat. Biotechnol.* 23, 329-336.

Feldkamp,M.M., Lala,P., Lau,N., Roncari,L., and Guha,A. (1999). Expression of activated epidermal growth factor receptors, Ras-guanosine triphosphate, and mitogen-activated protein kinase in human glioblastoma multiforme specimens. *Neurosurgery* 45, 1442-1453.

Fischer-Colbrie,J., Witt,A., Heinzl,H., Speiser,P., Czerwenka,K., Sevela,P., and Zeillinger,R. (1997). EGFR and steroid receptors in ovarian carcinoma: comparison with prognostic parameters and outcome of patients. *Anticancer Res.* 17, 613-619.

Fischer,O.M., Hart,S., Gschwind,A., and Ullrich,A. (2003). EGFR signal transactivation in cancer cells. *Biochem. Soc. Trans.* 31 , 1203-1208.

Fontanini,G., De Laurentiis,M., Vignati,S., Chine,S., Lucchi,M., Silvestri,V., Mussi,A., De,P.S., Tortora,G., Bianco,A.R., Gullick,W., Angeletti,C.A., Bevilacqua,G., and Ciardiello,F. (1998). Evaluation of epidermal growth factor-related growth factors and receptors and of neoangiogenesis in completely resected stage I-IIIa non-small-cell lung cancer: amphiregulin and microvessel count are independent prognostic indicators of survival. *Clin. Cancer Res.* 4, 241-249.

Frederick,L., Eley,G., Wang,X.Y., and James,C.D. (2000). Analyses of genomic rearrangements associated with EGRFvIII expression suggests involvement of Alu repeat elements. *Neuro. Oncol.* 2, 159-163.

Fujimoto,N., Wislez,M., Zhang,J., Iwanaga,K., Dackor,J., Hanna,A.E., Kalyankrishna,S., Cody,D.D., Price,R.E., Sato,M., Shay,J.W., Minna,J.D., Peyton,M.,

- Tang,X., Massarelli,E., Herbst,R., Threadgill,D.W., Wistuba,I.I., and Kurie,J.M. (2005). High expression of ErbB family members and their ligands in lung adenocarcinomas that are sensitive to inhibition of epidermal growth factor receptor. *Cancer Res.* 65, 11478-11485.
- Garrett,T.P., McKern,N.M., Lou,M., Elleman,T.C., Adams,T.E., Lovrecz,G.O., Zhu,H.J., Walker,F., Frenkel,M.J., Hoyne,P.A., Jorissen,R.N., Nice,E.C., Burgess,A.W., and Ward,C.W. (2002). Crystal structure of a truncated epidermal growth factor receptor extracellular domain bound to transforming growth factor alpha. *Cell* 110, 763-773.
- Gelderman,K.A., Tomlinson,S., Ross,G.D., and Gorter,A. (2004). Complement function in mAb-mediated cancer immunotherapy. *Trends Immunol.* 25, 158-164.
- Gentleman,R.C., Carey,V.J., Bates,D.M., Bolstad,B., Dettling,M., Dudoit,S., Ellis,B., Gautier,L., Ge,Y., Gentry,J., Hornik,K., Hothorn,T., Huber,W., Iacus,S., Irizarry,R., Leisch,F., Li,C., Maechler,M., Rossini,A.J., Sawitzki,G., Smith,C., Smyth,G., Tierney,L., Yang,J.Y., and Zhang,J. (2004). Bioconductor: open software development for computational biology and bioinformatics. *Genome Biol.* 5, R80.
- Giaccone,G., Gallegos,R.M., Le,C.T., Thatcher,N., Smit,E., Rodriguez,J.A., Janne,P., Oulid-Aissa,D., and Soria,J.C. (2006). Erlotinib for frontline treatment of advanced non-small cell lung cancer: a phase II study. *Clin. Cancer Res.* 12, 6049-6055.
- Gilbert,S.F. (1996). Cellular dialogues in organogenesis. *Birth Defects Orig. Artic. Ser.* 30, 1-12.
- Gow,C.H., Shih,J.Y., Chang,Y.L., and Yu,C.J. (2005). Acquired gefitinib-resistant mutation of EGFR in a chemonaive lung adenocarcinoma harboring gefitinib-sensitive mutation L858R. *PLoS. Med.* 2, e269.
- Graus-Porta,D., Beerli,R.R., Daly,J.M., and Hynes,N.E. (1997). ErbB-2, the preferred heterodimerization partner of all ErbB receptors, is a mediator of lateral signaling. *EMBO J.* 16, 1647-1655.
- Greulich,H., Chen,T.H., Feng,W., Janne,P.A., Alvarez,J.V., Zappaterra,M., Bulmer,S.E., Frank,D.A., Hahn,W.C., Sellers,W.R., and Meyerson,M. (2005).

Oncogenic transformation by inhibitor-sensitive and -resistant EGFR mutants. *PLoS. Med.* 2, e313.

Gross,M.E., Zorbas,M.A., Danels,Y.J., Garcia,R., Gallick,G.E., Olive,M., Brattain,M.G., Boman,B.M., and Yeoman,L.C. (1991). Cellular growth response to epidermal growth factor in colon carcinoma cells with an amplified epidermal growth factor receptor derived from a familial adenomatous polyposis patient. *Cancer Res.* 51, 1452-1459.

Gschwind,A., Zwick,E., Prenzel,N., Leserer,M., and Ullrich,A. (2001). Cell communication networks: epidermal growth factor receptor transactivation as the paradigm for interreceptor signal transmission. *Oncogene* 20, 1594-1600.

Gumbiner,B.M. (2005). Regulation of cadherin-mediated adhesion in morphogenesis. *Nat. Rev. Mol. Cell Biol.* 6, 622-634.

Guy,P.M., Platko,J.V., Cantley,L.C., Cerione,R.A., and Carraway,K.L., III (1994). Insect cell-expressed p180erbB3 possesses an impaired tyrosine kinase activity. *Proc. Natl. Acad. Sci. U. S. A* 91, 8132-8136.

Hanahan,D. and Weinberg,R.A. (2000). The hallmarks of cancer. *Cell* 100, 57-70.

Harding,J. and Burtneess,B. (2005). Cetuximab: an epidermal growth factor receptor chemeric human-murine monoclonal antibody. *Drugs Today (Barc.)* 41, 107-127.

Haura,E.B., Zheng,Z., Song,L., Cantor,A., and Bepler,G. (2005). Activated epidermal growth factor receptor-Stat-3 signaling promotes tumor survival in vivo in non-small cell lung cancer. *Clin. Cancer Res.* 11, 8288-8294.

Helin,K. and Beguinot,L. (1991). Internalization and down-regulation of the human epidermal growth factor receptor are regulated by the carboxyl-terminal tyrosines. *J. Biol. Chem.* 266, 8363-8368.

Heymach,J.V., Nilsson,M., Blumenschein,G., Papadimitrakopoulou,V., and Herbst,R. (2006). Epidermal growth factor receptor inhibitors in development for the treatment of non-small cell lung cancer. *Clin. Cancer Res.* 12, 4441s-4445s.

- Hirai,T., Kuwahara,M., Yoshida,K., Kagawa,Y., Hihara,J., Yamashita,Y., and Toge,T. (1998). Clinical results of transhiatal esophagectomy for carcinoma of the lower thoracic esophagus according to biological markers. *Dis. Esophagus*. *11*, 221-225.
- Hirsch,F.R. (2006). EGFR: a prognostic and/or a predictive marker? *J. Thorac. Oncol.* *1*, 395-397.
- Hirsch,F.R., Varella-Garcia,M., Cappuzzo,F., McCoy,J., Bemis,L., Xavier,A.C., Dziadziuszko,R., Gumerlock,P., Chansky,K., West,H., Gazdar,A.F., Crino,L., Gandara,D.R., Franklin,W.A., Bunn,P.A.. (2007) Combination of EGFR gene copy number and protein expression predicts outcome for advanced non-small-cell lung cancer patients treated with gefitinib. *Ann Oncol*, *18*, 752-760.
- Huang,S.M. and Harari,P.M. (1999). Epidermal growth factor receptor inhibition in cancer therapy: biology, rationale and preliminary clinical results. *Invest New Drugs* *17*, 259-269.
- Huang,Z.Q., Buchsbaum,D.J., Raisch,K.P., Bonner,J.A., Bland,K.I., and Vickers,S.M. (2003). Differential responses by pancreatic carcinoma cell lines to prolonged exposure to Erbitux (IMC-C225) anti-EGFR antibody. *J. Surg. Res.* *111*, 274-283.
- Huber,W., von,H.A., Sultmann,H., Poustka,A., and Vingron,M. (2002). Variance stabilization applied to microarray data calibration and to the quantification of differential expression. *Bioinformatics*. *18 Suppl 1*, S96-104.
- Hunter,T. (1998). The role of tyrosine phosphorylation in cell growth and disease. *Harvey Lect.* *94*, 81-119.
- Inukai,M., Toyooka,S., Ito,S., Asano,H., Ichihara,S., Soh,J., Suehisa,H., Ouchida,M., Aoe,K., Aoe,M., Kiura,K., Shimizu,N., and Date,H. (2006). Presence of Epidermal Growth Factor Receptor Gene T790M Mutation as a Minor Clone in Non-Small Cell Lung Cancer. *Cancer Res.* *66*, 7854-7858.
- Irizarry,R.A., Bolstad,B.M., Collin,F., Cope,L.M., Hobbs,B., and Speed,T.P. (2003). Summaries of Affymetrix GeneChip probe level data. *Nucleic Acids Res.* *31*, e15.
- Irmer,D., Funk,J.O., and Blaukat,A. (2007a). EGFR kinase domain mutations - functional impact and relevance for lung cancer therapy. *Oncogene* *26*, 5693-5701.



Irmer,D., Vocke,D., von Heydebreck,A., Amendt,C., Wienke,D., Blaukat,A. (2007b). Activity of the anti-EGFR antibody cetuximab in NSCLC cells with wildtype and mutant EGFR. Manuscript submitted.

Italiano,A. (2006). Targeting the epidermal growth factor receptor in colorectal cancer: advances and controversies. *Oncology* 70, 161-167.

Janmaat,M.L., Kruyt,F.A., Rodriguez,J.A., and Giaccone,G. (2003). Response to epidermal growth factor receptor inhibitors in non-small cell lung cancer cells: limited antiproliferative effects and absence of apoptosis associated with persistent activity of extracellular signal-regulated kinase or Akt kinase pathways. *Clin. Cancer Res.* 9, 2316-2326.

Janmaat,M.L. and Giaccone,G. (2003). The epidermal growth factor receptor pathway and its inhibition as anticancer therapy. *Drugs Today (Barc.)* 39 Suppl C, 61-80.

Janne,P.A., Engelman,J.A., and Johnson,B.E. (2005). Epidermal growth factor receptor mutations in non-small-cell lung cancer: implications for treatment and tumor biology. *J. Clin. Oncol.* 23, 3227-3234.

Jassem,J., Jassem,E., Jakóbkiewicz-Banecka,J., Rzyman,W., Badzio,A., Dziadziuszko,R., Kobierska-Gulida,G., Szymanowska,A., Skrzypski,M., Zylicz,M. (2004) P53 and K-ras mutations are frequent events in microscopically negative surgical margins from patients with nonsmall cell lung carcinoma. *Cancer*, 100, 1951-1960.

Ji,H., Zhao,X., Yuza,Y., Shimamura,T., Li,D., Protopopov,A., Jung,B.L., McNamara,K., Xia,H., Glatt,K.A., Thomas,R.K., Sasaki,H., Horner,J.W., Eck,M., Mitchell,A., Sun,Y., Al-Hashem,R., Bronson,R.T., Rabindran,S.K., Discafani,C.M., Maher,E., Shapiro,G.I., Meyerson,M., and Wong,K.K. (2006). Epidermal growth factor receptor variant III mutations in lung tumorigenesis and sensitivity to tyrosine kinase inhibitors. *Proc. Natl. Acad. Sci. U. S. A* 103, 7817-7822.

Jiang,W., Hiscox,S., Matsumoto,K., and Nakamura,T. (1999). Hepatocyte growth factor/scatter factor, its molecular, cellular and clinical implications in cancer. *Crit Rev. Oncol. Hematol.* 29, 209-248.

- Jo,M., Stolz,D.B., Esplen,J.E., Dorko,K., Michalopoulos,G.K., and Strom,S.C. (2000). Cross-talk between epidermal growth factor receptor and c-Met signal pathways in transformed cells. *J. Biol. Chem.* 275, 8806-8811.
- Johnston,J.B., Navaratnam,S., Pitz,M.W., Maniate,J.M., Wiechec,E., Baust,H., Gingerich,J., Skliris,G.P., Murphy,L.C., and Los,M. (2006). Targeting the EGFR pathway for cancer therapy. *Curr. Med. Chem.* 13, 3483-3492.
- Kakiuchi,S., Daigo,Y., Ishikawa,N., Furukawa,C., Tsunoda,T., Yano,S., Nakagawa,K., Tsuruo,T., Kohno,N., Fukuoka,M., Sone,S., and Nakamura,Y. (2004). Prediction of sensitivity of advanced non-small cell lung cancers to gefitinib (Iressa, ZD1839). *Hum. Mol. Genet.* 13, 3029-3043.
- Kobayashi,S., Ji,H., Yuza,Y., Meyerson,M., Wong,K.K., Tenen,D.G., and Halmos,B. (2005). An alternative inhibitor overcomes resistance caused by a mutation of the epidermal growth factor receptor. *Cancer Res.* 65, 7096-7101.
- Kokubo,Y., Gemma,A., Noro,R., Seike,M., Kataoka,K., Matsuda,K., Okano,T., Minegishi,Y., Yoshimura,A., Shibuya,M., and Kudoh,S. (2005). Reduction of PTEN protein and loss of epidermal growth factor receptor gene mutation in lung cancer with natural resistance to gefitinib (IRESSA). *Br. J. Cancer* 92, 1711-1719.
- Komurasaki,T., Toyoda,H., Uchida,D., and Morimoto,S. (1997). Epiregulin binds to epidermal growth factor receptor and ErbB-4 and induces tyrosine phosphorylation of epidermal growth factor receptor, ErbB-2, ErbB-3 and ErbB-4. *Oncogene* 15, 2841-2848.
- Krupp,M.N., Connolly,D.T., and Lane,M.D. (1982). Synthesis, turnover, and down-regulation of epidermal growth factor receptors in human A431 epidermoid carcinoma cells and skin fibroblasts. *J. Biol. Chem.* 257, 11489-11496.
- Kuroda,S., Fukata,M., Nakagawa,M., Fujii,K., Nakamura,T., Ookubo,T., Izawa,I., Nagase,T., Nomura,N., Tani,H., Shoji,I., Matsuura,Y., Yonehara,S., and Kaibuchi,K. (1998). Role of IQGAP1, a target of the small GTPases Cdc42 and Rac1, in regulation of E-cadherin- mediated cell-cell adhesion. *Science* 281, 832-835.
- Kwak,E.L., Sordella,R., Bell,D.W., Godin-Heymann,N., Okimoto,R.A., Brannigan,B.W., Harris,P.L., Driscoll,D.R., Fidias,P., Lynch,T.J., Rabindran,S.K.,

- McGinnis,J.P., Wissner,A., Sharma,S.V., Isselbacher,K.J., Settleman,J., and Haber,D.A. (2005). Irreversible inhibitors of the EGF receptor may circumvent acquired resistance to gefitinib. *Proc. Natl. Acad. Sci. U. S. A* *102*, 7665-7670.
- Laban,C., Bustin,S.A., and Jenkins,P.J. (2003). The GH-IGF-I axis and breast cancer. *Trends Endocrinol. Metab* *14*, 28-34.
- Laemmli,U.K. (1970). Cleavage of structural proteins during the assembly of the head of bacteriophage T4. *Nature* *227*, 680-685.
- Larsen,A.B., Pedersen,M.W., Stockhausen,M.T., Grandal,M.V., van,D.B., and Poulsen,H.S. (2007). Activation of the EGFR gene target EphA2 inhibits epidermal growth factor-induced cancer cell motility. *Mol. Cancer Res.* *5*, 283-293.
- Laskin,J.J. and Sandler,A.B. (2004). Epidermal growth factor receptor inhibitors in lung cancer therapy. *Semin. Respir. Crit Care Med.* *25 Suppl 1*, 17-27.
- Le,N.F., Andre,M., Greco,C., Billard,M., Sordat,B., Emile,J.F., Lanza,F., Boucheix,C., and Rubinstein,E. (2006). Profiling of the tetraspanin web of human colon cancer cells. *Mol. Cell Proteomics.* *5*, 845-857.
- Learn,C.A., Hartzell,T.L., Wikstrand,C.J., Archer,G.E., Rich,J.N., Friedman,A.H., Friedman,H.S., Bigner,D.D., and Sampson,J.H. (2004). Resistance to tyrosine kinase inhibition by mutant epidermal growth factor receptor variant III contributes to the neoplastic phenotype of glioblastoma multiforme. *Clin. Cancer Res.* *10*, 3216-3224.
- Lee,J.C., Vivanco,I., Beroukhim,R., Huang,J.H., Feng,W.L., DeBiasi,R.M., Yoshimoto,K., King,J.C., Nghiemphu,P., Yuza,Y., Xu,Q., Greulich,H., Thomas,R.K., Paez,J.G., Peck,T.C., Linhart,D.J., Glatt,K.A., Getz,G., Onofrio,R., Ziaugra,L., Levine,R.L., Gabriel,S., Kawaguchi,T., O'Neill,K., Khan,H., Liao,L.M., Nelson,S.F., Rao,P.N., Mischel,P., Pieper,R.O., Cloughesy,T., Leahy,D.J., Sellers,W.R., Sawyers,C.L., Meyerson,M., and Mellinghoff,I.K. (2006b). Epidermal growth factor receptor activation in glioblastoma through novel missense mutations in the extracellular domain. *PLoS. Med.* *3*, e485.
- Lee,J.M., Dedhar,S., Kalluri,R., and Thompson,E.W. (2006a). The epithelial-mesenchymal transition: new insights in signaling, development, and disease. *J. Cell Biol.* *172*, 973-981.

- Lee,J.W., Soung,Y.H., Kim,S.Y., Nam,H.K., Park,W.S., Nam,S.W., Kim,M.S., Sun,D.I., Lee,Y.S., Jang,J.J., Lee,J.Y., Yoo,N.J., and Lee,S.H. (2005). Somatic mutations of EGFR gene in squamous cell carcinoma of the head and neck. *Clin. Cancer Res.* 11, 2879-2882.
- Li,D., Ji,H., Zaghlul,S., McNamara,K., Liang,M.C., Shimamura,T., Kubo,S., Takahashi,M., Chirieac,L.R., Padera,R.F., Scott,A.M., Jungbluth,A.A., Cavenee,W.K., Old,L.J., Demetri,G.D., and Wong,K.K. (2007). Therapeutic anti-EGFR antibody 806 generates responses in murine de novo EGFR mutant-dependent lung carcinomas. *J. Clin. Invest* 117, 346-352.
- Li,S., Schmitz,K.R., Jeffrey,P.D., Wiltzius,J.J., Kussie,P., and Ferguson,K.M. (2005b). Structural basis for inhibition of the epidermal growth factor receptor by cetuximab. *Cancer Cell* 7, 301-311.
- Li,Z., McNulty,D.E., Marler,K.J., Lim,L., Hall,C., Annan,R.S., and Sacks,D.B. (2005a). IQGAP1 promotes neurite outgrowth in a phosphorylation-dependent manner. *J. Biol. Chem.* 280, 13871-13878.
- Lievre,A., Bachet,J.B., Le,C.D., Boige,V., Landi,B., Emile,J.F., Cote,J.F., Tomasic,G., Penna,C., Ducreux,M., Rougier,P., Penault-Llorca,F., and Laurent-Puig,P. (2006). KRAS mutation status is predictive of response to cetuximab therapy in colorectal cancer. *Cancer Res.* 66, 3992-3995.
- Lillie,F. R. (1908). *The Development of the Chick*. Henry Holt and Co, New York.
- Lim,W.T., Zhang,W.H., Miller,C.R., Watters,J.W., Gao,F., Viswanathan,A., Govindan,R., McLeod,H.L. (2007) PTEN and phosphorylated AKT expression and prognosis in early- and late-stage non-small cell lung cancer. *Oncol Rep*, 17, 853-857.
- Liu,B., Fang,M., Lu,Y., Mendelsohn,J., and Fan,Z. (2001). Fibroblast growth factor and insulin-like growth factor differentially modulate the apoptosis and G1 arrest induced by anti-epidermal growth factor receptor monoclonal antibody. *Oncogene* 20, 1913-1922.

- Lo,H.W., Hsu,S.C., li-Seyed,M., Gunduz,M., Xia,W., Wei,Y., Bartholomeusz,G., Shih,J.Y., and Hung,M.C. (2005). Nuclear interaction of EGFR and STAT3 in the activation of the iNOS/NO pathway. *Cancer Cell* 7, 575-589.
- Lo,H.W., Hsu,S.C., li-Seyed,M., Gunduz,M., Xia,W., Wei,Y., Bartholomeusz,G., Shih,J.Y., and Hung,M.C. (2005). Nuclear interaction of EGFR and STAT3 in the activation of the iNOS/NO pathway. *Cancer Cell* 7, 575-589.
- Lu,Y., Zi,X., Zhao,Y., Mascarenhas,D., and Pollak,M. (2001). Insulin-like growth factor-I receptor signaling and resistance to trastuzumab (Herceptin). *J. Natl. Cancer Inst.* 93, 1852-1857.
- Lu,Z., Ghosh,S., Wang,Z., and Hunter,T. (2003). Downregulation of caveolin-1 function by EGF leads to the loss of E-cadherin, increased transcriptional activity of beta-catenin, and enhanced tumor cell invasion. *Cancer Cell* 4, 499-515.
- Luetteke,N.C., Qiu,T.H., Fenton,S.E., Troyer,K.L., Riedel,R.F., Chang,A., and Lee,D.C. (1999). Targeted inactivation of the EGF and amphiregulin genes reveals distinct roles for EGF receptor ligands in mouse mammary gland development. *Development* 126, 2739-2750.
- Lynch,T.J., Bell,D.W., Sordella,R., Gurubhagavatula,S., Okimoto,R.A., Brannigan,B.W., Harris,P.L., Haserlat,S.M., Supko,J.G., Haluska,F.G., Louis,D.N., Christiani,D.C., Settleman,J., and Haber,D.A. (2004a). Activating mutations in the epidermal growth factor receptor underlying responsiveness of non-small-cell lung cancer to gefitinib. *N. Engl. J. Med.* 350, 2129-2139.
- Lynch,T.J., Lilenbaum,R.C., Bonomi,P., Ansari,R., Govindan,R., Janne,P.A. (2004b). A phase II trial of cetuximab as therapy for recurrent NSCLC. 40th Annual Meeting of the American Society of Clinical Oncology; 5–8June 2004 New Orleans: USA.
- Ma,P.C., Maulik,G., Christensen,J., and Salgia,R. (2003). c-Met: structure, functions and potential for therapeutic inhibition. *Cancer Metastasis Rev.* 22, 309-325.
- Madrid,L.V., Wang,C.Y., Guttridge,D.C., Schottelius,A.J., Baldwin,A.S., Jr., and Mayo,M.W. (2000). Akt suppresses apoptosis by stimulating the transactivation potential of the RelA/p65 subunit of NF-kappaB. *Mol. Cell Biol.* 20, 1626-1638.

- Mahtouk,K., Cremer,F.W., Reme,T., Jourdan,M., Baudard,M., Moreaux,J., Requirand,G., Fiol,G., De,V.J., Moos,M., Quittet,P., Goldschmidt,H., Rossi,J.F., Hose,D., and Klein,B. (2006). Heparan sulphate proteoglycans are essential for the myeloma cell growth activity of EGF-family ligands in multiple myeloma. *Oncogene* 25, 7180-7191.
- Matar,P., Rojo,F., Cassia,R., Moreno-Bueno,G., Di,C.S., Tabernero,J., Guzman,M., Rodriguez,S., Arribas,J., Palacios,J., and Baselga,J. (2004). Combined epidermal growth factor receptor targeting with the tyrosine kinase inhibitor gefitinib (ZD1839) and the monoclonal antibody cetuximab (IMC-C225): superiority over single-agent receptor targeting. *Clin. Cancer Res.* 10, 6487-6501.
- Mellstedt,H. (2003). Monoclonal antibodies in human cancer. *Drugs Today (Barc.)* 39 Suppl C, 1-16.
- Miettinen,P.J., Berger,J.E., Meneses,J., Phung,Y., Pedersen,R.A., Werb,Z., and Derynck,R. (1995). Epithelial immaturity and multiorgan failure in mice lacking epidermal growth factor receptor. *Nature* 376, 337-341.
- Moghal,N. and Sternberg,P.W. (2003). The epidermal growth factor system in *Caenorhabditis elegans*. *Exp. Cell Res.* 284, 150-159.
- Moroni,M., Veronese,S., Benvenuti,S., Marrapese,G., Sartore-Bianchi,A., Di,N.F., Gambacorta,M., Siena,S., and Bardelli,A. (2005). Gene copy number for epidermal growth factor receptor (EGFR) and clinical response to antiEGFR treatment in colorectal cancer: a cohort study. *Lancet Oncol.* 6, 279-286.
- Moscattello,D.K., Holgado-Madruga,M., Godwin,A.K., Ramirez,G., Gunn,G., Zoltick,P.W., Biegel,J.A., Hayes,R.L., and Wong,A.J. (1995). Frequent expression of a mutant epidermal growth factor receptor in multiple human tumors. *Cancer Res.* 55, 5536-5539.
- Mukherjee,S., Tessema,M., and Wandering-Ness,A. (2006). Vesicular trafficking of tyrosine kinase receptors and associated proteins in the regulation of signaling and vascular function. *Circ. Res.* 98, 743-756.
- Mukohara,T., Engelman,J.A., Hanna,N.H., Yeap,B.Y., Kobayashi,S., Lindeman,N., Halmos,B., Pearlberg,J., Tsuchihashi,Z., Cantley,L.C., Tenen,D.G., Johnson,B.E.,

and Janne,P.A. (2005). Differential effects of gefitinib and cetuximab on non-small-cell lung cancers bearing epidermal growth factor receptor mutations. *J. Natl. Cancer Inst.* *97*, 1185-1194.

Murillas,R., Larcher,F., Conti,C.J., Santos,M., Ullrich,A., and Jorcano,J.L. (1995). Expression of a dominant negative mutant of epidermal growth factor receptor in the epidermis of transgenic mice elicits striking alterations in hair follicle development and skin structure. *EMBO J.* *14*, 5216-5223.

Niho,S., Kubota,K., Goto,K., Yoh,K., Ohmatsu,H., Kakinuma,R., Saijo,N., and Nishiwaki,Y. (2006). First-line single agent treatment with gefitinib in patients with advanced non-small-cell lung cancer: a phase II study. *J. Clin. Oncol.* *24*, 64-69.

Noble,M.E., Endicott,J.A., and Johnson,L.N. (2004). Protein kinase inhibitors: insights into drug design from structure. *Science* *303*, 1800-1805.

Normanno,N., Bianco,C., De,L.A., Maiello,M.R., and Salomon,D.S. (2003). Target-based agents against ErbB receptors and their ligands: a novel approach to cancer treatment. *Endocr. Relat Cancer* *10*, 1-21.

Normanno,N., Bianco,C., Strizzi,L., Mancino,M., Maiello,M.R., De,L.A., Caponigro,F., and Salomon,D.S. (2005). The ErbB receptors and their ligands in cancer: an overview. *Curr. Drug Targets.* *6*, 243-257.

Ogiso,H., Ishitani,R., Nureki,O., Fukai,S., Yamanaka,M., Kim,J.H., Saito,K., Sakamoto,A., Inoue,M., Shirouzu,M., and Yokoyama,S. (2002). Crystal structure of the complex of human epidermal growth factor and receptor extracellular domains. *Cell* *110*, 775-787.

Okamoto,I., Kenyon,L.C., Emlet,D.R., Mori,T., Sasaki,J., Hirosako,S., Ichikawa,Y., Kishi,H., Godwin,A.K., Yoshioka,M., Suga,M., Matsumoto,M., and Wong,A.J. (2003). Expression of constitutively activated EGFRvIII in non-small cell lung cancer. *Cancer Sci.* *94*, 50-56.

Olayioye,M.A., Graus-Porta,D., Beerli,R.R., Rohrer,J., Gay,B., and Hynes,N.E. (1998). ErbB-1 and ErbB-2 acquire distinct signaling properties dependent upon their dimerization partner. *Mol. Cell Biol.* *18*, 5042-5051.

Ono,M. and Kuwano,M. (2006). Molecular mechanisms of epidermal growth factor receptor (EGFR) activation and response to gefitinib and other EGFR-targeting drugs. *Clin. Cancer Res.* 12, 7242-7251.

Paez,J.G., Janne,P.A., Lee,J.C., Tracy,S., Greulich,H., Gabriel,S., Herman,P., Kaye,F.J., Lindeman,N., Boggon,T.J., Naoki,K., Sasaki,H., Fujii,Y., Eck,M.J., Sellers,W.R., Johnson,B.E., and Meyerson,M. (2004). EGFR mutations in lung cancer: correlation with clinical response to gefitinib therapy. *Science* 304, 1497-1500.

Pao,W. and Miller,V.A. (2005). Epidermal growth factor receptor mutations, small-molecule kinase inhibitors, and non-small-cell lung cancer: current knowledge and future directions. *J. Clin. Oncol.* 23, 2556-2568.

Pao,W., Miller,V.A., Politi,K., Riely,G.J., Somwar,R., Zakowski,M.F., Kris,M.G., Varmus,H. (2005a). Acquired resistance of lung adenocarcinomas to gefitinib or erlotinib is associated with a second mutation in the EGFR kinase domain. *PLoS. Med.* 2, e73.

Pao,W., Wang,T.Y., Riely,G.J., Miller,V.A., Pan,Q., Ladanyi,M., Zakowski,M.F., Heelan,R.T., Kris,M.G., and Varmus,H.E. (2005b). KRAS mutations and primary resistance of lung adenocarcinomas to gefitinib or erlotinib. *PLoS. Med.* 2, e17.

Pastore,S., Mascia,F., Mariotti,F., Dattilo,C., Mariani,V., and Girolomoni,G. (2005). ERK1/2 regulates epidermal chemokine expression and skin inflammation. *J. Immunol.* 174, 5047-5056.

Pawson,T., Gish,G.D., and Nash,P. (2001). SH2 domains, interaction modules and cellular wiring. *Trends Cell Biol.* 11, 504-511.

Pece,S., Chiariello,M., Murga,C., and Gutkind,J.S. (1999). Activation of the protein kinase Akt/PKB by the formation of E-cadherin-mediated cell-cell junctions. Evidence for the association of phosphatidylinositol 3-kinase with the E-cadherin adhesion complex. *J. Biol. Chem.* 274, 19347-19351.

Pece,S. and Gutkind,J.S. (2000). Signaling from E-cadherins to the MAPK pathway by the recruitment and activation of epidermal growth factor receptors upon cell-cell contact formation. *J. Biol. Chem.* 275, 41227-41233.



- Pedersen,M.W., Meltorn,M., Damstrup,L., and Poulsen,H.S. (2001). The type III epidermal growth factor receptor mutation. Biological significance and potential target for anti-cancer therapy. *Ann. Oncol.* *12*, 745-760.
- Perez-Soler,R., Ling,Y-H., Lia,M., Kroog,G., Dai,Q., Zou,Y. (2003). Molecular mechanisms of sensitivity and resistance to the HER1/EGFR-tyrosine kinase inhibitor erlotinib (Tarceva). *Lung Cancer* 2003; 41 (Suppl 2): S72 (Abstract #O-247)).
- Perez-Torres,M., Guix,M., Gonzalez,A., and Arteaga,C.L. (2006). Epidermal growth factor receptor (EGFR) antibody down-regulates mutant receptors and inhibits tumors expressing EGFR mutations. *J. Biol. Chem.* *281*, 40183-40192.
- Piepkorn,M., Pittelkow,M.R., and Cook,P.W. (1998). Autocrine regulation of keratinocytes: the emerging role of heparin-binding, epidermal growth factor-related growth factors. *J. Invest Dermatol.* *111*, 715-721.
- Prenzel,N., Zwick,E., Daub,H., Leserer,M., Abraham,R., Wallasch,C., and Ullrich,A. (1999). EGF receptor transactivation by G-protein-coupled receptors requires metalloproteinase cleavage of proHB-EGF. *Nature* *402*, 884-888.
- Prenzel,N., Zwick,E., Leserer,M., and Ullrich,A. (2000). Tyrosine kinase signaling in breast cancer. Epidermal growth factor receptor: convergence point for signal integration and diversification. *Breast Cancer Res.* *2*, 184-190.
- Qian,X., Karpova,T., Sheppard,A.M., McNally,J., and Lowy,D.R. (2004). E-cadherin-mediated adhesion inhibits ligand-dependent activation of diverse receptor tyrosine kinases. *EMBO J.* *23*, 1739-1748.
- Radonic,A., Thulke,S., Mackay,I.M., Landt,O., Siegert,W., and Nitsche,A. (2004). Guideline to reference gene selection for quantitative real-time PCR. *Biochem. Biophys. Res. Commun.* *313*, 856-862.
- Ranson,M., Hammond,L.A., Ferry,D., Kris,M., Tullo,A., Murray,P.I., Miller,V., Averbuch,S., Ochs,J., Morris,C., Feyereislova,A., Swaisland,H., and Rowinsky,E.K. (2002). ZD1839, a selective oral epidermal growth factor receptor-tyrosine kinase inhibitor, is well tolerated and active in patients with solid, malignant tumors: results of a phase I trial. *J. Clin. Oncol.* *20*, 2240-2250.

- Remmelink,M., Mijatovic,T., Gustin,A., Mathieu,A., Rombaut,K., Kiss,R., Salmon,I., and Decaestecker,C. (2005). Identification by means of cDNA microarray analyses of gene expression modifications in squamous non-small cell lung cancers as compared to normal bronchial epithelial tissue. *Int. J. Oncol.* 26, 247-258.
- Resnick,M.B., Routhier,J., Konkin,T., Sabo,E., and Pricolo,V.E. (2004). Epidermal growth factor receptor, c-MET, beta-catenin, and p53 expression as prognostic indicators in stage II colon cancer: a tissue microarray study. *Clin. Cancer Res.* 10, 3069-3075.
- Riese,D.J. and Stern,D.F. (1998). Specificity within the EGF family/ErbB receptor family signaling network. *Bioessays* 20, 41-48.
- Rieske,P., Kordek,R., Bartkowiak,J., biac-Rychter,M., Biernat,W., and Liberski,P.P. (1998). A comparative study of epidermal growth factor receptor (EGFR) and MDM2 gene amplification and protein immunoreactivity in human glioblastomas. *Pol. J. Pathol.* 49, 145-149.
- Robertson,G.P. (2005). Functional and therapeutic significance of Akt deregulation in malignant melanoma. *Cancer Metastasis Rev.* 24, 273-285.
- Roche-Lestienne,C., Soenen-Cornu,V., Grardel-Duflos,N., Lai,J.L., Philippe,N., Facon,T., Fenaux,P., and Preudhomme,C. (2002). Several types of mutations of the Abl gene can be found in chronic myeloid leukemia patients resistant to STI571, and they can pre-exist to the onset of treatment. *Blood* 100, 1014-1018.
- Rubin,G.J., Melhem,M.F., Barnes,E.L., and Tweardy,D.J. (1996). Quantitative immunohistochemical analyses of transforming growth factor-alpha and epidermal growth factor receptor in patients with squamous cell carcinoma of the head and neck. *Cancer* 78, 1284-1292.
- Rusch,V., Klimstra,D., Venkatraman,E., Pisters,P.W., Langenfeld,J., and Dmitrovsky,E. (1997). Overexpression of the epidermal growth factor receptor and its ligand transforming growth factor alpha is frequent in resectable non-small cell lung cancer but does not predict tumor progression. *Clin. Cancer Res.* 3, 515-522.

- Salomon,D.S., Brandt,R., Ciardiello,F., and Normanno,N. (1995). Epidermal growth factor-related peptides and their receptors in human malignancies. *Crit Rev. Oncol. Hematol.* *19*, 183-232.
- Salomon,D.S., Bianco,C., and De,S.M. (1999). Cripto: a novel epidermal growth factor (EGF)-related peptide in mammary gland development and neoplasia. *Bioessays* *21*, 61-70.
- Saltz,L.B., Meropol,N.J., Loehrer,P.J., Sr., Needle,M.N., Kopit,J., and Mayer,R.J. (2004). Phase II trial of cetuximab in patients with refractory colorectal cancer that expresses the epidermal growth factor receptor. *J. Clin. Oncol.* *22*, 1201-1208.
- Samuels,Y. and Velculescu,V.E. (2004). Oncogenic mutations of PIK3CA in human cancers. *Cell Cycle* *3*, 1221-1224.
- Sanger,F., Nicklen,S., and Coulson,A.R. (1977). DNA sequencing with chain-terminating inhibitors. *Proc. Natl. Acad. Sci. U. S. A* *74*, 5463-5467.
- Sato,J.D., Kawamoto,T., Le,A.D., Mendelsohn,J., Polikoff,J., and Sato,G.H. (1983). Biological effects in vitro of monoclonal antibodies to human epidermal growth factor receptors. *Mol. Biol. Med.* *1*, 511-529.
- Schlessinger,J. (2000). Cell signaling by receptor tyrosine kinases. *Cell* *103*, 211-225.
- Shawver,L.K., Slamon,D., and Ullrich,A. (2002). Smart drugs: tyrosine kinase inhibitors in cancer therapy. *Cancer Cell* *1*, 117-123.
- She,Q.B., Solit,D., Basso,A., and Moasser,M.M. (2003). Resistance to gefitinib in PTEN-null HER-overexpressing tumor cells can be overcome through restoration of PTEN function or pharmacologic modulation of constitutive phosphatidylinositol 3'-kinase/Akt pathway signaling. *Clin. Cancer Res.* *9*, 4340-4346.
- Shilo,B.Z. (2003). Signaling by the *Drosophila* epidermal growth factor receptor pathway during development. *Exp. Cell Res.* *284*, 140-149.
- Shook,D. and Keller,R. (2003). Mechanisms, mechanics and function of epithelial-mesenchymal transitions in early development. *Mech. Dev.* *120*, 1351-1383.

Sibilia, M. and Wagner, E.F. (1995). Strain-dependent epithelial defects in mice lacking the EGF receptor. *Science* 269, 234-238.

Sihto, H., Puputti, M., Pulli, L., Tynninen, O., Koskinen, W., Aaltonen, L.M., Tanner, M., Bohling, T., Visakorpi, T., Butzow, R., Knuutila, A., Nupponen, N.N., and Joensuu, H. (2005). Epidermal growth factor receptor domain II, IV, and kinase domain mutations in human solid tumors. *J. Mol. Med.* 83, 976-983.

Skvortsov, S., Sarg, B., Loeffler-Ragg, J., Skvortsova, I., Lindner, H., Werner, O.H., Lukas, P., Illmensee, K., and Zwierzina, H. (2004). Different proteome pattern of epidermal growth factor receptor-positive colorectal cancer cell lines that are responsive and nonresponsive to C225 antibody treatment. *Mol. Cancer Ther.* 3, 1551-1558.

Sonnenberg, E., Meyer, D., Weidner, K.M., and Birchmeier, C. (1993). Scatter factor/hepatocyte growth factor and its receptor, the c-met tyrosine kinase, can mediate a signal exchange between mesenchyme and epithelia during mouse development. *J. Cell Biol.* 123, 223-235.

Sordella, R., Bell, D.W., Haber, D.A., and Settleman, J. (2004). Gefitinib-sensitizing EGFR mutations in lung cancer activate anti-apoptotic pathways. *Science* 305, 1163-1167.

Spivak-Kroizman, T., Lemmon, M.A., Dikic, I., Ladbury, J.E., Pinchasi, D., Huang, J., Jaye, M., Crumley, G., Schlessinger, J., and Lax, I. (1994). Heparin-induced oligomerization of FGF molecules is responsible for FGF receptor dimerization, activation, and cell proliferation. *Cell* 79, 1015-1024.

Strachan, L., Murison, J.G., Prestidge, R.L., Sleeman, M.A., Watson, J.D., and Kumble, K.D. (2001). Cloning and biological activity of epigen, a novel member of the epidermal growth factor superfamily. *J. Biol. Chem.* 276, 18265-18271.

Takano, T., Ohe, Y., Sakamoto, H., Tsuta, K., Matsuno, Y., Tateishi, U., Yamamoto, S., Nokihara, H., Yamamoto, N., Sekine, I., Kunitoh, H., Shibata, T., Sakiyama, T., Yoshida, T., and Tamura, T. (2005). Epidermal growth factor receptor gene mutations and increased copy numbers predict gefitinib sensitivity in patients with recurrent non-small-cell lung cancer. *J. Clin. Oncol.* 23, 6829-6837.

- Tang,J.M., He,Q.Y., Guo,R.X., Chang,X.J. (2006) Phosphorylated Akt overexpression and loss of PTEN expression in non-small cell lung cancer confers poor prognosis. *Lung Cancer*, *51*, 181-191.
- Tateishi,M., Ishida,T., Mitsudomi,T., Kaneko,S., and Sugimachi,K. (1990). Immunohistochemical evidence of autocrine growth factors in adenocarcinoma of the human lung. *Cancer Res.* *50*, 7077-7080.
- Thiery,J.P. (2002). Epithelial-mesenchymal transitions in tumor progression. *Nat. Rev. Cancer* *2*, 442-454.
- Thompson,E.W., Newgreen,D.F., and Tarin,D. (2005). Carcinoma invasion and metastasis: a role for epithelial-mesenchymal transition? *Cancer Res.* *65*, 5991-5995.
- Thomson,S., Buck,E., Petti,F., Griffin,G., Brown,E., Ramnarine,N., Iwata,K.K., Gibson,N., and Haley,J.D. (2005). Epithelial to mesenchymal transition is a determinant of sensitivity of non-small-cell lung carcinoma cell lines and xenografts to epidermal growth factor receptor inhibition. *Cancer Res.* *65*, 9455-9462.
- Threadgill,D.W., Dlugosz,A.A., Hansen,L.A., Tennenbaum,T., Lichti,U., Yee,D., LaMantia,C., Mourtou,T., Herrup,K., Harris,R.C., and . (1995). Targeted disruption of mouse EGF receptor: effect of genetic background on mutant phenotype. *Science* *269*, 230-234.
- Towbin,H., Staehelin,T., and Gordon,J. (1979). Electrophoretic transfer of proteins from polyacrylamide gels to nitrocellulose sheets: procedure and some applications. *Proc. Natl. Acad. Sci. U. S. A* *76*, 4350-4354.
- Toyooka,S., Kiura,K., and Mitsudomi,T. (2005). EGFR mutation and response of lung cancer to gefitinib. *N. Engl. J. Med.* *352*, 2136.
- Tsuchihashi,Z., Khambata-Ford,S., Hanna,N., and Janne,P.A. (2005). Responsiveness to cetuximab without mutations in EGFR. *N. Engl. J. Med.* *353*, 208-209.
- Uegaki,K., Nio,Y., Inoue,Y., Minari,Y., Sato,Y., Song,M.M., Dong,M., and Tamura,K. (1997). Clinicopathological significance of epidermal growth factor and its receptor in human pancreatic cancer. *Anticancer Res.* *17*, 3841-3847.

- van,d., V, Kumar,R., and Mendelsohn,J. (1991). Ligand-induced activation of A431 cell epidermal growth factor receptors occurs primarily by an autocrine pathway that acts upon receptors on the surface rather than intracellularly. *J. Biol. Chem.* *266*, 7503-7508.
- Van,O.E. (1994). Signaling through the insulin receptor and the insulin-like growth factor-I receptor. *Diabetologia* *37 Suppl 2* , S125-S134.
- Veale,D., Kerr,N., Gibson,G.J., Kelly,P.J., and Harris,A.L. (1993). The relationship of quantitative epidermal growth factor receptor expression in non-small cell lung cancer to long term survival. *Br. J. Cancer* *68*, 162-165.
- Velu,T.J., Beguinot,L., Vass,W.C., Zhang,K., Pastan,I., and Lowy,D.R. (1989). Retroviruses expressing different levels of the normal epidermal growth factor receptor: biological properties and new bioassay. *J. Cell Biochem.* *39*, 153-166.
- Viloria-Petit,A., Crombet,T., Jothy,S., Hicklin,D., Bohlen,P., Schlaeppli,J.M., Rak,J., and Kerbel,R.S. (2001). Acquired resistance to the antitumor effect of epidermal growth factor receptor-blocking antibodies in vivo: a role for altered tumor angiogenesis. *Cancer Res.* *61*, 5090-5101.
- Wiley,H.S. (2003). Trafficking of the ErbB receptors and its influence on signaling. *Exp. Cell Res.* *284*, 78-88.
- Williams,K.J., Telfer,B.A., Brave,S., Kendrew,J., Whittaker,L., Stratford,I.J., and Wedge,S.R. (2004). ZD6474, a potent inhibitor of vascular endothelial growth factor signaling, combined with radiotherapy: schedule-dependent enhancement of antitumor activity. *Clin. Cancer Res.* *10*, 8587-8593.
- Witta,S.E., Gemmill,R.M., Hirsch,F.R., Coldren,C.D., Hedman,K., Ravdel,L., Helfrich,B., Dziadziuszko,R., Chan,D.C., Sugita,M., Chan,Z., Baron,A., Franklin,W., Drabkin,H.A., Girard,L., Gazdar,A.F., Minna,J.D., and Bunn,P.A., Jr. (2006). Restoring E-cadherin expression increases sensitivity to epidermal growth factor receptor inhibitors in lung cancer cell lines. *Cancer Res.* *66*, 944-950.
- Wong,C., Rougier-Chapman,E.M., Frederick,J.P., Datto,M.B., Liberati,N.T., Li,J.M., and Wang,X.F. (1999). Smad3-Smad4 and AP-1 complexes synergize in

transcriptional activation of the c-Jun promoter by transforming growth factor beta. *Mol. Cell Biol.* **19**, 1821-1830.

Wu,X., Fan,Z., Masui,H., Rosen,N., and Mendelsohn,J. (1995). Apoptosis induced by an anti-epidermal growth factor receptor monoclonal antibody in a human colorectal carcinoma cell line and its delay by insulin. *J. Clin. Invest* **95**, 1897-1905.

Yamashita,S., Miyagi,C., Fukada,T., Kagara,N., Che,Y.S., and Hirano,T. (2004). Zinc transporter LIV1 controls epithelial-mesenchymal transition in zebrafish gastrula organizer. *Nature* **429**, 298-302.

Yamauchi,T., Ueki,K., Tobe,K., Tamemoto,H., Sekine,N., Wada,M., Honjo,M., Takahashi,M., Takahashi,T., Hirai,H., Tushima,T., Akanuma,Y., Fujita,T., Komuro,I., Yazaki,Y., and Kadowaki,T. (1997). Tyrosine phosphorylation of the EGF receptor by the kinase Jak2 is induced by growth hormone. *Nature* **390**, 91-96.

Yarden,Y. and Sliwkowski,M.X. (2001). Untangling the ErbB signaling network. *Nat. Rev. Mol. Cell Biol.* **2**, 127-137.

Yauch,R.L., Januario,T., Eberhard,D.A., Cavet,G., Zhu,W., Fu,L., Pham,T.Q., Soriano,R., Stinson,J., Seshagiri,S., Modrusan,Z., Lin,C.Y., O'Neill,V., and Amler,L.C. (2005). Epithelial versus mesenchymal phenotype determines in vitro sensitivity and predicts clinical activity of erlotinib in lung cancer patients. *Clin. Cancer Res.* **11**, 8686-8698.

Yoon,S. and Seger,R. (2006). The extracellular signal-regulated kinase: multiple substrates regulate diverse cellular functions. *Growth Factors* **24**, 21-44.

Zeineldin,R., Rosenberg,M., Ortega,D., Buhr,C., Chavez,M.G., Stack,M.S., Kusewitt,D.F., and Hudson,L.G. (2006). Mesenchymal transformation in epithelial ovarian tumor cells expressing epidermal growth factor receptor variant III. *Mol. Carcinog.* **45**, 851-860.

Zhang,X., Gureasko,J., Shen,K., Cole,P.A., and Kuriyan,J. (2006). An allosteric mechanism for activation of the kinase domain of epidermal growth factor receptor. *Cell* **125**, 1137-1149.

---

Zou,H.Y., Li,Q., Lee,J.H., Arango,M.E., McDonnell,S.R., Yamazaki,S., Koudriakova,T.B., Alton,G., Cui,J.J., Kung,P.P., Nambu,M.D., Los,G., Bender,S.L., Mroczkowski,B., and Christensen,J.G. (2007). An orally available small-molecule inhibitor of c-Met, PF-2341066, exhibits cytoreductive antitumor efficacy through antiproliferative and antiangiogenic mechanisms. *Cancer Res.* 67, 4408-4417.



## Acknowledgements

First, I would like to thank Professor Dr. Christoph Turck for promoting this work at the Ludwig-Maximilians-Universität in Munich and for his sustained support, as well as for the helpful and guiding discussions.

I am thankful to my supervisor at Merck KGaA, PD Dr. Jens Oliver Funk, for his generous and motivating support and for the possibility to conduct my PhD thesis in the division TA Oncology at the Merck KGaA in Darmstadt.

I am particularly thankful to Dr. Andree Blaukat, who escorted my work scientifically and personally. He was at all times open for my inquiries and was always ready to support me with his prudential advice. I also want to thank him for backing my economic education.

I would further like to thank Dr. Nina Heiss, for offering me the initial opportunity to start my PhD thesis at Merck, for guiding me during my first year and for introducing me to translational cancer research.

I am also very grateful to Dr. Dirk Wienke, who has steadily helped me with his valuable scientific advice and his willingness to formally and scientifically supervise Andrea and Mara.

I am grateful to Melanie Kühnl in the lab of Dr. Detlef Güssow for performing the whole genome Affymetrix expression analyses, to Dr. Anja von Heydebreck for the statistical evaluation of the Affymetrix data, to Gerhard Schuster und Monika Schaefer in the lab of Dr. Christiane Amendt for carrying out the murine xenograft experiments, to Dr. Oliver Poeschke for his support with the BRET assays, as well as to Jens Baumgärtner and Tobias Haas for their support and evaluation of the expression data from the Low-Density Arrays.

In addition I would like to thank Dr. Arne Sutter, Dr. Christofer Stroh, Dr. Joyce Beherens and Dr. Frank Zenke for scientific discussions and their positive reinforcement. I am grateful to Jürgen, Christoph, Iris, Irina, Silvia, Martin, Frank, Dagmar, Katharina, Elisabeth and all other current and former members of the TA Oncology for technical support and for creating a positive and welcome working atmosphere. Furthermore, I thank Horst for his administrative and personal help.

I thank Andrea and Mara for their contribution in characterizing the long-term treated cancer cell lines and the stably transfected NIH3T3 cells and for the joyful

discussions we had. Further I would like to thank my interns Alex, Conny and Jana for their experimental and personal support and their interest in this work.

A special “thank you” goes to Dirk, Elena, Friederike, Jessi, Katharina, Katja, Ralf and Vanessa and the former members of the “Doktorandenlabor” for their amicable teamwork and the recreative discussions we shared during the last three years.

I thank my mother for their enduring encouragement and motherly affection. I thank my father for his support and interest in my work.

Ultimately, I thank my little son Ben Leonard for distracting me from writing this thesis and for his smile and play.

I thank Doro for her love.

## Curriculum Vitae

Name: Denis Irmer  
Date of birth: June 29<sup>th</sup>, 1976  
Place of birth: Recklinghausen  
Status: Married, one son  
Address: Benrodestraße 57  
40597 Düsseldorf

- 1982 - 1986: Grundschule, Immenstaad am Bodensee.
- 1986 - 1995: Gymnasium Überlingen (Allgemeine Hochschulreife).
- 1995 - 1996: Civil Service, Storchstation Salem.
- 1996 - 2003: Studies of Biology at the University of Tübingen, California State University Long Beach (CSULB) and Ludwig-Maximilians- Universität (LMU) München.
- 01 - 06/2000: Research Project in the laboratory of Prof. Dr. Olaf Schneewind, Institute of Immunology and Microbiology, University of California Los Angeles (UCLA):  
“The role of YscX and YscY for the type III secretion system in *Yersinia enterocolitica*”.
- 01 - 11/2003: Diploma thesis in the laboratory of Prof. Dr. Rudolf Grosschedl, Institute for Biochemistry, LMU München:  
“The role of PIASy for cellular STAT-Signaling, Wnt-Signaling and Sumoylation”.
- 2004 - 2007: PhD thesis at Merck KGaA, Darmstadt, represented at the Institute for Biochemistry by Prof. Dr. Christoph Turck, LMU München:  
“Molecular analyses of resistance and sensitivity mechanisms to anti-EGFR directed tumor therapy”.
- 2007 - : Consultant, Bayer Business Services GmbH, Business Consulting, R&D, Leverkusen.

**Publications:**

Irmer,D., Funk,J.O., and Blaukat,A. (2007). EGFR kinase domain mutations - functional impact and relevance for lung cancer therapy. *Oncogene* 26, 5693-5701.

Irmer,D., Vocke,D., von Heydebreck,A., Amendt,C., Wienke,D., Blaukat,A. (2007). Activity of the anti-EGFR antibody cetuximab in NSCLC cells with wildtype and mutant EGFR. Manuscript submitted.

Ruff,M.\*, Irmer,D.\*, Vocke,D., Wienke, D., Blaukat,A. (2007). Biological activity of the anti-EGFR antibody cetuximab in a stably transfected model cell line expressing EGFR kinase domain mutations. Manuscript in preparation. (\* these authors contributed equally to the publication).